# SPATIO-TEMPORAL MODELLING OF REFERENCE CROP EVAPOTRANSPIRATION ACROSS KARNATAKA STATE, INDIA

**Thesis**

**Submitted in partial fulfilment of the requirements for the degree of**

**DOCTOR OF PHILOSOPHY**

**by**

**NIRANJAN S**

**DEPARTMENT OF WATER RESOURCES AND OCEAN ENGINEERING**

**NATIONAL INSTITUTE OF TECHNOLOGY KARNATAKA**

**SURATHKAL, MANGALURU - 575025**

**APRIL, 2023**

# SPATIO-TEMPORAL MODELLING OF REFERENCE CROP EVAPOTRANSPIRATION ACROSS KARNATAKA STATE, INDIA

**Thesis**

**Submitted in partial fulfilment of the requirements for the degree of**

**DOCTOR OF PHILOSOPHY**

**by**

**NIRANJAN S**

**Reg. No. 165066AM16F05**

**Research Guide**

**Prof. LAKSHMAN NANDAGIRI**

**DEPARTMENT OF WATER RESOURCES AND OCEAN ENGINEERING**

**NATIONAL INSTITUTE OF TECHNOLOGY KARNATAKA**

**SURATHKAL, MANGALURU - 575025**

**APRIL, 2023**

## DECLARATION

*by the Ph.D. Research Scholar*

I hereby *declare* that the Research Thesis entitled **"Spatio-temporal Modelling of Reference Crop Evapotranspiration across Karnataka State, India"**, which is being submitted to the **National Institute of Technology Karnataka Surathkal** in partial fulfilment of the requirements for the award of the Degree of ***Doctor of Philosophy*** in the **Department of Water Resources and Ocean Engineering (Formerly Department of Applied Mechanics and Hydraulics)** is a *bonafide report of the research work carried out by me*. The material contained in this thesis has not been submitted to any University or Institution for the award of any degree.

**Niranjan S**
Register No.: 165066AM16F05
Department of Water Resources and Ocean Engineering
Formerly Department of Applied Mechanics and Hydraulics

Place: NITK, Surathkal

Date: 28/04/2023.

## CERTIFICATE

This is to *certify* that the Research Thesis entitled **"Spatio-temporal Modelling of Reference Crop Evapotranspiration across Karnataka State, India"**, submitted by **Niranjan S** (Register Number: 165066AM16F05) as the record of the research work carried out by him, is *accepted* as the *Research Thesis submission* in partial fulfillment of the requirements for the award of degree of **Doctor of Philosophy**.

**Prof. Lakshman Nandagiri**
Research Guide
(Name and Signature with Date and Seal)

Dr. LAKSHMAN NANDAGIRI
Professor
Dept. of Water Resources & Ocean Engineering
National Institute of Technology Karnataka
Surathkal, Srinivasnagara, Mangaluru - 575 025

**Chairperson - DRPC**
(Signature with Date and Seal)
Department of Water Resources and Ocean Engineering
Formerly Department of Applied Mechanics and Hydraulics

Chairman (DRPC)
Dept. of Water Resources & Ocean Engineering

Dept. of Water Resources & Ocean Engineering
NITK Surathkal

# Acknowledgements

This Thesis marks the end of an enriching, challenging and memorable time as a student at NITK Surathkal. This journey has been the exhilarating and successful completion of years of effort would be incomplete without mentioning the people who have helped me sail smoothly over the crests and troughs.

First and foremost, I am grateful and indebted to have Prof. Lakshman Nandagiri as a research supervisor. His profound wisdom and inimitable technical expertise have helped in attaining the required skills with ease and achieving my research objective. His constant persuasion for originality and constructive criticism have refined my research writing, which aided me in completing this colossal task of journal and thesis writing. Apart from the technical engagements, his constant words of encouragement have helped me in my personal development. It is difficult to overstate my gratitude and put it into words. He shall remain a source of inspiration throughout my life.

I am grateful to the Water Resources and Development Organization (WRDO), Government of Karnataka for providing the hydro-meteorological data used in the study. I reserve special thanks to Mrs. Thara N., Assistant Engineer, Hydrology Unit for coordination during the data collection.

I am sincerely thankful to the Research Progress Assessment Committee (RPAC) panel members: the Late Prof. Paresh Chandra Deka and Prof. G. S. Dwarakish (Department of Water Resources and Ocean Engineering), and Prof. Subhash C. Yaragal (Department of Civil Engineering) for their valuable inputs during the progress assessment which helped me to bring the report to the present form.

I am greatly obliged to Dr. K. Varija the present Head of the Department and Prof. Doddamani B.M., Prof. Amai Mahesha, and Prof. Amba Shetty, the former Heads of the Department of Water Resources and Ocean Engineering, NITK, Surathkal, for their support and granting permissions to use the departmental computing facilities necessary for my research.

I express my gratitude to Dr. Debabrata Karmakar and Dr. Prithviraj U for providing the lab facilities.

I gratefully express my gratitude to faculty members of Civil Engineering: Prof. Ravishankar U., Dr. Prashanth M.H., Prof. Narasimhan C., Prof. Srihari S., and Prof. Swaminathan K and all the faculty from Water Resources and Ocean Engineering department for their constant mentoring during my days at the institute.

A special thank goes to my colleagues and friends for their closeness and support throughout the stay at NITK and their constant support through hard times and celebration of each accomplishment. I am extremely grateful to my Labmates: Dr. Praveen K. M., Dr. Venkateshawarulu, Anjali Vijay, Ayilo Kikon.

I also thank my friends who have rendered their input and emotional support during the course of the journey Dr. Abhishek Pathak, Dr. Usha A., Chandrashekharayya Hiremath, Dr. Sinan Nizar, Dr. Diwan Mohaideen, Punithraj, Venkannagouda, Surajith, Dr. Sandesh Upadhyaya, Swathi Shetty, Murugan, Dr. Pramod K., Pandu, Dr. Geetha K., Saicharan, Vinod, Sahaj, Poojitha, Salma Shaik, for being a part of this journey and being helpful in numerous ways.

I sincerely acknowledge the help and support rendered by all the non-teaching staff for their guidance in all official works: Mr. Balakrishna, Mr. Seetharam, Mrs. Prathima, Mr. Anil Kumar and Ms. Sweekritha.

Most importantly, this endeavour would not have been possible without the cooperation and support of my family members. Heartfelt thanks to my parents for their support and encouragement that always kept me on the right path to follow my dreams. Special thanks to my sister, Nayana S. for being a support system. I am thankful to my maternal uncle Dr. B. Balakrishna, and paternal uncle Dr. Doddaiah S.V. for being an inspiration and for their continuous encouragement. I am also thankful for the help received from all the cousins. Thanks to my entire family for being there with me throughout this journey.

Finally, I thank God for letting me through all the difficulties and for the blessings.

**Thank You All**

**Niranjan S**

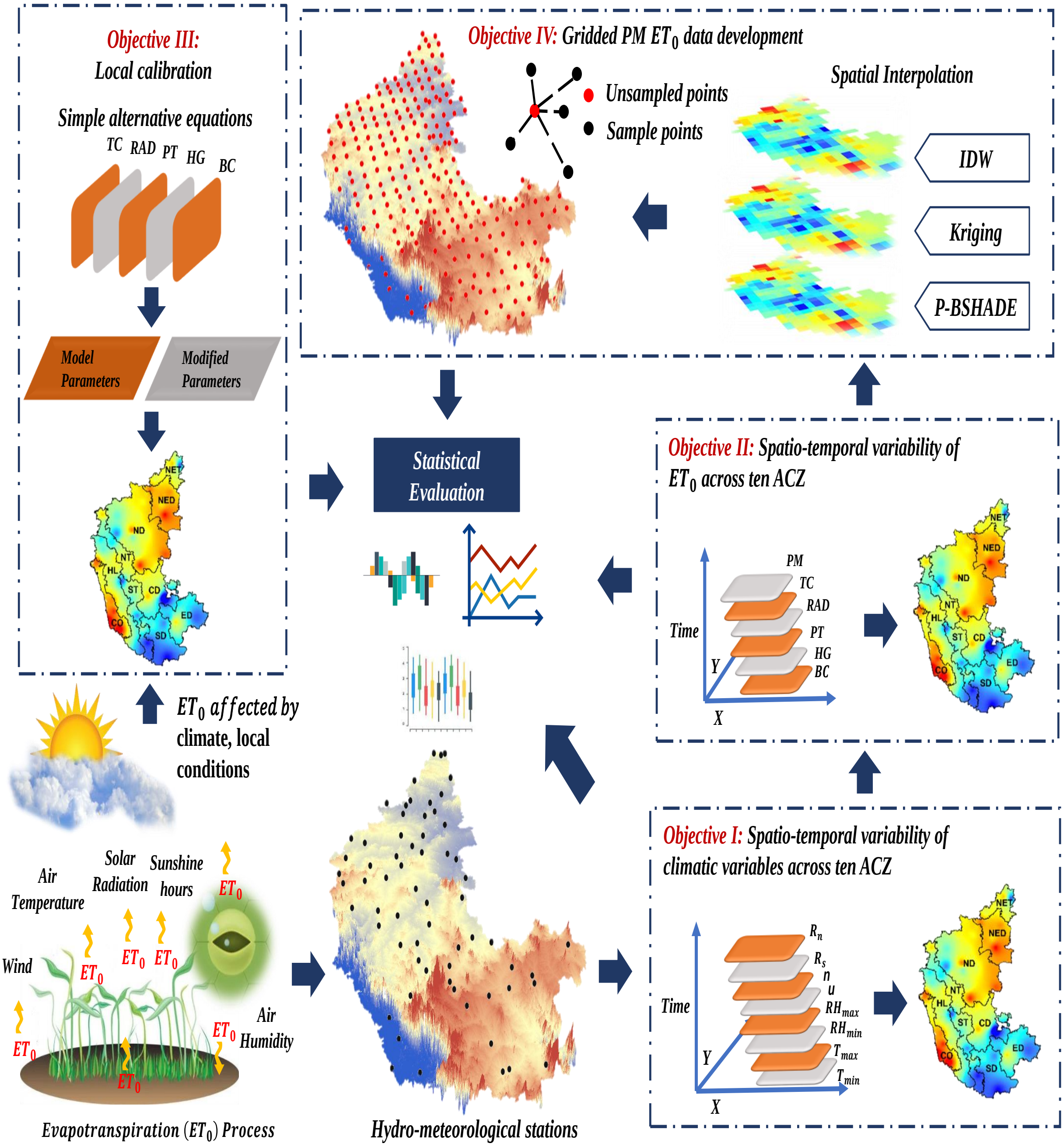
Objective III:
Local calibration
Simple alternative equations
TC RAD PT HG BC
Model Parameters
Modified Parameters
Objective IV: Gridded PM $ET_0$ data development
Unsampled points
Sample points
Spatial Interpolation
IDW
Kriging
P-BSHADE
Statistical Evaluation
Objective II: Spatio-temporal variability of $ET_0$ across ten ACZ
Time
Y
X
PM
TC
RAD
PT
HG
BC
$ET_0$ affected by climate, local conditions
Objective I: Spatio-temporal variability of climatic variables across ten ACZ
$R_n$
$R_s$
n
u
$RH_{max}$
$RH_{min}$
$T_{max}$
$T_{min}$
Air Temperature
Solar Radiation
Sunshine hours
Wind
Air Humidity
Evapotranspiration ($ET_0$) Process
Hydro-meteorological stations

## ABSTRACT

Reference crop evapotranspiration ($ET_0$) is a key variable required in the computation of crop water and irrigation water requirements and also as an input in hydrological modelling. Due to the non-availability of direct $ET_0$ measurements, $ET_0$ is usually estimated using regularly recorded climate data. The physically-based FAO-56 Penman-Monteith (PM) equation has been identified as a reliable method for this purpose but suffers from the disadvantage that it requires input data pertaining to a large number of climate variables. Therefore, in data short situations, simpler empirical to semi-empirical temperature and radiation-based methods may have to be used to estimate $ET_0$. However, their performances in diverse climates and the effect of local calibration on their accuracies have not been extensively studied.

Therefore, the present study was taken up with the following objectives: 1) Assessment of spatio-temporal variations of climatic variables associated with the calculation of reference crop evapotranspiration ($ET_0$) over Karnataka State, India for the historical period 2006-2016 2) Assessment of spatio-temporal variations of Penman-Monteith (PM) $ET_0$ for the study area for the same historical period 3) Performance evaluation of simpler alternative $ET_0$ equations relative to PM $ET_0$ with and without local calibration of parameters and 4) Development of a gridded PM $ET_0$ product for Karnataka State. For this purpose, historical climate data from the period 2006-2016 for 67 stations located in various agro-climatic zones of Karnataka State, India was used.

Spatio-temporal variability assessment was carried out on the historical data of eight climatic variables from 67 stations using statistical indices, box-whisker plots and spatial maps. The dataset consisted of daily values of six climatic variables, namely maximum air temperature ($T_{max}$), minimum air temperature ($T_{min}$), maximum relative humidity ($RH_{max}$), minimum relative humidity ($RH_{min}$), actual hours of sunshine (n) and wind speed (u). The analysis clearly demonstrated the prevalence of distinct climatic regimes ranging from humid to arid. The overall characterization of climate variables indicates the northern agroclimatic zones (ND, NED, and NT) exhibited high temperature, low humidity, and high sunshine values. Similarly, the southern region is characterized by low temperature and high humidity. Since the climate of Karnataka State is largely influenced by the monsoon phenomenon, distinct variations in climatic variables arise on its account. A similar influence of the monsoon was seen in the intra-annual variations of mean $ET_0$ estimates. It was seen that $ET_0$ values peak during the month of April (4.5-5 $\mathrm{mm\ d^{-1}}$) and with the onset of the monsoon rains in May-June and begin to decrease to around 3.0-4 $\mathrm{mm\ d^{-1}}$. The spatial variability of $ET_0$ across the Karnataka State indicates lower values in the southern, coastal, and hilly regions in comparison to northern regions. This difference is caused probably on account of the topographical effect created by the Western Ghat mountains which are located in the western part of the State.

The primary objective of the present research was to develop a comprehensive methodology for the evaluation of the performances of simpler $ET_0$ equations with and without local calibration of parameters at a large number of climate stations located in Karnataka State, India. To achieve this objective, five simpler popular alternative $ET_0$ equations namely, temperature-based Blaney-Criddle (BC) and Hargreaves (HG), radiation-based FAO-24 Radiation (RAD), Priestly-Taylor (PT) and Turc (TC) equations were tested for their performance against the physically-based combination-based FAO-56 PM method. Initially, the accuracies of monthly $ET_0$ estimates obtained by the five alternative methods for the period of record were assessed relative to PM $ET_0$ estimates using the coefficient of determination ($R^2$), root mean square error (RMSE) and mean bias error (MBE) as performance measures. Overall, results indicate that the original PT equation performed the best among the 4 alternative simpler equations in terms of $R^2$ and RMSE in most of the agroclimatic zones of the study area. However, the equation consistently over-estimated $ET_0$ values relative to the PM equation in several of the zones.

Subsequently, numerical coefficients in the original forms of the alternative equations were treated as unknown parameters and optimized for each station using PM $ET_0$ estimates as a reference. Results from local calibration of the five alternative $ET_0$

methods indicated significant improvement in their prediction accuracies. Mean values of model parameters for different agro-climatic zones in the study area and also maps showing spatial variability of the parameters were developed for the benefit of practitioners who wish to obtain estimates of $ET_0$ comparable to the PM method using limited climate data. However, replacing the $T_{mean}$ term (with equal weightage for $T_{max}$ and $T_{min}$) with an alternative $T_{eff}$ with variable weightages for these variables did not lead to any substantial improvement in the accuracy of $ET_0$ estimates by the alternative equations.

Furthermore, to provide $ET_0$ estimates at large spatial scales in the State the study developed a gridded daily PM $ET_0$ product for a period of 2006-2016 at 0.25°×0.25° resolution using spatial interpolation techniques. Three interpolation techniques namely, inverse distance weightage (IDW), Kriging and P-BSHADE were chosen as possible candidates. Prior to application, the three spatial interpolation methods were evaluated for their prediction accuracies using a limited sample of climate stations. Accordingly, the conceptually and computationally simpler IDW method was selected since the prediction accuracies were more or less the same for all the methods. Using daily PM $ET_0$ estimates obtained at the 67 climate stations for the period 1st January 2006 to 31st December 2016, the IDW method was implemented to derive daily $ET_0$ estimates at the 260 grid points. The accuracy of the gridded data product developed in this study was compared with three other global $ET_0$ data products available in the public domain. Results indicated that the gridded product developed in this study provided the most accurate estimates of $ET_0$ in all the agroclimatic zones of Karnataka State. Web links for the gridded data product have been created in an effort to share the data on $ET_0$ which is a critical input in a variety of studies in earth sciences. It is hoped that researchers and practitioners will benefit from this unique data product.

**Keywords:** Reference crop evapotranspiration, Local-calibration, Modified-method, Spatial-interpolation, Gridded data, Climate variables, Agro-climatic zones

# TABLE OF CONTENTS

## LIST OF FIGURES

# LIST OF TABLES

# CHAPTER 1

# INTRODUCTION

## 1.1 GENERAL

Water scarcity and the detrimental impacts of climate change on freshwater resources are considered to be major environmental problems confronting humanity in the 21st century. Anthropogenic activities of an ever-increasing human population are causing significant changes in climatic regimes and the spatiotemporal dynamics of the hydrological cycle. In these circumstances, available water resources must be utilized most efficiently across all sectors. Globally agriculture accounts for 70% of global freshwater withdrawals and up to 90% in some fast-growing economies. Crop yields from irrigated agriculture are 2.7 times more than that of rainfed farming (UN WWDR 2012). However, depleting freshwater resources and increasing water demands from other sectors are leading to less water being available for agriculture. Hence there is a need to design more efficient irrigation systems which provide maximum agricultural output with minimum water input. To achieve this, crop water requirements (CWR) and irrigation water requirements (IWR) need to be accurately assessed for different crops taking into consideration prevailing climatic conditions. A key variable in procedures for estimation of CWR and IWR is potential evapotranspiration, nowadays more precisely defined as “Reference Crop Evapotranspiration.”

## 1.2 REFERENCE CROP EVAPOTRANSPIRATION

Evapotranspiration can be defined as the combination of two separate processes whereby water is lost on the one hand from the soil surface by evaporation and on the other hand from the crop by transpiration (Allen et al. 1998). Nearly 75% of the total annual precipitation on land surfaces is returned to the atmosphere by evaporation and transpiration (Singh 1989). This phenomenon is often ignored component of the hydrologic cycle, unlike other components which can be physically visualized. Nonetheless, this invisible flux of water vapour is persistent in its ability to remove water from the soil and in many cases leads to a devastating situation of drought.

The rate at which water is removed by evapotranspiration from a cropped surface is influenced by several factors. These factors can be broadly classified into weather parameters, crop characteristics, management/environmental factors and available soil moisture levels. The weather parameters include radiation, air temperature, humidity and wind speed. Crop characteristics that affect evapotranspiration are crop type, variety, and development stage. Soil salinity, water content, plant density, and land fertility are the environmental factors that influence evapotranspiration. Management factors that affect evapotranspiration include cultivation method, fertilizer application, and type of irrigation. The availability of sufficient soil moisture in the crop root zone is vital for the process of evapotranspiration to be sustained. When moisture levels reduce below field capacity, the rate of evapotranspiration also reduces rapidly and becomes negligible at the permanent wilting point. The objective of irrigation is to ensure sufficient soil moisture availability so that evapotranspiration is maximum thereby resulting in maximum crop yield.

Given the complexity of the evapotranspiration phenomenon, the concept of 'potential' evapotranspiration (PET) was introduced by Thornthwaite and Penman in 1948 considering a hypothetical green alfalfa crop with unlimited soil moisture supply, in which case the rate of evapotranspiration is purely a function of prevailing climatic conditions. The concept of PET was improved upon by Jensen et al. (1970) who defined it as "the upper limit or maximum evapotranspiration that occurs under given climatic conditions from a field having a well-watered agricultural crop with an aerodynamically rough surface such as alfalfa with 12 in. to 18 in. of top growth". By considering the physically-based PM evapotranspiration model, Allen et al. (1998) presented a more precise and unambiguous concept of potential evapotranspiration through the definition of "reference crop evapotranspiration ($ET_0$)."$ET_0$ is the rate of water loss due to evapotranspiration from a hypothetical green grass crop of 0.12 m in height, with a surface resistance of 70 $\mathrm{s\ m^{-1}}$, an albedo of 0.23 and not short of water supply. Figure 1.1 provides a schematic representation of the concept underlying the definition of $ET_0$. Again, it is to be noted that $ET_0$ is a function of only the prevailing climate. The report of Allen et al. (1998), more popularly known as the FAO-56 report, provides complete details of how as a first step $ET_0$ may be computed from ground-based climate records and in subsequent steps CWR and IWR may be estimated by taking into account factors related to vegetation, management/environmental and adequate rainfall.

Several existing $ET_0$ models are derived for arid, semi-arid humid environments with most of the comparisons of models in the United States (Allen 1996; Blaney-Criddle 1962; Jensen et al. 1997). Therefore, it can be seen that studies suggest incorporating local conditions into these models before application (McMahon et al. 2013; Mohan 1991; Nandagiri and Kovoor 2006; Xu and Singh 2002). Globally studies have found the performance of the calibrated models has significantly improved estimations than the uncalibrated models (Pandey et al. 2014; Tabari and Talaee 2011; Trajkovic 2007). Also, practically due to the varying geographies and local conditions it is important that the $ET_0$ models be calibrated before application. In the past several research have been carried out in calibrating $ET_0$ methods to local conditions and found that FAO-56 PM is a superior alternative in yielding accurate $ET_0$ estimations against measured $ET_0$ across varied environments (Bormann 2011; Garcia et al. 2004; Itenfisu et al. 2003; Jhajharia et al. 2012; Masanta and Srinivas 2021; McKenney and Rosenberg 1993; McVicar et al. 2007; Mohan 1991; Verma et al. 2008; Xu and Singh 2002; Zhang et al 2007). Therefore, several researchers have calibrated simpler alternative methods taking PM $ET_0$ as a standard method. Since the PM $ET_0$ requires 5-6 climatic input variables simpler approaches with 1-2 variables remain a popular approach however these equations require local calibration to yield better estimates. Therefore, the present study is driven by the idea of developing a methodology for the entire Karnataka state to estimate accurate $ET_0$ estimates with the minimum number of inputs.

## 1.3 SPECTRUM OF EVAPOTRANSPIRATION MODELS

The dynamics and thermodynamics of the atmosphere are fundamentally influenced by exchanges of momentum, heat, and moisture between the atmosphere and the earth's surface. Over the years there has been a profound understanding of these physiological aspects that govern these processes. The evapotranspiration process

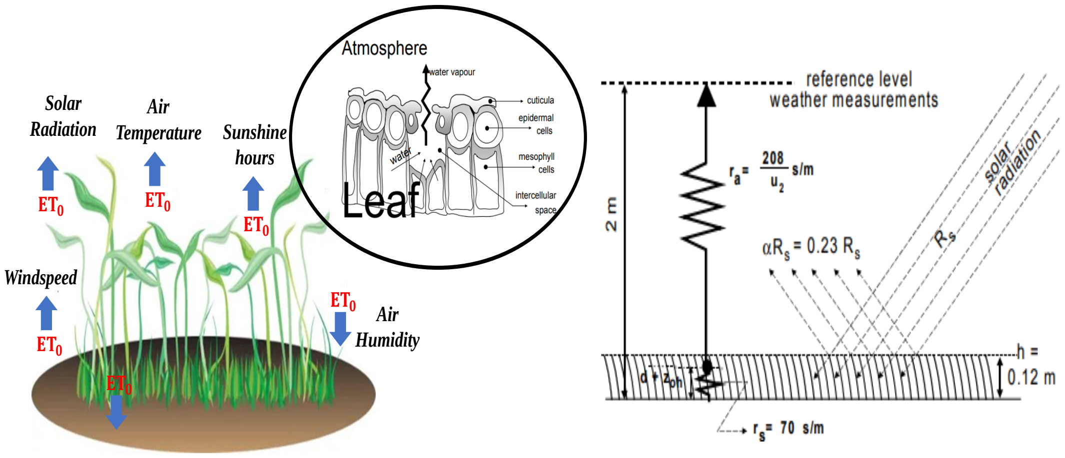


**Figure 1.1: Schematic representation of the concept of reference crop evapotranspiration (Source: FAO-56, Allen et al. 1998)**

involves two processes evaporation and transpiration occurring simultaneously and there is no easy way to distinguish the two (Allen et al. 1998; Schmugge and Andre 1998). This complexity in the process is a daunting task for any researcher, furthermore, various factors like radiation, wind, humidity, and wind speed alter the process thus there is a need for a multidisciplinary approach to precisely quantify the process. The scientific quantification of evaporation and evapotranspiration can be made by direct field measurements and indirect approaches by numerical modelling by energy balance equations and meteorological methods (McMahon et al. 2013; Mohan 1991; Xu and Singh 2002). The history of evaporation theory development can be traced to Dalton's gas law in 1802 which gave meteorologists a concept of water vapour pressure difference which substantially redefined the understanding of evaporation. Jensen (2010) gives historical knowledge of this equation where they largely were remote and remained in the United Kingdom (UK), and the United States of America (USA). The earlier investigations considered air temperature and second wind speed as the only variables causing ET later with technological developments in field measurements many comprehensive models of evapotranspiration recognized solar radiation to be the primary factor for causing ET. Later, incorporating meteorological parameters Thornthwaite 1948 coined PET, and defined it as the evapotranspiration from large vegetation covering the surface with adequate moisture at all times, this study also differentiated global climate based upon PET moisture indices. Penman in 1948 combined the aerodynamic approach and energy equations and presented a new physics-based theoretical complex equation of evaporation rates for open water, bare soil, and green grass from standard meteorological data (Chattopadhyay and Hulme 1997; George 2012; McMahon et al. 2013) advanced modern combination form of this equation with standard reference is referred as Penman-Monteith equation. During the 1950-the 60s, temperature and radiation-based equations were given by Blaney-Criddle popularly known as an FAO-24 method (Doorenbos and Pruitt 1977; Frevert et al. 1983). Further, the United Nations (UN) Food and Agriculture Organization (FAO) has proposed standardized procedures for the calculation of $ET_0$ using ground-based climatological measurements (Allen et al. 1998; Doorenbos and Pruitt 1977; Jensen et al. 1970) which perhaps is widely accepted as a sole method for $ET_0$ calculations. The present study utilizes these equations in determining the $ET_0$ prominently.

In these aspects, evapotranspiration has received considerable attention but the diversity of techniques makes it difficult to model the process, the situation is furthermore complicated as there exists confusion among researchers related to hypothetical evaporation rates: potential evaporation, potential evapotranspiration, and reference evapotranspiration adding to this problem is the data-intensive format for these equations. With the advent of satellites determination of the consumptive use of plants has been transformed from just site-based measuring systems to remote sensing. Large-scale crop inventory and yield prediction studies are aiding precision farming. Developments in this field are largely driven by the Surface Energy Balance approach, these fluxes are measured through the measurement of latent heat flux in several models like Surface Energy Balance System (SEBS), Surface Energy Balance Algorithm for Land (SEBAL), and Mapping Evapotranspiration at high Resolution with Internalized Calibration (METRIC) (Allen et al. 2007) are developing with help of satellites like LANDSAT, MODIS and ECOSTRESS are enhancing the imagery to near-surface measurements (Fisher 2020; Karthikeyan et al. 2020; Khan et al. 2020; Schmugge and Andre 1998). Though there is wide scope for research in the application of these investigations in ET mapping, they are not under the umbrella of the present study. The present study investigates the computational methodology of reference crop evapotranspiration from a ground-based weather station with an inadequate climatic data approach.

## 1.4 CONSTRUCTION OF SPATIAL $ET_0$ DATA

As explained in earlier paragraphs the estimates of evapotranspiration are an important factor in determining the CWR/IWR and it's also a primary input to many hydrological models. Since $ET_0$ estimates are primarily dependent on the ground-based climate network for data input however owing to multiple factors the availability of ground-based $ET_0$ is sparse. This problem is critical in developing nations such as India where there is a low density of climatic stations. As per the India Meteorological Department (IMD), the total number of agrometeorological observatories in India is around 224 and only 3 evapotranspiration stations (https://www.imdagrimet.gov.in/). Similarly in the Karnataka State, a total of 36 surface observatories only 3 stations provide evapotranspiration with a limited temporal scale. Owing to the limited availability of limited climate stations studies rely on available gridded $ET_0$ products and ancillary products (weather inputs) to derive $ET_0$ estimates. However, these products especially the ancillary products are global products largely derived through reanalysis (Globalweather 2018) therefore these are to be evaluated before use. Under the aegis of the National Hydrology Project, several data products have been made available to the public but only actual evapotranspiration data is available at a shorter temporal scale derived from the satellite products (NRSC 2021). Also, reference crop evapotranspiration data and historical data are not available. In Karnataka at a regional scale, there has been no such gridded $ET_0$ product. One of the long-term plans of the Indian Meteorological Society Vision 2030 is to promote the use of local data and IMD advisories for farm-level operations (IMS Vision 2030). Therefore, the development of gridded products will benefit large interdisciplinary applications related to $ET_0$.

Accordingly, a number of studies in India have been carried out to quantify the spatiotemporal dynamics of rainfall and temperature to enable the creation of global and regional spatial datasets (Pai et al. 2014; Rajeevan and Bhate 2014; Srivastava 2009) for the application of distributed hydrological/agricultural/climate models. However, similar efforts have been lacking in characterizing spatio-temporal variabilities of $ET_0$ with the intention of creating gridded datasets as an aid to modellers (Srivastava et al. 2009). The need for such studies gets amplified since the density of climate stations is significantly lower than rain gauge stations in most countries of the world. In data scare situations, the modeller is left with no other option than to 1) use areal average $ET_0$ values as input or 2) use approximate, less data-intensive $ET_0$ estimation procedures. Several worldwide studies have shown that the use of such simpler options can reduce the accuracy of hydrological model output (e.g., Bai et al 2016; Remesan and Holman 2015; Zhao et al. 2013). Therefore, there is a need to develop a methodology for creating gridded datasets of $ET_0$ at temporal and spatial scales appropriate for more accurate application of hydrological, agricultural and climate models.

Although attempts have been made to study the evapotranspiration dataset, however, the development of spatial datasets of $ET_0$ is rendered difficult and requires answers to the following important research issues:

1. $ET_0$ represents a complex process that is influenced by a large number of highly variable climatic characteristics which in turn may be inter-correlated and also vary with terrain features such as elevation, aspect, and slope

2. Accurate estimation of $ET_0$ using the best model may not be feasible due to the non-availability of data pertaining to all the influencing climate variables. Therefore, the choice of an estimation model is many times limited by the nature of the available dataset and a need may arise for local calibration to improve accuracies

3. Also, when simple methods are used, the error introduced in $ET_0$ estimates needs to be assessed against an established standard

4. Implementation of interpolation algorithms to estimate $ET_0$ at unsampled locations which is a necessary step in creating gridded data is complicated due

to a large number of influencing climate variables and also the sparse nature of available data networks. Therefore, the interpolation algorithm to be adopted needs to be rigorously tested before use.

## 1.5 MAJOR RESEARCH ISSUES CONCERNING REFERENCE CROP EVAPOTRANSPIRATION

For the present research, a review of the literature highlighted a few major issues which require further study and analysis. These issues are presented in the following discussion and a review of relevant literature and study objectives are presented in subsequent sections.

**Issue No. 1:**

Indian studies focus on mapping temporal and spatial variabilities of $ET_0$ over large areas such as State are limited in number. Understanding the variations of $ET_0$ over a state will benefit the preparation of water resources development plans and also in the planning and design of irrigation schemes. No such studies seem to have been taken up for Karnataka State, India.

**Issue No. 2:**

$ET_0$ is subject to significant variations with respect to time. This is on account of temporal variations in the climatic variables involved in the computation of $ET_0$. Especially because of global climate changes which are prevalent in recent times, there is an urgent need to characterize the magnitude and direction of long-term trends in climatic variables such as temperature, humidity, radiation, and wind speed in Karnataka. At the same time trends in $ET_0$ values also need to be assessed and explanations for changes in patterns of $ET_0$ need to be linked to trends in climatic variables.

**Issue No. 3:**

Upon examination of the climatic inputs for each $ET_0$ method and the equations associated with each of the methods, it is apparent that the climatic variables do not appear directly in them. This means that several other supporting equations need to be used to convert input climate variables into variables that appear in the $ET_0$ equations. However, for some of the variables which appear in the $ET_0$ equations, several alternative supporting equations have been proposed in the literature, which may lead to differences in final results. Also, alternative supporting equations have been developed for use when measured data on one or more of the climate variables are not available. Again, the use of such simpler equations may lead to significantly large differences in $ET_0$ estimates.

**Issue No. 4:**

Most of the methods proposed for the estimation of $ET_0$ are either empirical or semi-empirical with the sole exception of the FAO-56 PM method which has a more physical basis. Therefore, Allen et al. (1998) recommend the use of this method in preference to other methods. However, a major limitation in the widespread use of the FAO-56 PM method is that it requires input data pertaining to a large number of climatic variables which may not be available at all climate stations. Therefore, a large number of studies have been undertaken to evaluate the performances of the simpler methods relative to the FAO-56 PM approach. A major finding of such comparative analyses has been that the climate of the region plays an important role in deciding which of the alternative methods provides $ET_0$ estimates comparable to the FAO-56 PM method. Also, it has been noted that the performance of the simpler equations can be significantly improved by adopting local calibration.

## 1.6 OBJECTIVES OF THE PRESENT STUDY

1. Assess spatiotemporal variabilities in historical records of climatic variables associated with the computation of Penman-Monteith (PM) Reference Crop Evapotranspiration ($ET_0$) at climate stations located in Karnataka State.

2. To compute PM $ET_0$ using ground-based climate data and assess spatiotemporal variabilities across Karnataka State

3. To evaluate the relative performances of simpler $ET_0$ methods in comparison to the PM $ET_0$ model with and without local calibration.

4. To develop appropriate methods for accurate spatial interpolation of $ET_0$ and develop gridded datasets of $ET_0$ for Karnataka State.

## 1.7 SCOPE OF THE PRESENT STUDY

The main focus of the present study will be to characterize temporal and spatial variabilities of reference crop evapotranspiration across Karnataka State, India. Historical records of climatic variables for stations located in the State will be used in the present study. As part of the study, climatic variables involved in $ET_0$ computation using the FAO-56 Penman-Monteith model will be assessed and linked to corresponding trends in $ET_0$ values. Also, alternative methods such as temperature-based and radiation-based methods for $ET_0$ estimation during the non-availability of all climatic variables will be evaluated. Also, the study will focus on the evaluation of alternative methods of computing variables in data scare situations and the ability of local calibration to improve $ET_0$ estimates.

## 1.8 OVERVIEW OF RESEARCH METHODOLOGY ADOPTED

Figure 1.2 gives an overview of the overall methodology adopted in this research work. Firstly, the obtained dataset is checked for quality any erroneous data was removed. After processing the data, six different $ET_0$ algorithms were used to calculate $ET_0$ at 67 stations from 2006 to 2016. Later the $ET_0$ results are analyzed and the performance of the simpler five different $ET_0$ methods was tested against the benchmark FAO-56 PM method. Further $ET_0$ equations are locally calibrated to obtain local parameters. Finally, different interpolation techniques are used to generate gridded $ET_0$ at the point scale.

## 1.9 ORGANIZATION OF THESIS

A brief explanation of the chapter-wise description of the thesis is presented here. *Chapter 1* gives an introduction to the scope and main objectives of the present work. *Chapter 2* provides details of the study area and hydro-meteorological dataset used in the study. *Chapter 3* describes the FAO-56 PM method and results of the PM method along with the spatio-temporal assessment of climatic variables associated with PM $ET_0$ methods. *Chapter 4* presents the methodology and results of the performance of the Hargreaves $ET_0$ equation with and without calibration. Additionally, the effect of replacing the mean temperature with an effective temperature on the performance

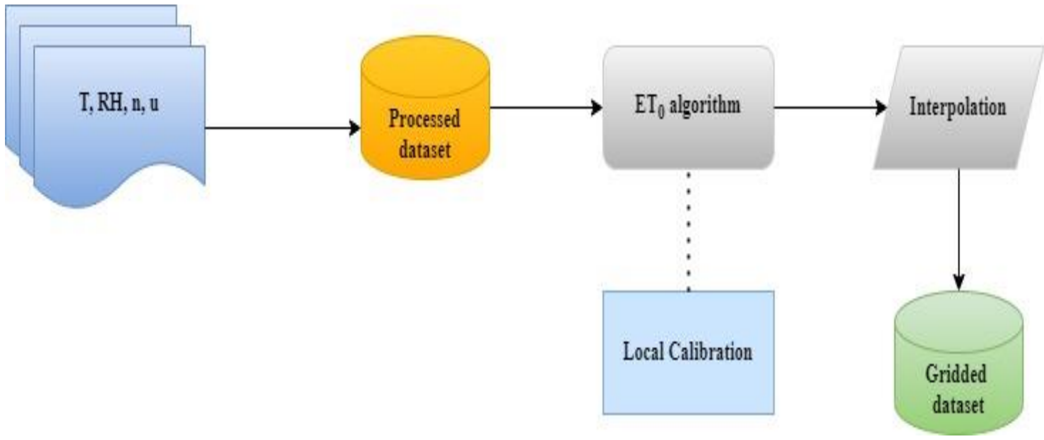


**Figure 1.2: Overview of the methodology adopted**

of the Hargreaves equation is also assessed. *Chapter 5* elucidates the methodology adopted involved in calibrating simpler $ET_0$ equations along with the performance of simpler $ET_0$ equations. *Chapter 6* presents the overall performance of simpler equations with and without calibration. Also, the mean parameters and spatio-temporal maps across agro-climatic zones are provided which can be used when using models in Karnataka State. *Chapter 7* elucidates the methodology adopted in the development of gridded $ET_0$ development. This chapter provides a comprehensive analysis of different spatial interpolation techniques. Also, this chapter provides a framework for accessing the developed dataset. *Chapter 8* gives an overview of the conclusions from this research work and suggests avenues for future research.

For the sake of clarity and readability, a review of relevant literature is not provided as a separate chapter, instead pertinent literature is reviewed in each chapter of the thesis.

## CHAPTER 2

## STUDY AREA AND DATA

### 2.1 DESCRIPTION OF THE STUDY AREA

The study area under consideration is Karnataka State located in the southern part of India. The geographical area of the State is 19.1 Mha and is situated between 11°40′ and 18°27′ North latitudes and 74°5′ and 78°33′ East longitudes and accounts for 5.8% of India's total geographical area. The state is surrounded by a chain of mountains in the west called the Western Ghats and in the south-east by the Eastern Ghats. There exists a large diversity in geographic and physiographic conditions in the State which is responsible for the climatic differentiation from arid to semi-arid in the plateau region, sub-humid to humid tropical in the Western Ghats mountains, and humid tropical monsoon type in the west coast plains (Initiative – Karnataka B. C. C. 2011). For meteorological purposes, the State has been divided into three sub-divisions; Coastal Karnataka, North Interior Karnataka, and South interior Karnataka. As per Koppen's classification, the State has three climatic types; tropical monsoon, hot seasonally dry tropical savanna climate and hot semi-arid, tropical steppe type while Thornthwaite's classification is based upon soil moisture indices yields per-humid, semi-arid, moist sub-humid, dry-humid zone, arid zone and humid zones.

The south-west monsoon is the primary source of rainfall during this period the state receives a copious amount of 74% annual rainfall (Guhathakurta et al. 2020). Typically, the rainy season extends for four months (June-September) with maximum rainfall occurring on the windward side of the mountainous chain of Western Ghats with an annual average of 3350 mm. Contrasting to this the leeward side receives as low as 600-700 mm. Apart from this 12 % of rainfall is received during the north-east monsoon season (October-December) and 7% during the summer season. The average annual rainfall is about 530-1319 mm for the entire state.

## 2.2 DATA SOURCES

### 2.2.1 Hydro-meteorological (HM) data

The study relies on a consistent and concurrent climatic dataset drawn from a network of over 89 hydro-meteorological stations maintained by the Water Resources Development Organization (WRDO), Government of Karnataka. The stations are equipped with standard ground-based instruments; alcohol and wet-bulb thermometers, sunshine recorder, cup anemometer, and mercury thermometers. Readings are taken twice a day at 0830 and 1730 hours. For each station, the data set used comprised daily values of maximum air temperature ($T_{max}$) (°C), minimum air temperature ($T_{min}$) (°C), maximum relative humidity ($RH_{max}$) (%), minimum relative humidity ($RH_{min}$) (%), actual hours of sunshine (n) (hour) and 24 h windspeed (u) ($T_{max}$). Though the agency performs quality checks before supplying to users of dataset, missing entries that existed were identified and erroneous data were eliminated manually. After quality checks and eliminating outliers from the raw dataset, records pertaining to the variables listed above for a total of 67 stations for the period 2006-2016 ($N_d$=4018 days) were available for analysis. The obtained dataset was structured to the required format for implementing the six $ET_0$ estimation methods. Since data requirement was highest for the PM method, a master dataset comprising relevant climate variables was prepared. The algorithms for the other less data-intensive $ET_0$ methods derived relevant inputs from this master dataset. The overall procedure of climate data pre-processing and master dataset creation is shown in Figure 2.1.

### 2.2.2 CFSR data

The Climate Forecast System Reanalysis (CFSR) weather data the Texas A&M University spatial sciences website,(Globalweather 2018) was obtained for a bounding box of Karnataka State. This is a global high-resolution ( 38 km resolution) reanalysis data available on a daily scale for a time period of 1979 to 2014. The dataset consists of five variables precipitation (mm), maximum and minimum temperature (°C), relative humidity (%), windspeed ($\mathrm{m\ s^{-1}}$), and solar radiation ($\mathrm{MJm^{-2}day^{-1}}$).

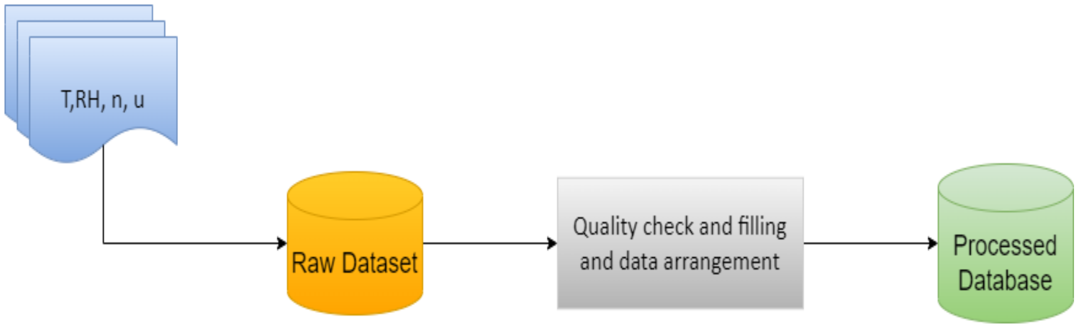


**Figure 2.1: Components of data processing**

### 2.2.3 Agro-climatic zones

Taking into consideration the rainfall pattern quantum and distribution, soil types, texture, depth and physiochemical properties, elevation and topography major crops and type of vegetation the Karnataka state is divided into 10 agro-climatic zones (Ramachandra et al. 2004; KSDA, Government of Karnataka 2018). The map of the study area with the agro-climatic zones is shown in Figure 2.2(a) and Table 2.2. The ten agro-climatic zones are Central Dry (CD), Coastal (CO), Eastern Dry (ED), Hilly (HL), North Eastern Dry (NED), North Eastern Transition (NET), Northern Dry (ND), Northern Transition (NT), Southern Dry (SD) and Southern Transition (ST). The zone-wise classification helps in better evaluation and understanding of climatic variability at a regional scale and was, therefore, adopted in the present study.

### 2.2.4 Climatic dataset used

The climatic dataset was obtained from hydro-meteorological stations (HM) observatories operated and maintained by the Water Resources Development Organization (WRDO), Government of Karnataka State, India. From a network of over 89 HM stations, data from 67 stations for the period 2006-2016 was chosen for the present study (Figure 2.2(a)). The list of selected climate stations located in the 10 agro-climatic zones along with their locational details is provided in Table 2.2. The dataset consisted of daily values of six climatic variables, namely maximum air temperature ($T_{max}$), minimum air temperature ($T_{min}$), maximum relative humidity ($RH_{max}$), minimum relative humidity ($RH_{min}$), actual hours of sunshine (n) and wind speed (u). Despite quality checks by WRDO, data gaps existed at each station for varying percentages of time in the historical period considered (Figure 2.2(b)). These were filled in from the nearest neighbour for short periods (1–5 days). For longer periods of missing data, the corresponding values from the nearest grid point (Figure 2.2(b)) of the Climate Forecast System Reanalysis (CFSR) were used (Fuka 2013, Dile and Srinivasan 2012, Saha 2012, ). Finally, for each of the selected 67 stations, a dataset comprising six climatic variables for 11 years (2006-2016) was prepared for $ET_0$ analysis. Daily values of the climate variables were converted into monthly mean daily values and a total of 132 months were considered in the analysis.

**Table 2.1: Various climatic input variables required for each of the $ET_0$ estimation methods considered in this study.**

| Method | Input Data Requirements | | |
|---|---|---|---|
| | Site | Climate | |
| | | Primary | Secondary |
| FAO-56 Penman-Monteith | $z$ , $z_w$ , $\varphi$ | $T_{max}$, $T_{min}$, $RH_{max}$, $RH_{min}$, $u_z$, n | |
| FAO-24 Blaney-Criddle | $z_w$ , $\varphi$ | $T_{max}$ , $T_{min}$ | $RH_{min}$ , $u_z$ , $u_r$ , n |
| FAO-24 Radiation | $z$ , $z_w$ , $\varphi$ | $T_{max}$ , $T_{min}$, n | $RH_{max}$ , $RH_{min}$ , $u_z$ , $u_r$ |
| Priestley-Taylor | $z$ , $\varphi$ | $T_{max}$ , $T_{min}$ , n | |
| Turc | $\varphi$ | $T_{max}$ , $T_{min}$ , $RH_{max}$, $RH_{min}$ , n | |
| FAO-56 Hargreaves | $\varphi$ | $T_{max}$ , $T_{min}$ , n | |

where z is the elevation of the site above mean sea level (m), $z_w$ is the height of wind measurement (m), $\varphi$ is the latitude of the place (radians), $u_z$ is the wind speed measured at any other height ($z_w$), $u_r$ is the ratio of day to night time windspeed.

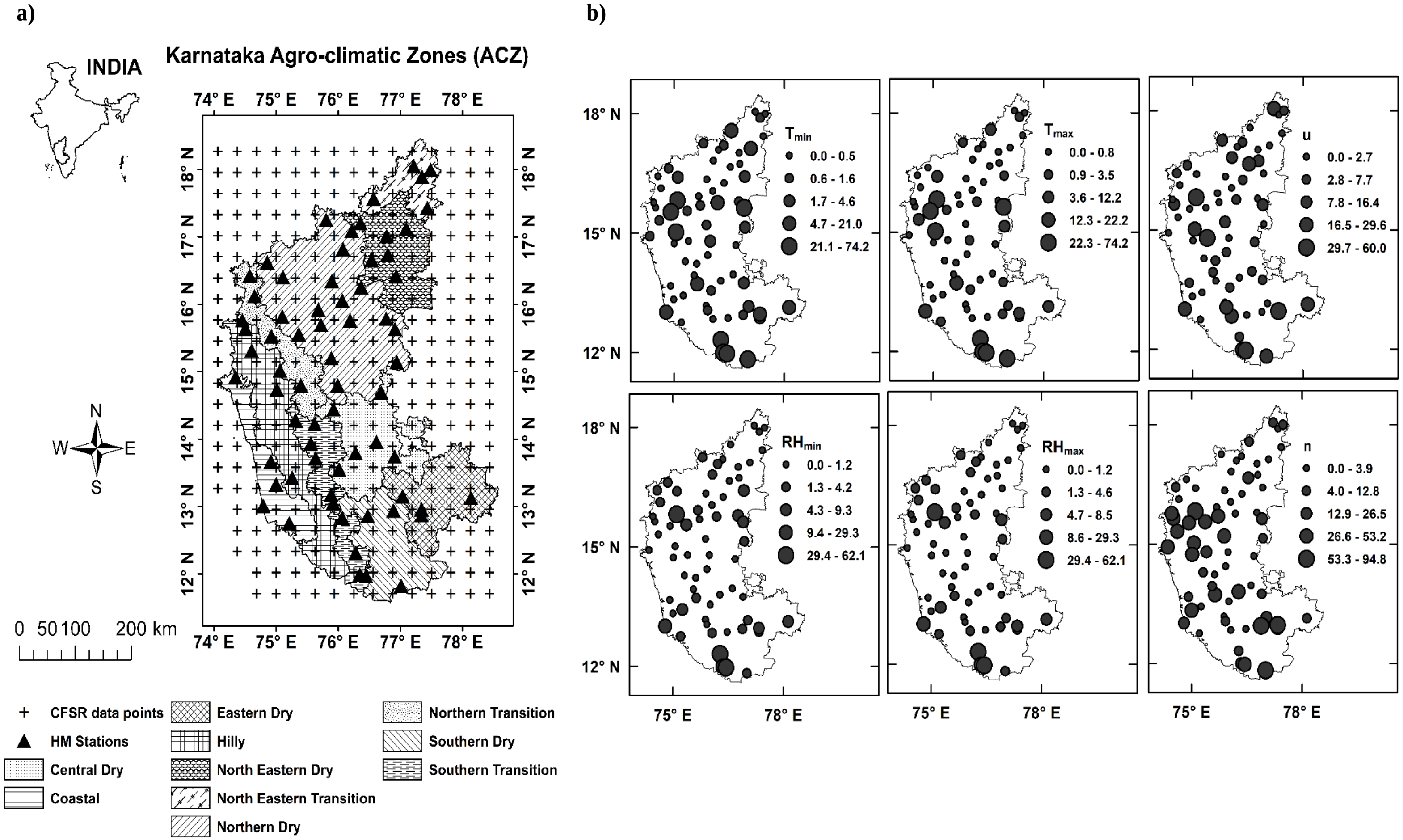


**Figure 2.2: (a) Map of the study area, climatic stations, CFSR grid points (b) Climate dataset availability (in percentage): 0 means no missing and upto N%**

**Table 2.2: Location details of selected climate stations in different agro-climatic zones**

| Zone | Zone ID | Station | Station ID | Altitude (m) | Latitude (N) | Longitude (E) |
|---|---|---|---|---|---|---|
| Central Dry | CD | Davangere | CD1 | 606 | 14° 26′ | 75° 55′ |
| | | Hiriyur | CD2 | 616 | 13° 57′ | 76° 36′ |
| | | Hosadurga | CD3 | 735 | 13° 47′ | 76° 16′ |
| | | Kadur | CD4 | 775 | 13° 33′ | 76° 00′ |
| | | Rayapura | CD5 | 590 | 14° 41′ | 76° 41′ |
| | | Sira | CD6 | 654 | 13° 44′ | 76° 54′ |
| Coastal | CO | Ajekar | CO1 | 66 | 13° 19′ | 74° 59′ |
| | | Hosangadi | CO2 | 69 | 13° 40′ | 74° 54′ |
| | | Kadra | CO3 | 24 | 14° 55′ | 74° 20′ |
| | | Puttur | CO4 | 118 | 12° 45′ | 75° 12′ |
| | | Surathkal | CO5 | 26 | 13° 00′ | 74° 47′ |
| Eastern Dry | ED | Hebbur | ED1 | 811 | 13° 09′ | 77° 02′ |
| | | Kolar | ED2 | 839 | 13° 07′ | 78° 07′ |
| | | Manchanbele | ED3 | 726 | 12° 52′ | 77° 20′ |
| | | Thippagondanahalli | ED4 | 762 | 12° 57′ | 77° 20′ |
| Hilly | HL | Bachanaki | HL1 | 573 | 15° 01′ | 75° 03′ |
| | | Barchi | HL2 | 477 | 15° 18′ | 74° 36′ |
| | | Dharma | HL3 | 596 | 14° 44′ | 75° 00′ |
| | | Khanapur | HL4 | 680 | 15° 38′ | 74° 30′ |
| | | Sringeri | HL5 | 672 | 13° 25′ | 75° 15′ |
| North Eastern Dry | NED | Afzalpur | NED1 | 423 | 17° 12′ | 76° 21′ |
| | | Bheemarayanagudi | NED2 | 451 | 16° 44′ | 76° 47′ |
| | | Chittapur | NED3 | 425 | 17° 07′ | 77° 05′ |
| | | Deodurga | NED4 | 398 | 16° 24′ | 76° 55′ |
| | | Jewargi | NED5 | 413 | 17° 00′ | 76° 46′ |
| | | Kembhavi | NED6 | 496 | 16° 39′ | 76° 32′ |
| | | Narayanpur | NED7 | 477 | 16° 15′ | 76° 21′ |
| North Eastern Transtion | NET | Aland | NET1 | 514 | 17° 34′ | 76° 33′ |
| | | Bhalki | NET2 | 593 | 18° 02′ | 77° 12′ |
| | | Chincholi | NET3 | 454 | 17° 25′ | 77° 25′ |
| | | Halhalli | NET4 | 633 | 17° 53′ | 77° 20′ |
| | | Janwada | NET5 | 557 | 17° 59′ | 77° 28′ |
| Northern Dry | ND | Almatti | ND1 | 548 | 16° 20′ | 75° 53′ |
| | | Almel | ND2 | 449 | 17° 05′ | 76° 13′ |
| | | Badami | ND3 | 566 | 15° 55′ | 75° 40′ |
| | | Bellary | ND4 | 453 | 15° 08′ | 76° 56′ |
| | | Devara Hipparagi | ND5 | 539 | 16° 49′ | 76° 04′ |
| | | Harapanahalli | ND6 | 632 | 14° 47′ | 75° 59′ |
| | | Hungund | ND7 | 535 | 16° 03′ | 76° 03′ |
| | | Kudachi | ND8 | 553 | 16° 37′ | 74° 51′ |
| | | Kushtagi | ND9 | 639 | 15° 45′ | 76° 11′ |
| | | Mahalingpur | ND10 | 584 | 16° 24′ | 75° 06′ |
| | | Mundargi | ND11 | 530 | 15° 12′ | 75° 53′ |
| | | Navalgund | ND12 | 581 | 15° 33′ | 75° 21′ |
| | | Navilutheerta | ND13 | 657 | 15° 49′ | 75° 05′ |

| | | | | | | |
|---|---|---|---|---|---|---|
| | | Ron | ND14 | 579 | 15° 41′ | 75° 43′ |
| | | Sindhanur | ND15 | 397 | 15° 47′ | 76° 46′ |
| | | Siruguppa | ND16 | 381 | 15° 37′ | 76° 54′ |
| | | Zalki | ND17 | 479 | 17° 15′ | 75° 48′ |
| Northern Transition | NT | Chikkodi | NT1 | 644 | 16° 25′ | 74° 34′ |
| | | Haveri | NT2 | 583 | 14° 47′ | 75° 23′ |
| | | Hidkal Dam | NT3 | 676 | 16° 07′ | 74° 39′ |
| | | Santibastwad | NT4 | 764 | 15° 45′ | 74° 27′ |
| | | Walmi | NT5 | 699 | 15° 31′ | 74° 55′ |
| Southern Dry | SD | Gorur | SD1 | 901 | 12° 50′ | 76° 03′ |
| | | Marconahalli | SD2 | 737 | 12° 56′ | 76° 53′ |
| | | Shravanabelgola | SD3 | 871 | 12° 51′ | 76° 28′ |
| | | Suvarnavathi | SD4 | 764 | 11° 49′ | 77° 00′ |
| Southern Transition | ST | BR Project | ST1 | 639 | 13° 43′ | 75° 38′ |
| | | Belur | ST2 | 994 | 13° 10′ | 75° 52′ |
| | | Channahally | ST3 | 985 | 13° 03′ | 75° 55′ |
| | | Honnali | ST4 | 585 | 14° 13′ | 75° 37′ |
| | | Hunsur | ST5 | 801 | 12° 18′ | 76° 16′ |
| | | Kabini | ST6 | 710 | 11° 59′ | 76° 20′ |
| | | Kutrahalli | ST7 | 603 | 14° 17′ | 75° 18′ |
| | | Nugu | ST8 | 736 | 11° 58′ | 76° 26′ |
| | | Shimoga | ST9 | 606 | 13° 56′ | 75° 33′ |

# CHAPTER 3

# SPATIO-TEMPORAL VARIABILITIES OF CLIMATE VARIABLES AND PENMAN-MONTEITH $ET_0$

## 3.1 GENERAL

Numerous studies have indicated the reliance of $ET_0$ methods on ground-based climate data and its influence on the applicability. Several studies have evaluated the performance of different $ET_0$ equations of different $ET_0$ methods across various climatic regimes and have indicated the superiority of combination-type $ET_0$ equations. In particular, several worldwide studies have shown the $ET_0$ estimates of FAO-56 Penman-Monteith (PM) are accurate across different climatic regimes (Awal et al. 2020; Kovoor 2005; McKenney and Rosenberg 1993; Mohan 1991; Xu and Singh 2002). Therefore, owing to the better and consistence performance in $ET_0$ estimations across different climatic environments the United Nations Food and Agriculture Organization (FAO) Penman-Monteith methodology popularly known as the FAO-56 PM method has been widely accepted as a standard method for $ET_0$ computation. This chapter describes in detail the methodology adopted for PM $ET_0$ calculations and its variability across Karnataka state. Also, the associated climatic variables and their spatio-temporal analysis help to characterize the hydrology and understand long-term variability across varying spaces and times within the study area.

Studies on reference crop evapotranspiration have been carried out by a large number of researchers from various disciplines such as hydrology, agronomy, irrigation, agriculture, soil physics, and climate. Because of this multi-disciplinary focus, a significantly large body of literature exists on various aspects related to this variable. Therefore, the literature review presented herein only focuses on the following aspects: 1) Large-scale and long-term studies of $ET_0$ 2) studies wherein relative performances of various $ET_0$ estimation methods have been evaluated 3) methods adopted by previous researchers to calibrate simpler $ET_0$ according to the local climate.

## 3.2 LARGE AND LONG-TERM $ET_0$ STUDIES

The average annual per capita water availability as per the 2011 census in India is 1545 cubic meters in the country as a whole, which is reducing progressively due to the increasing population. In particular, Jain et al. (2007) estimate India's evapotranspiration to be 69.5%, primarily being an agrarian nation evapotranspiration plays a key role in the hydrologic cycle and has a major influence on crop management and economic development. Accurate estimates of daily CWR/IWR will help farmers with the all-important decisions of when and how much water to apply. The measurement of ET in India is both by direct and indirect measurements. The direct method of measurement has been by lysimeters, pan evaporation method as per India Meteorological Department (IMD) 550 surface weather stations are equipped with complete measuring instruments. As a developing economy, there are difficulties in implementing state of art automatic weather stations. Owing to economic expenditures and time direct measurements are difficult therefore indirect methods of measuring evapotranspiration are preferred (Mall and Gupta 2002).
Largely indirect measurement of evapotranspiration has been either by using water balance models or commonly used methods such as Penman, Blaney Criddle during limited data availability Hargreaves method has been in existence. There have been numerous significant studies on measuring regional potential evapotranspiration in India through PM and BC equations. Sarma et al. (2014) studied the spatial distribution of potential evapotranspiration by the Penman equation across 194 stations in India from 1961 to 1995. The study reports significant decreases, increases, and no trends are noticed in annual PET both in space and time. Annual PET for the country as a whole increased in the latter half of the 20th century. Goyal (2004) studied the sensitivity of evapotranspiration to global warming in the arid zone of Rajasthan and reports ET changes with the change of long-term meteorological variables of 32 years (1971-2002). The important contribution of the study is that it bifurcates the individual effect of meteorological variables on ET. Vicar et al. (2012) reviewed the stilling phenomenon globally across 148 studies reporting terrestrial windspeed trends worldwide and found an average of about -0.014 $\mathrm{m\,s^{-1}}$ for studies with more

than 30 sites observing data for more than 30 years, which confirmed that stilling was widespread. The study confirms the declining rates of $ET_0$; average trends were 3.19 mm. The study identified the reasons for evaporative demand trends occurring from four primary meteorological variables i.e., windspeed, atmospheric humidity, radiation, and air temperature. Also, it reported that 36 studies highlighted the importance of windspeed variability. The significance of sensitivity rates of evaporative demand to changing windspeed was identified with the relative contributions of aerodynamic and radiative changes that were globally observed.

Almorox (2015) assessed 11 representatives temperature-based $ET_0$ methods considering large 4362 climatological stations worldwide and evaluated the applicability of the different $ET_0$ approaches using the Koppen climate classification of the stations. The FAO-56 PM was taken as a benchmark for assessing the $ET_0$ methods. Performance analysis of various methods showed Hargreaves–Samani equation yielded accurate $ET_0$ estimates in arid, semiarid, temperate, cold, and polar climates. Likewise, Thornthwaite and McCloud methods were least successful across climate classes. Results showed the temperature-based methods yielded high errors with a low average correlation against PM in tropical climates. Debnath and Samui (1988) found the normal weekly potential evapotranspiration values of 47 stations situated over different parts of the country varying from 5 mm on the west coast of peninsular India to 24 mm over the northwest part of the country. The peak of weekly oscillation maximum value is around the end of February/ March over the extreme southwest coast of the country, while it is the third week of June over northwest Rajasthan northeast India and small pockets around Rajahmundry of Andhra Pradesh and Bihar. The significant argument the study makes is the existence of a negative correlation between latitude and the seasonal potential water demand of crops at different seasons in each of the groups which are inversely proportional to an increase in latitudinal value. Chattopadhyay and Hulme (1997) observed trends of temperature for 50 years (1940-90) and potential evapotranspiration trends with recent and future climate change for about 27 stations across India were reported. The important finding of the study comes out is both evaporation and evapotranspiration decreased, because of climatological variables such as cloud cover and humidity.

Irmark (2012) conducted a detailed analysis of the association between $ET_0$ and all meteorological variables with an integrated approach of practical and robust procedures to estimate necessary climate variables data to be used in Penman-Monteith equations. The study analyzed the trends and magnitudes of change in meteorological variables for a 116-yr period from 1893 to 2008 in the agriculture-dominated Platte River Basin in central Nebraska, USA. A significant increase in $T_{min}$ and $T_{avg}$ was observed while the windspeed and vapour pressure deficit were found to be insignificant. But the decrease in $ET_0$ is most likely to occur from increasing precipitation that results in a significant reduction in solar and net radiation which reduced $ET_0$. Jaswal et al. (2008) show a significant annual decreasing evaporation from 1971-2000 for 45 well-distributed stations over India. Verma et al. (2008) studied thirty years of meteorological time series data from 1976-2007 for twenty well-distributed locations in India and computed evapotranspiration using the FAO PM method. They found potential evapotranspiration to be lowest at Buralikson (1100 mm) and highest (2109 mm) at Bellary.

Jaswal and Rao (2010) studied annual trends of meteorological parameters temperature, rainfall, relative humidity, and clouds for ten stations in Jammu and Kashmir for the period 1976-2007. Results of trend analysis showed increasing temperature over the state with a significant increase in both maximum and maximum temperature in the Kashmir and Jammu region respectively. Jhajharia et al. (2012) studied trends in $ET_0$ for 8 stations in the humid regions of northeast India and reported in the last 22 years, and found a significant decrease in $ET_0$ at annual and seasonal time scales for 6 sites in northeast India. The decrease in $ET_0$ was due to the net radiation and wind speed. Priya et al. (2015) studied the sensitivity of $ET_0$ to changes in different climatic variables and the effect of temperature change and elevated $CO_2$ on $ET_0$ at Akola. The FAO-56 PM equation was used to estimate $ET_0$ during 1970-2008, the results showed temperature influenced $ET_0$ the most followed by vapour pressure deficit, solar radiation, and windspeed. Gundalia and Dholakia (2017) modelled $ET_0$ based on the most dominant meteorological variables in the Middle South

Saurashtra region of Gujarat (India). This section provided an overall gist of large $ET_0$ assessment specifically to India but there exist very few studies analyzing individual meteorological variables and their variability with $ET_0$, especially cloud cover and sunshine whereby minuscule studies reported these effects.

Bandyopadhyay (2009) presented the temporal trend of $ET_0$ and region-wise spatial variation, for 32 years (1971–2002) for monthly meteorological data across 133 stations evenly distributed over different agroecological regions (AERs) of India. FAO-56 PM was used in determining $ET_0$. The study reported missing solar radiation and sunshine hour data for most of the stations only 29 stations measured either or both. Overall, out of 133 stations considered, a significant falling trend in $ET_0$ was observed at 20 stations and 11 stations did not show any significant trend. Among the 29 stations with measured solar radiation and/or sunshine data, a significant decreasing trend was observed while two stations each showed an increasing and insignificant trend. Hargreaves $ET_0$ was calculated from estimated solar radiation and measured values. Thus, the $ET_0$ estimated by both methods were equally correlated.

## 3.3 FAO-56 PENMAN-MONTEITH REFERENCE CROP EVAPOTRANSPIRATION EQUATION

As per Allen et al. (1998) [hereinafter referred to as FAO-56], the recommended form of the PM equation is:

$$ET_0 = \frac{0.408\Delta(R_n - G) + \gamma\frac{900}{T_{mean} + 273}u_2(e_s - e_a)}{\Delta + \gamma(1 + 0.34u_2)} \tag{3.1}$$

where $ET_0$ is the reference evapotranspiration ($\mathrm{mm\ d^{-1}}$); $R_n$ is the net radiation at the crop surface ($\mathrm{MJm^{-2}day^{-1}}$); G is the soil heat flux density ($\mathrm{MJm^{-2}day^{-1}}$); $\mathrm{T_{mean}}$ is the mean daily air temperature at 2 m height (°C); $\mathrm{u_2}$ is the wind speed at 2m height ($\mathrm{m\ s^{-1}}$); $\mathrm{e_s}$ is the saturation vapour pressure (kPa); $\mathrm{e_a}$ is the actual vapour pressure (kPa); $\mathrm{e_s}$-$\mathrm{e_a}$ is the saturation vapour pressure deficit (kPa); Δ is the slope of saturation vapour pressure temperature curve (kPa $^\circ\mathrm{C}^{-1}$) and $\gamma$ is the psychrometric constant (kPa $^\circ\mathrm{C}^{-1}$).

## 3.4 SECONDARY VARIABLES OF PM $ET_0$

The FAO-56 recommends equations for computing the secondary parameters which form an input to the above-mentioned primary equation. The following sections provide a detailed explanation of these equations.

### 3.4.1 Saturation Vapor Pressure ($e_s$)

An estimate of mean daily $e_s$ is obtained as,

$$\underset{(\mathrm{kPa})}{e_S} = \frac{e^0\left(T_{\max}\right) + e^0\left(T_{\min}\right)}{2} \tag{3.2}$$

where $T_{max}$ and $T_{min}$ are maximum and minimum air temperatures (°C) respectively and saturation vapour pressures (kPa) corresponding to these are obtained from,

$$e_a = e^0_{(\mathrm{kPa})}\left(T_{\mathrm{dew}}\right) = 0.6108 \exp\left[\frac{17.27 T_{\mathrm{dew}}}{T_{dew} + 237.3}\right] \tag{3.3}$$

in which $T_{dew}$ (°C) may be either $T_{max}$ or $T_{min}$ and $e^0(T_{dew})$ is saturation vapour pressure at air temperature $T_{dew}$ (kPa).

### 3.4.2 Actual Vapor Pressure ($e_a$)

$$e_a = \frac{\left[e^0\left(T_{\min}\right)\frac{\mathrm{RH}_{\max}}{100} + e^0\left(T_{\max}\right)\frac{\mathrm{RH}_{\min}}{100}\right]}{2} \tag{3.4}$$

where $RH_{max}$ and $RH_{min}$ are maximum and minimum values of relative humidity (%) respectively.

### 3.4.3 Slope of Vapor Pressure Curve (Δ)

$$\Delta = \frac{4098\left[0.6108 \exp\left(\frac{17.27\bar{T}}{\bar{T} + 237.3}\right)\right]}{(\bar{T} - 237.3)^2} \tag{3.5}$$

where $\bar{T}$ is the mean air temperature defined as,

$$\bar{T} = \frac{T_{max} + T_{min}}{2} \tag{3.6}$$

### 3.4.4 Psychrometric Constant ($\gamma$)

$$\gamma = 0.665 \times 10^{-3} P \tag{3.7}$$

where P is the atmospheric pressure (kPa) which is obtained from,

$$P = 101.3 \left[ \frac{293 - 0.0065z}{293} \right]^{5.76} \tag{3.8}$$

where z is the elevation of the site above mean sea level (m).

### 3.4.5 Net Radiation at Crop Surface ($R_n$)

According to the principle of radiation balance,

$$R_n = R_{\mathrm{ns}} - R_{\mathrm{n1}} \tag{3.9}$$

where $\mathrm{R_{ns}}$ is the net short wave solar radiation ($\mathrm{MJm^{-2}day^{-1}}$) and $\mathrm{R_{nl}}$ is the net longwave radiation ($\mathrm{MJm^{-2}day^{-1}}$). Procedures to calculate $\mathrm{R_{ns}}$ vary depending on the type of radiation measurements made at the location. In this work, the computation of $\mathrm{R_{ns}}$ is done using measurements of actual sunshine hours (n). Accordingly, the relevant procedure proceeds by considering the incident and reflected components of incoming short-wave solar radiation ($R_n$). Net short-wave solar radiation is calculated as,

$$R_{ns} = (1 - \alpha) R_s \tag{3.10}$$

where $\alpha$ is the albedo or canopy reflection coefficient. FAO-56 suggests that for hypothetical grass reference crop,

$$\alpha = 0.23 \tag{3.11}$$

Incoming solar radiation ($\mathrm{MJm^{-2}day^{-1}}$) is calculated as,

$$R_s = \left( 0.25 + 0.5 \frac{n}{N} \right) R_a \tag{3.12}$$

where $R_a$ is extra-terrestrial solar radiation at the top of the atmosphere ($MJm^{-2}day^{-1}$), n is the actual duration of sunshine (hours) and N is the maximum possible duration of sunshine (hours). N is dependent on the time of year and latitude and may be obtained as,

$$N = \frac{24}{\pi}\omega_s \tag{3.13}$$

where $\omega_s$ is the sunset hour angle (radians) and is computed as,

$$\omega_s = \arccos(-\tan\varphi\tan\delta) \tag{3.14}$$

in which $\varphi$ is the latitude of the place (radians) and $\delta$ is the solar declination (radians) which, for any day number of the year (J) may be calculated as,

$$\delta = 0.409\,\mathrm{Sin}\left(\frac{2\pi J}{365} - 1.39\right) \tag{3.15}$$

Extra-terrestrial solar radiation ($R_a$) is also related to the time of year (J and $\delta$) and latitude ($\varphi$) through the relationship,

$$R_a = \frac{24(60)}{\pi}G_{sc}d_r\left[\omega_s\,\mathrm{Sin}\,\varphi\,\mathrm{Sin}\,\delta + \mathrm{Cos}\,\varphi\,\mathrm{Cos}\,\delta\,\mathrm{Sin}\,\omega_s\right] \tag{3.16}$$

where $G_{sc}$ is the solar constant (= 0.0820 $MJm^{-2}min^{-1}$) and $d_r$ is the inverse relative distance from Earth to Sun may be obtained from,

$$d_r = 1 + 0.033\,\mathrm{Cos}\left(\frac{2\pi J}{365}\right) \tag{3.17}$$

Net long wave solar radiation ($R_{nl}$) in Eq. (3.9) is computed as,

$$R_{nl} = \sigma_{SB}\left(\frac{T^4{}_{\mathrm{maxk}} + T^4_{\mathrm{mink}}}{2}\right)(0.34 - 0.14\sqrt{e_a})\left(1.35\frac{R_S}{R_{so}} - 0.35\right) \tag{3.18}$$

where $\sigma_{SB}$ is Stephan Boltzmann constant ($= 4.903 \times 10^9 MJK^{-4}m^{-2}day^{-1}$), $T_{maxk}$ is the maximum temperature in (K) and $T_{mink}$ is the minimum temperature (K) and clear sky short wave radiation ($R_{so}$) may be calculated using,

$$R_{so} = \left(0.75 + 2 * 10^{-5} z\right) R_a \qquad (3.19)$$

### 3.4.6 Wind Speed at 2.0 m above Ground Surface ($u_2$)

The FAO-56 procedure uses wind speed ($u_2$) measured at 2 m above the ground surface and suggests the following equation to convert wind speed ($u_z$) measured at any other height ($z_w$) into equivalent $u_2$ values. The 24-hour wind speed was recorded in $\mathrm{kmh^{-1}}$ and hence necessary correction was applied to convert it to $\mathrm{m\ s^{-1}}$ to conform to its application in Equation 2.1.

$$\underset{(m/s)}{u_2} = u_z \frac{4.87}{\ln\left[67.8 z_W - 5.42\right]} \qquad (3.20)$$

### 3.4.7 Soil Heat Flux Density (G)

According to FAO-56, soil heat flux (G) needs to be calculated only when $ET_0$ is computed using mean monthly climatological records. The recommended equation for G is,

$$\underset{(\mathrm{MJ/m^2}/d)}{G_{\mathrm{month},i}} = 0.14 \left(T_{\mathrm{month,i}} - T_{\mathrm{month,i-1}}\right) \qquad (3.21)$$

where T month,i is the mean air temperature for month i and T month , i – 1 is the mean air temperature for month i-1.

### 3.4.8 Day Number (J)

For monthly calculations, J at the middle of the month is found to give satisfactory results and is calculated by,

$$J = \mathrm{INTEGER}\left(30.4 * J_1 - 15\right) \qquad (3.22)$$

where $J_1$ is the number of the month (J1 = 1, 2, ........,12).

The algorithm implementing the use of Eqs. (3.2) – (3.22) for computation of $ET_0$ of grass reference crop by Equation 3.1 is summarized in Box-11, Chapter 4 of Allen et al. (1998). A computer program based on this algorithm was developed in this study to derive estimates of all parameters and PM $ET_0$ using daily and monthly mean climatological and other relevant inputs. The program was validated using the numerical example given in Example 17,18 (Chapter 4) of FAO – 56 and reproduced the same results with respect to all parameters and $ET_0$ estimates.

## 3.5 SPATIAL AND TEMPORAL VARIABILITIES OF CLIMATIC VARIABLES

Mean values ($\bar{x}$) of each of the eight climate variables $T_{max}$ (°C), $T_{min}$ (°C), $RH_{max}$ (%), $RH_{min}$ (%), u ($\mathrm{m\ s^{-1}}$), n (hours), $R_s$ ($\mathrm{MJm^{-2}day^{-1}}$) and $R_n$ ($\mathrm{MJm^{-2}day^{-1}}$) were computed at each station considering the entire period of record (2006-2016). Using these values, maps depicting the spatial variabilities of each climatic variable across the 10 agro-climatic zones as well as the entire Karnataka State were generated using inverse distance interpolation (Figure 3.1). Values of standard deviation (SD) (not shown here for brevity) and coefficient of variation (CV) were also computed and used to assess the temporal variability of the climatic variables at each station.
Figure 3.1 depicts the typical climate characteristics of Karnataka state across each zone varying from drier northern regions to humid regions adjoining the western ghats. The overall mean temperature values were found to be maximum in the northern regions with $T_{min}$ found to be maximum in NED and CO regions. $T_{max}$ values were found to be highest in the plains of NED and NET zone accompanied by lower SD and CV values, which showed less variability. The relative humidity values reflect the northern regions to be dry with as low as 43% (both $RH_{min}$ and $RH_{max}$) in the ND region. However, the mean relative humidity values were high in regions transitioning from drier to hilly to plateaus in the southern region. The maximum humidity was found too high in CO and SD regions. The overall windspeed was found to be the lowest ranging from 0.15 to 2.63 $\mathrm{m\ s^{-1}}$ and clusters of high values were found in the ND zone. As sunshine hours (n) and radiation ($R_n$ and $R_n$) are correlated variables; Figure 3.1 portrays this relationship with the northern region showing high variability with lower values in the southern regions. However, a cluster of lower values can be observed in the ND zones.

## 3.6 BOX-WHISKERS PLOTS OF CLIMATIC VARIABLES

A more robust analysis of the spatio-temporal variabilities of the climate variables across ten different zones was assessed using box-whisker plots. Box plots were used in grouping stations into specific zones based on their similar statistical characteristics. Therefore, box plots for the period 2006-2016 were used to check the data integrity and remove existing outliers within each station. Temporal statistical characteristics of 67 stations were assessed based on four seasons of the year – pre-monsoon (March to May), monsoon (June to September), post-monsoon (October to December) and winter (January to February) was performed using box-whisker plots. Typically, the height of the box represents the inter-quartile range (difference between the 75th percentile and 25th percentile) of the data and the median value is represented by a horizontal line within the box. The whiskers on either side of the box represent the minimum and maximum values of the variable and all values lower/higher than these are represented as outliers beyond the whiskers. Box-whisker plots thereby provide complete information on the variability within a given dataset in a concise manner. Figure 3.3 shows box-whisker plots for each of the climate variables for each season considering the historical period of observation (2006-2016). The seasonal temperature variability was high during the monsoon and post-monsoon seasons, $T_{min}$ values were positively skewed in the winter season however during other months the distribution seems to be negatively skewed. It can be seen for all the seasons the $T_{max}$ appears to be normally distributed and the overall median is above 30 °C. In the case of $RH_{min}$, the values seem to be positively skewed across all seasons with the least outliers but $RH_{max}$ values are opposite to these values with the overall median across all seasons appearing to be as high as 80 % with negative skewness. In the case of windspeed, the whiskers indicate the maximum values to be less than 5 $\mathrm{m\ s^{-1}}$ with the overall median positively skewed. Apparently, the lower windspeed median values were accompanied by high outliers with maximum values being 20 $\mathrm{m\ s^{-1}}$. Sunshine hours showed higher median values of more than 8 hours in the winter indicating the possibility of negative skewness where higher mean values are observed but during other seasons the data seems to be positively skewed.

Similar higher median values were observed with $R_n$ and $R_n$ values. It can be seen that the upper whiskers in the case of n, $R_n$ and $R_n$ are short against the lower whisker which is longer indicating the large values following within the lower quartiles.

From the overall spatio-temporal analysis of climatic variables, the variability revealed both the $T_{min}$ and $T_{max}$ were considerably high in north-eastern regions relative to the southern regions where the temperature was found to be moderate to low values. Interestingly $T_{min}$ was found to be maximum in the CO zone at 23 °C. On the contrary, the examination of relative humidity revealed high values of $RH_{min}$ and $RH_{max}$ values near coastal and hilly environments. From the overall variability of climatic variables, it was observed that geographical features such as elevation largely affected the climatic variability.

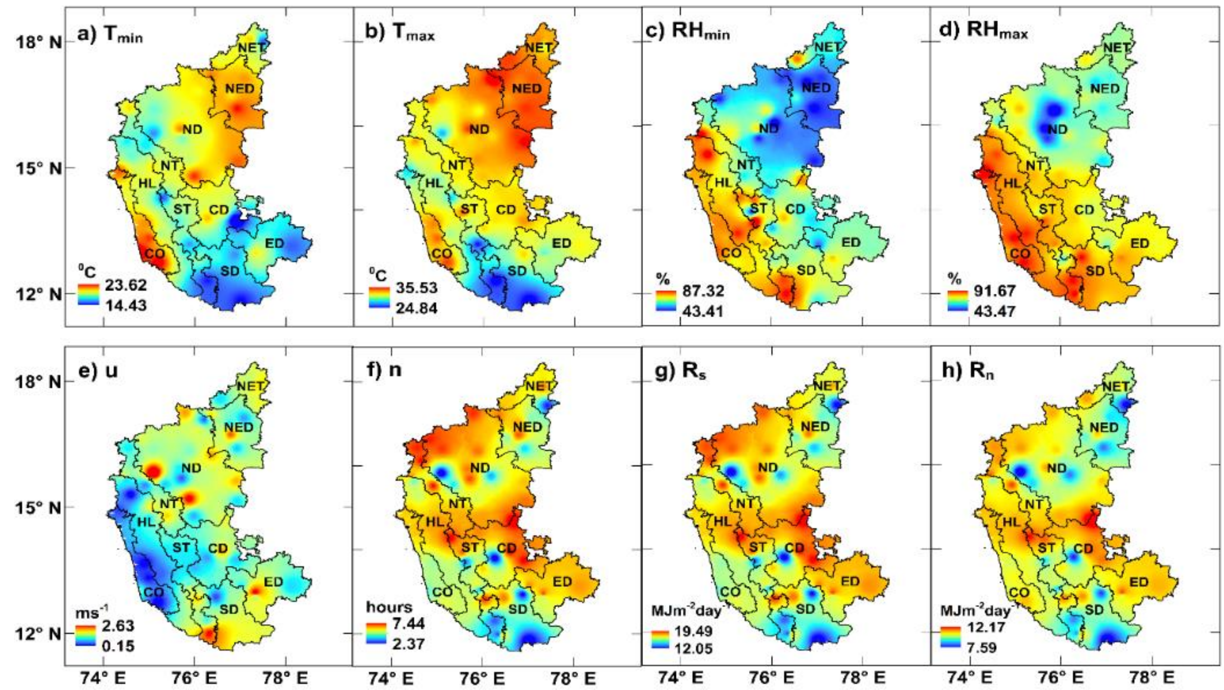


**Figure 3.1: Average variability of climatic variables over the study area**

## 3.7 SPATIAL AND TEMPORAL VARIABILITY OF PM $ET_0$

It can be seen from Figure 3.4 that the average maximum PM $ET_0$ values were found to increase from the southern region to the northern region. Significant clusters of high values were observed in the NED, ND and also some portions of the CD region. Since $ET_0$ variability is subjected to dependent climatic variables and other

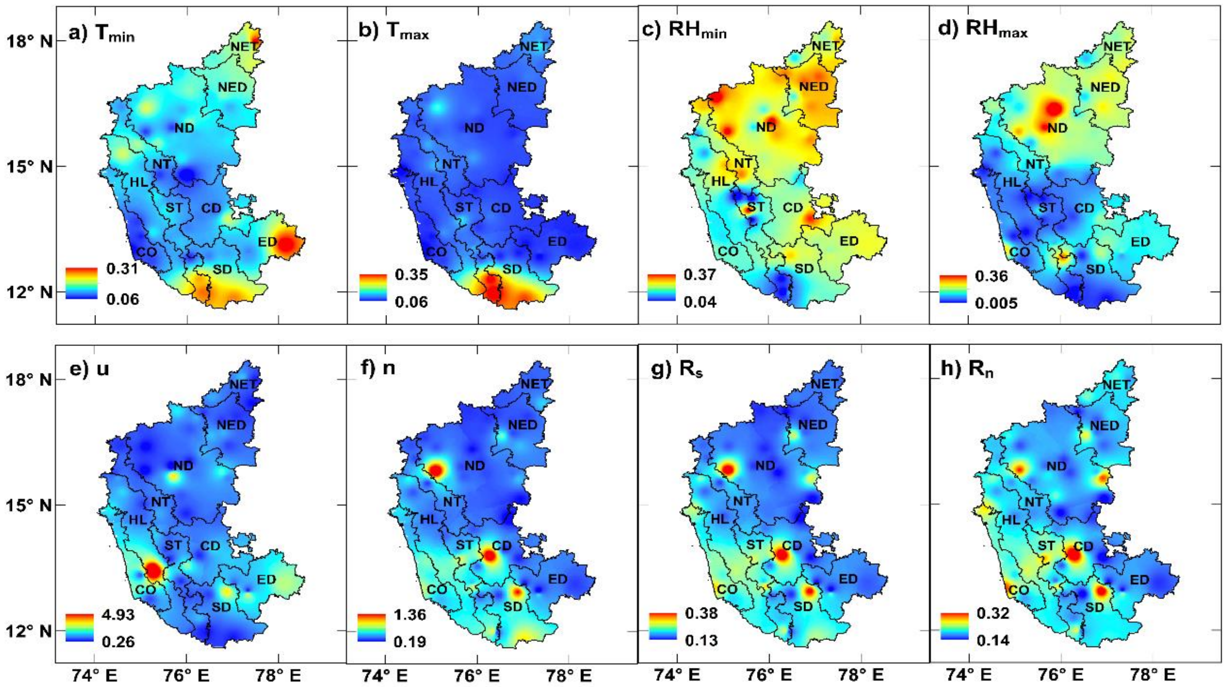


**Figure 3.2: Average CV values of climatic variables over the study area**

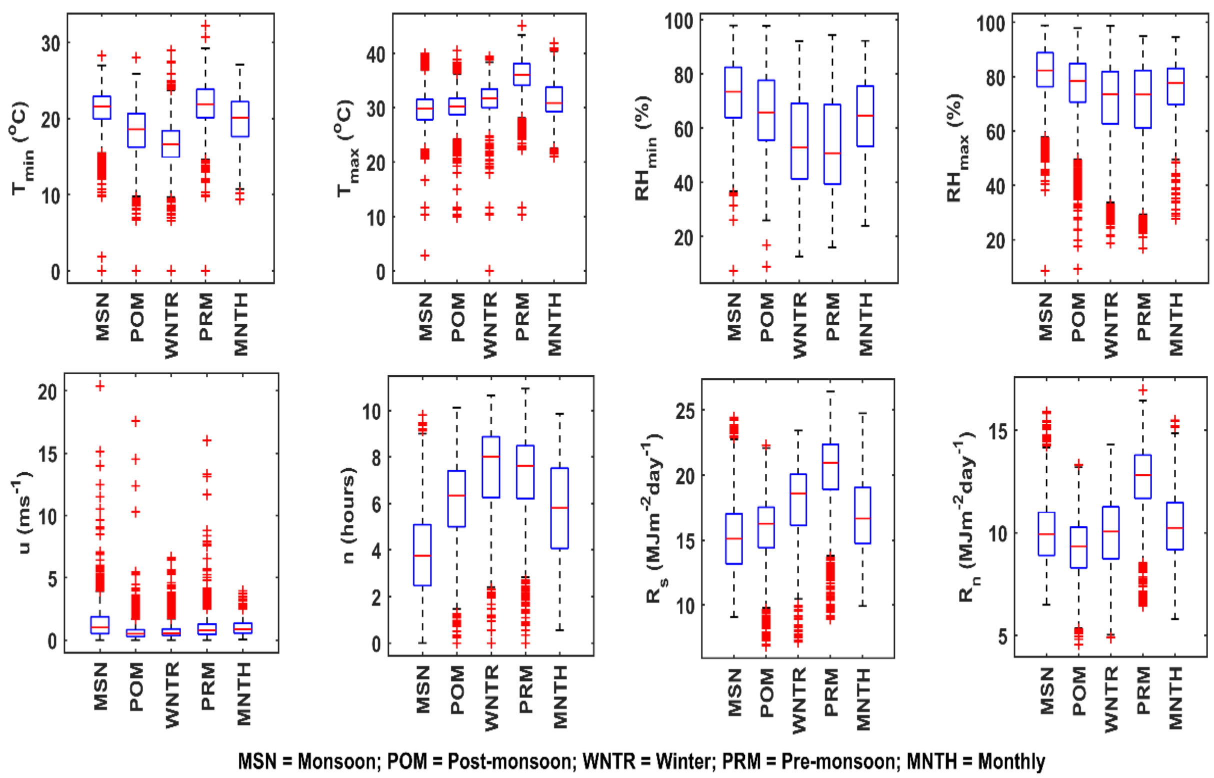


**Figure 3.3: Seasonal variability of climatic variables**

geographical conditions (Zhang et al. 2018) it can be observed that $ET_0$ values are high in the plains and dry regions. Whereas the mountainous, hilly and coastal regions varied from lower to moderate values of $ET_0$ values. The overall average PM $ET_0$ for the entire state ranged from 2.68 to 4.58 $\mathrm{mm\ d^{-1}}$ with CV values of 0.16 to 0.42. Significant high average values of $ET_0$ clusters can be observed in the NED and ND zones which indicate the occurrence of higher rates of $ET_0$. However, this cluster is accompanied by inconsistent CV values for example at Navilutheertha the $ET_0$ values are significantly less accompanied by higher CV values. Since Navilutheeratha contained large amounts of missing climatic variables, possible higher CV values may be due to low-quality input climatic variables. As it is clear from the figure higher $ET_0$ values were in the plains and little portion of the coastal areas. It is also evident in the western ghat's hilly regions significantly lower $ET_0$ values were observed especially at the confluence of western and eastern ghats in the SD zone yielded the lowest values of $ET_0$ values. These values are accompanied by lower CV values thereby indicating the possibility of a decrease in PM $ET_0$ values with a significant rise in elevation. However, further assessment has to be carried out to identify such changes.

Figure 3.5 shows the seasonal variability where increasing $ET_0$ values are observed during the summer season with a maximum in the NED zone yielding 6 $\mathrm{mm\ d^{-1}}$ during May. Amongst different zones, during the summer season, the lowest $ET_0$ was observed in March about 3.9 mm d−1 in the SD zone. It is apparent from Figure 3.5 there is an increase in $ET_0$ values from March to April across all zones and reaching its peak in May, with $ET_0$ values of 5.86 in the NED and NET zones. As the temperature starts declining beginning from monsoon and reaching the lowest during the winter season the $ET_0$ values also start to decrease across zones. As the state receives maximum rainfall during monsoon sharp decline in $ET_0$ values from summer to monsoon season was observed. Interestingly post-monsoon seasons NT and CO showed increasing values during September and October months. The winter season showed the lowest $ET_0$ values for all seasons. Overall least $ET_0$ of 2.93 mm d−1 in January was observed in NED with a maximum of 4.11 mm d−1 in the ED zone.

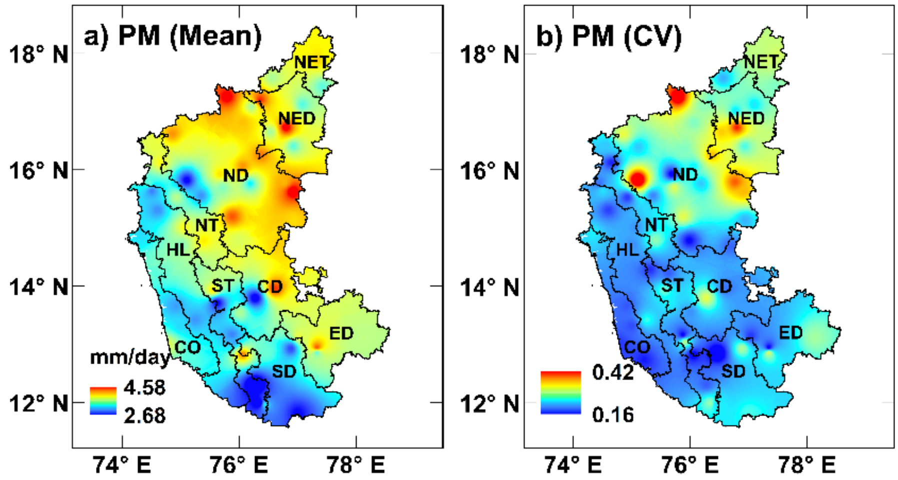


**Figure 3.4: Spatial variability of mean and CV values of PM $ET_0$**

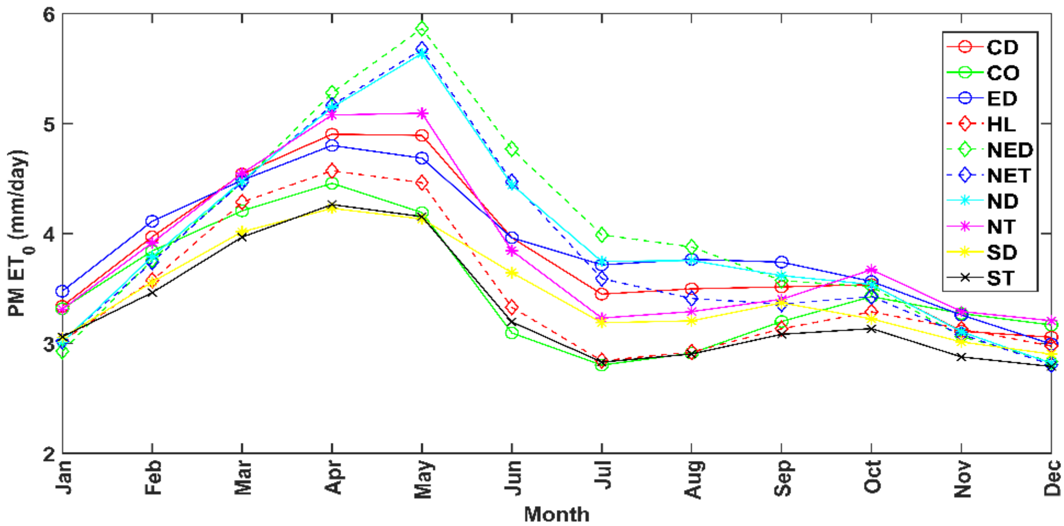


**Figure 3.5: Temporal variability of PM $ET_0$ across different ACZ's**

CHAPTER 4

# LOCAL CALIBRATION OF THE HARGREAVES EQUATION

## 4.1 GENERAL

Increasing anthropogenic activities are significantly altering climatic regimes and the spatiotemporal dynamics of the hydrological cycle. These changes are affecting freshwater availability thereby decreasing the per-capita water availability in water-stressed countries such as India. Therefore, there is a need to efficiently use available water resources in all sectors and more so in the agricultural sector which is the largest consumer of freshwater in India. In this situation, improving water management practices through more efficient irrigation scheduling aimed at delivering water to satisfy crop needs for maximum yield is essential. A key variable in procedures for the estimation of crop water requirement (CWR) and irrigation water requirement (IWR) is 'Reference Crop Evapotranspiration' ($ET_0$). Since direct measurement of $ET_0$ is difficult, several methods for its estimation using regularly recorded climate data have been proposed by previous researchers. The United Nations (UN) Food and Agriculture Organization (FAO) has proposed standardized procedures for the calculation of $ET_0$ using ground-based climatological measurements (Allen et al. 1998; Doorenbos and Pruitt 1977). In particular, the FAO-56 report (Allen et al. 1998) recommends the sole use of the physically-based Penman-Monteith (PM) equation for computation of $ET_0$ and provides detailed procedures equations for converting observed climatological measurements into variables necessary for the application of the PM equation. However, since the PM equation requires data pertaining to 5-6 climate variables that may not be available at all locations, several other empirical to semi-empirical $ET_0$ equations that require fewer climate variables continue to remain popular amongst researchers and practitioners (Jabloun and Sahli 2008; McKenney and Rosenberg 1993; Mohan 1991; Urrea et al. 2006; Xu and Singh 2002). Over the past few decades, a large number of studies have been taken up to evaluate the accuracies of these simpler $ET_0$ equations relative to the PM equation in various climatic

regions of the world (Almorox et al. 2015; Espador et al. 2011; Garcia 2004; Jensen et al. 1997; Jhajharia et al. 2012; Itenfisu et al. 2003; Nandagiri and Kovoor 2006; Temesgen et al. 2005). The results of comparative studies have indicated the need for local calibration of parameters present in the simpler empirical to semi-empirical equations to attain acceptable levels of accuracy (e.g., Valero et al. 2013; Valiantzas 2013, 2015). One such simpler equation is the Hargreaves (HG) equation proposed by Hargreaves and Samani (1985). This temperature-based equation has been subject to comparisons with the PM equation in several parts of the world and found to provide reasonably accurate estimates of $ET_0$ in certain climatic conditions (e.g., Valiantzas 2015; Sentelhas 2010). Allen et al. (1998) recommend the use of the HG equation as an alternative to the PM equation in data-scarce situations.
However, a few studies have shown that the HG equation may require local calibration to provide $ET_0$ estimates comparable to the PM equation (Pandey et al. 2014; Shahidian et al. 2013; Tabari and Talaee 2011; Trajkovic 2007). For example, Gavilan et al. (2006) evaluated the HG equation in semi-arid conditions in Southern Spain using data from 86 meteorological stations. Accuracies of daily $ET_0$ estimates were evaluated relative to the FAO-56 PM equation and it was found that the performance of the HG equation varied with location with deviations being larger in coastal and inland areas. They reported significantly better performance of the HG equation when regional calibration of parameters was carried out using two methods by calibrating climate variables and kriging spatial interpolation. Martinez-Cob and Tejero-Juste (2004) evaluated the performance of the HG equation in windy and non-windy conditions in semi-arid north-east Spain and recommended local calibration at non-windy locations. Trajkovic (2007) calibrated the HG equation in the humid western Balkan region of south-east Europe and found that $ET_0$ estimates were in close agreement with the PM method. Tabari and Talaee (2011) studied the effect of local calibration on the performances of the HG and Priestley-Taylor (PT) methods relative to the PM method in arid and cold climates of Iran using historical climate records of 12 stations. They obtained parameter values that were significantly different from the standardized values which yielded smaller errors in $ET_0$ estimates. Pandey et al.

(2014) evaluated the effect of local calibration of the HG equation in east Sikkim, India using daily, weekly, and monthly time steps and noted a significant reduction in error for all three-time steps. Subburayan et al. (2011) calibrated the HG equation for a hot and humid location in India. The study found that the average underestimation of HG against PM was 28%. The exponent in the Hargreaves was found to be 0.653 which deviated from the standard HG exponent of 0.5. Though the results of original HG $ET_0$ estimates indicated a deviation from the FAO56 PM method but a significant decrease in standard error estimates was observed in modified HG estimates. Patel et al. (2014) calibrated the HG equation using the fuzzy logic method at eight locations across four climatic regions in India. The study used CLIMWAT datasets for input climatic variables and the results showed significant improvements in $ET_0$ estimates by the modified HG method across all climatic zones in India. Berti et al. (2014) calibrated the HG equation in north-eastern Italy using climate records of 35 agro-meteorological stations for the period 1994-2006. They found that local calibration of one parameter in the HG equation reduced the overestimation in $ET_0$ estimates relative to the PM equation to 2.6%. Mendicino and Senatore (2013) calibrated the HG equation in southern Italy and found the adjusted HG equation provided better estimates of daily $ET_0$. They developed a quadratic regression relationship between one of the HG parameters and the mean temperature. Vanderlinden et al. (2004) applied the HG equation at 16 meteorological stations in southern Spain during 1961-1998 and reported a gain in unbiasedness and precision due to local calibration. From the review of previous studies, it is evident that the optimal parameters involved in the HG equation exhibit significant deviations from the standard values suggested by Hargreaves and Samani (1985) and Allen et al. (1998) in different climatic regimes of the world. Therefore, the application of the HG equation in data-scarce situations requires local calibration if accurate estimates of $ET_0$ are to be obtained. However, since either the measured value of $ET_0$ or those estimated by the data-intensive PM equation is required for local calibration, there is a need to develop procedures for regionalizing the parameters so that they may be estimated at locations where calibration data is unavailable. Such regionalization efforts can be successful only when a large number of climate stations covering a wide variety of climatic conditions are considered.

In addition to the calibration of parameters, efforts have been made to redefine the mean daily temperature which forms the most important input in temperature-based $ET_0$ estimation methods such as the Thornthwaite and Blaney-Criddle equation. Instead of using mean temperature calculated as an average of the maximum and minimum temperatures, alternate forms of an 'effective' temperature have been used with the Thornthwaite equation by Pereira and Pruitt (2004) and Dinpashoh (2006) resulting in more accurate estimates of $ET_0$. Similar efforts involving the use of effective temperature in the Blaney-Criddle $ET_0$ equation have been made (e.g., Fooladmand and Ahmadi 2009; Fooladmand 2011) and a reduction in estimation errors have been reported. However, no such efforts involving the use of effective temperature with the HG equation seem to have been taken up.

The present study was taken up to evaluate the performance of the HG $ET_0$ equation with and without local calibration of parameters. Additionally, the effect of replacing the mean temperature with an effective temperature on the performance of the HG equation was also assessed. Since measured $ET_0$ is rarely available, it was proposed to determine optimal HG model parameters and so also parameters of the effective temperature variable using $ET_0$ estimates obtained with the PM equation. In addition to temporal variabilities, the intention was to assess the spatial variabilities in $ET_0$ estimates and parameters at a regional scale with significant heterogeneity in climatic conditions. It is for this reason that the selected study area was Karnataka State located in south India.

## 4.2 HARGREAVES (HG) $ET_0$ EQUATIONS

The Hargreaves (HG) equation (Hargreaves and Samani, 1985; Allen et al., 1998) for daily $ET_0$ estimation is given by,

$$ET_{0,H} = 0.0023 \times (T_{\text{mean}} + 17.8) \times (T_{\max} - T_{\min})^{0.5} \times R_a \tag{4.1}$$

where $ET_{0,H}$ is the daily reference evapotranspiration estimated by the 'original' HG equation ($\mathrm{mm\ d^{-1}}$), $T_{\max}$ is the maximum air temperature ( °C), $T_{\min}$ is the minimum air temperature (°C) $T_{mean}$ is the mean air temperature (°C) = ($T_{max}$ + $T_{min}$)/2 and $R_a$ is the extra-terrestrial radiation ($\mathrm{mm\ d^{-1}}$).

In this study, Equation (4.1) is rewritten in a general form as,

$$ET_{M,H} = a_H\,(\,T_{mean} + b_H)\,(T_{\max} - T_{\min})^{c_H}\,R_a \tag{4.2}$$

where $ET_{M,H}$ is the daily reference evapotranspiration estimated by the 'modified' HG equation ($\mathrm{mm\ d^{-1}}$) and the other variables retain the same definitions as above. $a_H$, $b_H$, and $c_H$ are model parameters that need to be determined by calibration.

Three more versions of the HG equation were obtained by replacing the mean air temperature ($T_{mean}$) in Equation 4.2 with effective air temperature ($T_{eff}$). That is,

$$ET_{M,Heff} = a_H\,(\,T_{eff} + b_H)\,(T_{\max} - T_{\min})^{c_H}\,R_a \tag{4.3}$$

Effective air temperature ($T_{eff}$) may be defined by any one of the following expressions.

$$T_{eff,K} = 0.5K_H\,(3\,T_{\max} - T_{\min}) \tag{4.4a}$$

$$T_{eff,f} = f_H\,T_{\min} + (1 - f_H)\,T_{\max} \tag{4.4b}$$

$$T_{eff,gh} = g_H\,T_{\min} + h_H\,T_{\max} \tag{4.4c}$$

where $K_H$, $f_H$, $g_H$, and $h_H$ are model parameters that need to be determined by calibration. While Equation 4.4a was suggested by Fooladmand and Ahmadi (2009), Equation 4.4b and 4.4c were proposed by Ma and Guttorp (2013). The following notations are used for $ET_0$ values calculated using $T_{eff}$ values instead of $T_{mean}$ in Equation 4.2: $ET_{M,HK}$, $ET_{M,Hf}$, and $ET_{M,Hgh}$ when Equation 4.4a, Equation 4.4b and Equation 4.4c respectively are used. In effect, the present study uses 5 different versions of the HG equation for estimating daily $ET_0$ using monthly mean climate inputs for the period of record.

## 4.3 COMPUTATION OF $ET_0$ AND CALIBRATION PROCEDURE

A computer program was developed in MATLAB® to calculate daily $ET_0$ values ($\mathrm{mm\ d^{-1}}$) by the PM model (Equation 3.1), the HG model (Eqs. 4.1-4.2), and the HG models using $T_{eff}$ defined by Eqs. 4.3, 4.4a, 4.4b, 4.4c at each station (Table 2.1) for each month in the period of record (2006-2016). The accuracy of the developed program was verified using numerical examples given by Allen et al. (1998).
Since the record length of 11 years was too short to carry out a month-wise analysis, the HG equations (Eqs. 4.1-4.3) were locally calibrated at each station using the annual period. Accordingly, the available month-wise data was divided into a calibration set and a validation set. The period January 2006 – December 2012 (84 months) was used for calibrating the HG equations and was validated for the period January 2013 – December 2016 (48 months). At each station, calibration was performed in two steps: 1) $ET_{M,H}$ values (Equation 4.2) were first used with corresponding values of $ET_{0,PM}$ (Equation 3.1) to determine optimal values of parameters $a_H$, $b_H$, and $c_H$ 2) Retaining these optimal values of $a_H$, $b_H$, and $c_H$, the other three versions of the HG equation with $T_{mean}$ replaced by alternate definitions of $T_{eff}$ (Eqs. 4.3, 4.4a, 4.4b, 4.4c) were calibrated separately with corresponding values of $ET_{0,PM}$ to obtain optimal model parameters $K_H$, $f_H$, and $g_H$ and $h_H$ for each station. In all cases of local calibration, optimal model parameters were obtained by minimizing the sum of squared errors (SSE) between PM $ET_0$ estimates and those obtained from the HG equation. That is,

$$SSE = \sum_{i=1}^{N} (Y_i - X_i)^2 \tag{4.5}$$

where $Y_i$ is the $ET_{0,PM}$ and $X_i$ is the $X_i$ or $ET_{M,HK}$ or $ET_{M,Hf}$ or $ET_{M,Hgh}$ depending on the particular HG equation being calibrated and N is the total number of months. In this study, optimal model parameters were obtained using the SOLVER Add-in in *Microsoft® Excel®* (2013) by minimizing SSE (Equation 4.5) by adopting the Generalized Reduced Gradient (GRG) Nonlinear method.
Accuracy assessment of the HG equations (Eqs. 4.1-4.3) relative to the PM equa-

tion was accomplished in both calibration and validation phases using the coefficient of determination ($R^2$), root mean square error (RMSE), and mean bias error (MBE) statistics computed as,

$$R^2 = \left[ \frac{N\Sigma Y_i \Sigma X_i - \Sigma Y_i \Sigma X_i}{\sqrt{[N\Sigma Y_i^2 - (\Sigma Y_i^2)] - [N\Sigma X_i^2 - (\Sigma X_i^2)]}} \right]^2 \tag{4.6}$$

$$RMSE = \sqrt{\frac{\Sigma(Y_i - X_i)^2}{N}} \tag{4.7}$$

$$MBE = \frac{\Sigma_{i=1}^{n}(Y_i - X_i)}{N} \tag{4.8}$$

where Y is the $ET_{0,PM}$ and X is the $ET_{0,H}$ or $ET_{M,H}$ or $ET_{M,HK}$ or $ET_{M,Hf}$, or $ET_{M,Hgh}$ depending on which of the HG equations is being evaluated. For a perfect estimation, $R^2$ = 1, RMSE = 0 and MBE = 0. A convenient method for interpreting the overall performance of a given HG equation using the above three statistics across the 67 stations was devised in which a 'score' which was computed using the following steps: 1) Considering a particular HG equation, one of the statistic, say $R^2$ is selected and the number of stations at which this HG equation yielded the highest value of $R^2$ relative to the other equations is noted 2) A similar count is made for the number of stations at which the HG equation yielded the lowest RMSE and lowest MBE 3) Next the ratio of the number of stations at which the particular HG equation yielded the best values of statistics to the total number of stations is calculated 4) The same steps are applied to all the HG equations whose performance was evaluated to identify the equation which performed best at the largest number of stations in each zone and also in the study area as a whole.

## 4.4 RESULTS AND DISCUSSION

Mean monthly $ET_{0,PM}$ values obtained using the PM method (Equation 3.1) are shown in Figures 3.4 and 3.5 to provide an overview of the magnitudes and intra-annual variability. It can be seen that $ET_0$ values are in the range of 3.0 $\mathrm{mm\ d^{-1}}$ in January and increase monotonically over the summer season to reach peak values of 5.0 $\mathrm{mm\ d^{-1}}$ in May. With the onset of the South-west monsoon rainfall in June, $ET_0$ values reduce and remain constant at about 3.5 $\mathrm{mm\ d^{-1}}$ during the monsoon season which lasts upto October. Subsequently, during the winter season, $ET_0$ values reduce to 3.0 $\mathrm{mm\ d^{-1}}$. However, the standard deviation bars (not shown here for brevity) indicate significant variations in monthly $ET_0$ values across the 67 stations located in different agro-climatic zones. The spatial variability as indicated by larger values of standard deviation appears to be more during April, May, and June and reduces during peak monsoon months of July-August and the winter season (November-February).

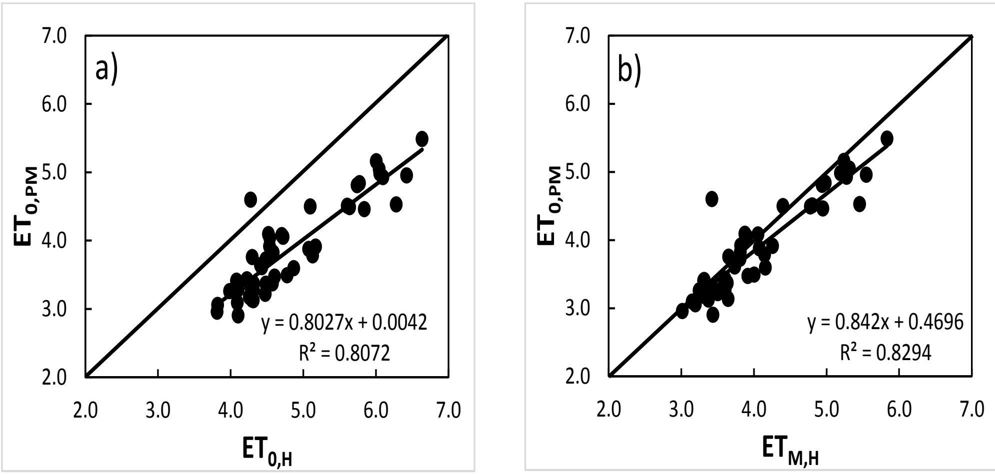


**Figure 4.1: Comparison of estimates by PM equation ($ET_{0,PM}$) with estimates by the a) original HG equation ($ET_{0,H}$) and b) modified HG equation ($ET_{M,H}$) for the validation phase at Davangere station (CD1)**

### 4.4.1 Original vs modified HG equations

The effect of local calibration on the performance of the HG equation relative to the PM equation was analysed through the implementation of Equation 4.1, Equation 4.2, and Equation 3.1 at each of the stations using the procedure described in the previous section. As an example, a comparison of $ET_0$ estimates during the validation phase is presented for the Davangere station (CD1) located in the Central Dry (CD) agro-climatic zone. The scatter plot showing $ET_0$ estimates by the PM equation ($ET_{0,PM}$) versus estimates by the original HG equation ($ET_{0,H}$) for 48 months (2013-16) in the validation phase at the Davangere station is shown in Figure 4.1. The original HG equation with standard values of parameters (Equation 4.1a) overestimates $ET_0$ values in comparison to the PM equation (Equation 3.1) with the overestimation being slightly larger for higher values of $ET_0$. Although a reasonably high value of $R^2$ =

0.8072 (Equation 4.6) was obtained, the values of RMSE (Equation 4.7) and MBE (Equation 4.8) of 1.006 $\mathrm{mm\,d^{-1}}$ and 0.9493 $\mathrm{mm\,d^{-1}}$ are indicative of somewhat large errors and bias in the $ET_{0,H}$ estimates. Calibration of the modified HG equation (Equation 4.2) using PM $ET_0$ estimates for 84 months during 2006-12 at the Davangere station yielded the following optimal values for the parameters: $a_H$ = 0.00424, $b_H$ = -1.0024, and $c_H$ = 0.4054. While the difference between the optimal value of parameters $c_H$ is not very different from the standard values of 0.5 (Equation 4.1), parameters $a_H$ and $b_H$ are significantly different from the standard value of 0.0023 and 17.8 respectively. With these values of optimal parameters, application of the modified HG equation (Equation 4.2) for the validation period yielded $ET_{M,H}$ values which are compared with the corresponding values of $ET_{0,PM}$ in Figure 4.1b for the Davangere station. The effect of local calibration is evident from the significant reduction in bias (MBE = 0.171 $\mathrm{mm\,d^{-1}}$) even though there is not much improvement in the value of $R^2$ (0.8294). RMSE was also reduced to 0.3473 $\mathrm{mm\,d^{-1}}$ for the modified HG equation (Figure 4.1b). Therefore, it may be concluded that for the Davangere station, local calibration of the HG equation resulted in a significant reduction in error and also a bias in $ET_0$ estimates. Results of a similar performance analysis during the validation phase for the original and modified HG equations relative to the PM equation for all 67 stations are presented in Table 4.1. For brevity minimum and maximum values of $R^2$, RMSE and MBE obtained for stations pooled in each agro-climatic zone in the State are shown therein separately for $ET_{0,H}$ and $ET_{M,H}$ estimates in comparison to $ET_{0,PM}$ estimates.

Examination of minimum and maximum values of $R^2$ indicates that the modified HG equation (Equation 4.2) yields $ET_{M,H}$ estimates which are better than $ET_{0,H}$ estimates provided by the original HG equation (Equation 4.1) in six out of the ten agro-climatic zones, and for the State as a whole (Table 4.1). In terms of $R^2$, it appears that local calibration does not provide any benefit in the Coastal (CO), Hilly (HL), Northern Transition (NT), and Southern Transition (ST) zones. However, the examination of RMSE values (Table 4.1) for the $ET_{0,H}$, and $ET_{M,H}$estimates indicate that for the State and in all zones, local calibration results in a significant reduction in error with the reduction in some cases being more than 50%. The only exception is the NT zone where RMSE values are in favour of the original HG $ET_{0,H}$ estimates. From Table 4.1 it can also be seen that $ET_{M,H}$ estimates by the modified HG equation (Equation 4.2) with the local calibration of parameters yields significantly lower values of MBE in all cases in comparison to the $ET_{0,H}$ estimates by the original HG equation (Equation 4.1). Therefore, it appears from the results shown in Table 4.1 that local calibration of the HG equation results in a significant reduction in both error and bias at stations located across the 10 agro-climatic zones of the study area. Considering the State as a whole, the modified HG equation appears to be superior to the original HG equation based on all three performance statistics (Table 4.1).

Table 4.2 shows the optimal parameters for the modified HG equation (Equation 4.2) whose performance assessment was shown in Table 4.1. Calibration of the modified HG equation to obtain optimal model parameters $a_H$, $b_H$, and $c_H$ in Equation 4.2 was performed as described in Article 4.2. Again for brevity, rather than showing parameter values for individual stations, mean values and standard deviations for stations pooled under each agro-climatic zone are shown therein. The last row in Table 4.2 shows mean parameter values and associated standard deviations for all 67 stations considered in the analysis.

It can be seen that although the mean value of the parameter $a_H$ of 0.0049 for the State as a whole (Table 4.2) deviates significantly from the standard value of $a_H$ = 0.0023 in the original HG equation (Equation 4.1), not only is the standard deviation quite high but significant departures from the standard value can be seen when stations are pooled under different zones. Mean values of $a_H$ range from as low as 0.0032 in the Northern Transition Zone (NT) to as high as 0.0067 in the Northern Dry (ND) zone. This implies that the original HG equation is not applicable without local calibration of this parameter in the study area. A similar conclusion can be drawn by examining the values of the parameter $b_H$ (Table 4.1) which show variations from as low as – 0.74 in the Coastal zone (CO) to as high as 34.95 in the Eastern Dry zone (ED) which are quite different from the standard value of 17.8 proposed by the original HG equation (Equation 4.1). Parameter $c_H$ (Table 4.1) while showing relatively lower variability across the zones still deviates from the standard value of 0.5 (Equation 4.1) with a mean value of 0.27 for the study area as a whole. The lowest value of $c_H$ = 0.20 was recorded in the Hilly zone (HL) with a moderate SD of 0.13 among the 5 stations, whereas the Eastern Dry (ED) zone with 4 stations yielded the highest mean value of $c_H$ = 0.39 with a higher SD of 0.25. Figure 4.2 shows maps depicting the spatial variabilities of the optimized HG model parameters $a_H$, $b_H$, and $c_H$ over the study area. These maps were derived by interpolating station-wise values of parameters using the inverse distance method. While Figures (4.2a) and (4.2b) indicate significant variations in parameters $a_H$ and $b_H$ with some clustering in certain areas, the variability of parameter $c_H$ appears to be more uniform across the study area (Figure 4.2c). An effort was made to explore the possibility of a correlation between station-wise values of $a_H$ and $b_H$ with station elevations but no significant relationships could be extracted. However, when mean values of parameters for the agro-climatic zones (Table 4.2) were regressed against mean elevations for the zones, it was found that parameter $a_H$ was negatively correlated with elevation with $R^2$ = 0.6305 and parameter $b_H$ was positively correlated with $R^2$ = 0.5944. These results indicate that elevation explains about 60% of the observed variability in these two parameters. Whether other terrain factors have an additional influence needs to be investigated in future studies aimed at the regionalization of parameters.

### 4.4.2 Performance of HG equations with effective temperature

The performances of the HG equations with mean temperature ($T_{mean}$) being replaced with effective temperature ($T_{eff}$) (Equation 4.3) defined by three alternative methods (Eqs. 4.4a, 4.4b, 4.4c) were evaluated using the procedure described in Article 4.2. While retaining the optimal values of parameters $a_H$, $b_H$ and $c_H$ obtained through calibration of HG $ET_0$ estimates by Equation 4.2 with those from the PM method (Equation 3.1), the HG equation with $T_{eff}$ (Equation 4.3) was again calibrated with the PM method. Optimal values of parameters $K_H$ (Equation 4.4a), $f_H$ (Equation 4.4b), and $g_H$ and $h_H$ (Equation 4.4c) were obtained by calibration with $ET_0$ estimates by the PM method (Equation 3.1) using the monthly values for the period January

**Table 4.1: Minimum and maximum values of validation phase performance statistics of the original (Equation 4.1) and modified (Equation 4.2) HG equations and HG equation using effective temperature (Eqs. 4.3, 4.4a, 4.4c) relative to the PM equation (Equation 4) for stations pooled in each agro-climatic zone**

| Zone | No. of | Statistic | $R^2$ | | | | RMSE (mm $d^{-1}$) | | | | MBE (mm $d^{-1}$) | | | |
|---|---|---|---|---|---|---|---|---|---|---|---|---|---|---|
| | Stations | Equation | $ET_{0,H}$ | $ET_{M,H}$ | $ET_{M,HK}$ | $ET_{M,Hgh}$ | $ET_{0,H}$ | $ET_{M,H}$ | $ET_{M,HK}$ | $ET_{M,Hgh}$ | $ET_{0,H}$ | $ET_{M,H}$ | $ET_{M,HK}$ | $ET_{M,Hgh}$ |
| CD | 6 | Min | 0.38 | 0.41 | 0.37 | 0.41 | 0.69 | 0.25 | 0.39 | 0.25 | 0.61 | 0.004 | 0.005 | 0.01 |
| | | Max | 0.88 | 0.92 | 0.83 | 0.92 | 2.07 | 1.32 | 1.28 | 1.29 | 1.86 | -1.24 | -1.2 | -1.21 |
| CO | 5 | Min | 0.26 | 0.30 | 0.17 | 0.30 | 0.69 | 0.54 | 0.57 | 0.54 | 0.17 | 0.38 | 0.35 | 0.37 |
| | | Max | 0.40 | 0.36 | 0.45 | 0.30 | 0.98 | 0.75 | 0.69 | 0.78 | 1.9 | 0.57 | 0.61 | 0.57 |
| ED | 4 | Min | 0.14 | 0.14 | 0.03 | 0.13 | 1.00 | 0.71 | 0.91 | 0.68 | -0.19 | 0.34 | 0.41 | 0.36 |
| | | Max | 0.35 | 0.69 | 0.46 | 0.71 | 2.09 | 1.23 | 1.63 | 1.34 | 1.88 | 0.69 | 0.93 | 0.73 |
| HL | 5 | Min | 0.52 | 0.52 | 0.48 | 0.46 | 0.67 | 0.30 | 0.34 | 0.30 | 0.34 | 0.03 | 0.002 | 0.03 |
| | | Max | 0.91 | 0.86 | 0.87 | 0.86 | 1.66 | 0.96 | 0.99 | 0.96 | 1.59 | -0.75 | -0.83 | -0.72 |
| NED | 7 | Min | 0.48 | 0.43 | 0.47 | 0.42 | 0.98 | 0.38 | 0.50 | 0.38 | 0.88 | 0.19 | 0.16 | 0.12 |
| | | Max | 0.92 | 0.93 | 0.88 | 0.93 | 1.88 | 1.20 | 1.04 | 1.23 | 1.74 | 0.93 | 0.7 | 0.95 |
| NET | 5 | Min | 0.51 | 0.53 | 0.44 | 0.53 | 0.91 | 0.36 | 0.48 | 0.36 | 0.002 | -0.05 | 0.03 | -0.05 |
| | | Max | 0.83 | 0.90 | 0.76 | 0.90 | 1.58 | 0.94 | 1.00 | 0.94 | 1.17 | -0.35 | -0.83 | -0.35 |
| ND | 17 | Min | 0.11 | 0.15 | 0.17 | 0.15 | 0.85 | 0.21 | 0.24 | 0.21 | 0.37 | -0.02 | 0.03 | -0.02 |
| | | Max | 0.91 | 0.92 | 0.91 | 0.92 | 2.09 | 2.01 | 2.08 | 2.01 | 2.02 | -1.11 | 1.05 | -1.1 |
| NT | 5 | Min | 0.52 | 0.30 | 0.35 | 0.35 | 0.36 | 0.80 | 0.39 | 0.39 | 0.33 | 0.00 | -0.03 | 0.002 |
| | | Max | 0.81 | 0.78 | 0.87 | 0.87 | 0.88 | 1.64 | 1.14 | 1.15 | 1.33 | -0.7 | -0.71 | -0.68 |
| SD | 4 | Min | 0.28 | 0.50 | 0.43 | 0.50 | 0.77 | 0.25 | 0.32 | 0.25 | -0.17 | -0.1 | -0.16 | -0.09 |
| | | Max | 0.84 | 0.85 | 0.79 | 0.86 | 2.07 | 1.02 | 1.17 | 1.02 | 1.91 | -0.79 | -0.9 | -0.79 |
| ST | 9 | Min | 0.21 | 0.20 | 0.20 | 0.17 | 0.41 | 0.39 | 0.39 | 0.39 | -0.04 | -0.01 | -0.03 | -0.01 |
| | | Max | 0.89 | 0.87 | 0.89 | 0.87 | 1.78 | 1.03 | 1.00 | 1.03 | 1.6 | -0.83 | -0.84 | -0.83 |
| State | 67 | Min | 0.11 | 0.14 | 0.03 | 0.13 | 0.41 | 0.21 | 0.24 | 0.21 | 0.02 | 0.00 | 0.002 | 0.002 |
| | | Max | 0.92 | 0.93 | 0.91 | 0.93 | 2.09 | 2.01 | 2.08 | 2.01 | 2.02 | -1.24 | -1.2 | -1.21 |

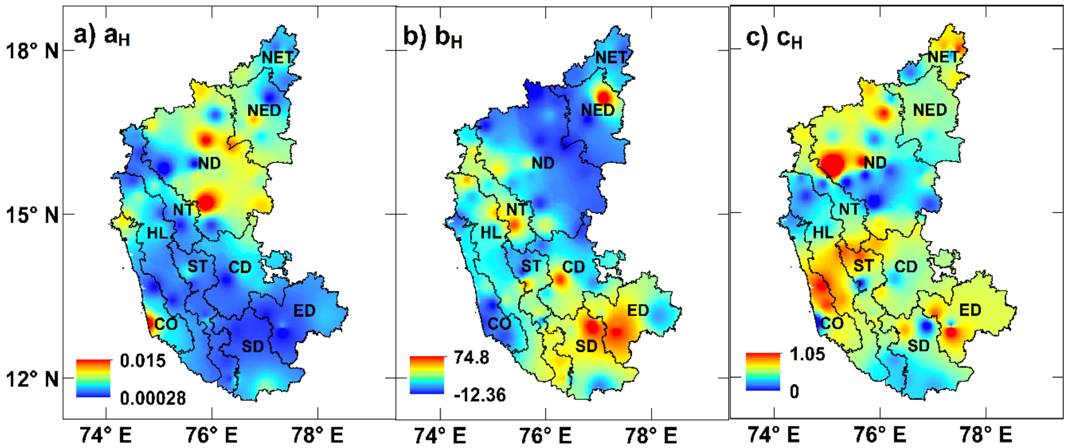


**Figure 4.2: Maps depicting spatial variations of optimized HG model parameters $a_H$, $b_H$, and $c_H$ (Equation 4.1) over the study area**

2006 – December 2012 (84 months) and were validated for the period January 2013 – December 2016 (48 months).

As an example, Figure 4.3 shows the results of the comparative evaluation of $ET_0$ estimates by these methods during the validation phase for the Davangere station (CD1) located in the Central Dry (CD) agro-climatic zone. The scatter plot (Figure 4.3a) shows $ET_0$ estimates by the PM equation ($ET_{0,PM}$) versus estimates by the HG equation with $T_{eff}$ defined by Equation 4.4a ($ET_{M,HK}$). The optimal value of the parameter $K_H$ = 0.6947 yielded these results with optimal values of parameters $a_H$ = 0.00424, $b_H$ = -1.0024 and $c_H$ = 0.4054 obtained in the earlier step. From the scatter plot (Figure 4.3a) it is evident that $ET_{M,HK}$ estimates deviate from the $ET_{0,PM}$ estimates with a large scatter for medium-range values and overestimation for higher values of $ET_0$. Performance evaluation yielded values of $R^2$ = 0.7411, RMSE = 0.4403 $\mathrm{mm\ d^{-1}}$ and MBE = 0.182 $\mathrm{mm\ d^{-1}}$ for this case. On the other hand, Figure 5.3b indicates a better comparison between estimates $ET_{M,Hf}$ and $ET_{0,PM}$ with an optimized parameter value of $f_H$= 0.4992. Although a slight overestimation for higher values still exists, the use of Equation 4.4b to define $T_{eff}$ significantly improves the performance of the HG model (Equation 4.3). While $R^2$ increases to 0.8294, RMSE and MBE reduce to 0.3481 $\mathrm{mm\ d^{-1}}$ and 0.172 $\mathrm{mm\ d^{-1}}$ respectively when Equation (4.3 and 4.4b) are implemented for the Davangere station (Figure 4.3b). However, since the value of

**Table 4.2: Mean and standard deviations of optimal HG equation parameters (Equation 4.2) for stations pooled in each agro-climatic zone**

| Zone | No. of Stations | $a_H$ | | $b_H$ | | $c_H$ | |
|---|---|---|---|---|---|---|---|
| | | Mean | Std. Dev | Mean | Std. Dev | Mean | Std. Dev |
| CD | 6 | 0.0042 | 0.0018 | 11.61 | 22.64 | 0.30 | 0.09 |
| CO | 5 | 0.0065 | 0.0045 | -0.74 | 11.53 | 0.30 | 0.22 |
| ED | 4 | 0.0025 | 0.0017 | 34.95 | 26.09 | 0.39 | 0.25 |
| HL | 5 | 0.0035 | 0.0020 | 25.07 | 17.89 | 0.20 | 0.13 |
| NED | 7 | 0.0063 | 0.0030 | 6.83 | 30.44 | 0.26 | 0.04 |
| NET | 5 | 0.0048 | 0.0023 | 3.14 | 5.68 | 0.30 | 0.17 |
| ND | 17 | 0.0067 | 0.0038 | 3.75 | 14.20 | 0.27 | 0.26 |
| NT | 5 | 0.0032 | 0.0016 | 26.73 | 17.86 | 0.26 | 0.10 |
| SD | 4 | 0.0033 | 0.0019 | 32.53 | 27.48 | 0.21 | 0.17 |
| ST | 9 | 0.0034 | 0.0014 | 18.76 | 20.24 | 0.27 | 0.15 |
| State | 67 | 0.0049 | 0.0029 | 13.30 | 20.83 | 0.27 | 0.17 |

$f_H$= 0.4992, the results shown in Figure 4.1b are almost the same as those shown for $ET_{M,H}$ in Figure 3b which uses $T_{mean}$ with a weightage of 0.5 for $T_{min}$. Therefore, for the Davangere station, the use of Equation 4.3 with $T_{eff}$ defined by Equation 4.4b does not yield any additional benefit. While the same inference is true for the comparison between estimates of $ET_{0,PM}$ and $ET_{M,Hgh}$ shown in Figure 4.3c with optimal parameter values of $g_H$ = 0.5021 and $h_H$ = 0.4990, later analysis showed that for other stations values of g and h deviated significantly from 0.5.

Using a similar procedure, $ET_{M,Hf}$ estimates by the HG equation (Equation 4.3) with $T_{eff}$ defined by Equation 4.4b were used to calibrate the parameter $f_H$ at the remaining 66 stations using $ET_{0,PM}$ estimates. Station-wise optimal values of $f_H$(not shown for brevity) indicated that they varied between 0.49 to 0.54. For the study area as a whole, the mean value of $f_H$= 0.50 with a standard deviation of 0.01 was obtained from which it may be concluded that Equation 4.4b does not offer any significant improvement in accuracy over the use of $T_{mean}$ in the HG equation (Equation 4.2). Since $ET_{M,Hgh}$ values were almost identical to $ET_{M,H}$ estimates, the former approach was discarded from all further analysis of this study.

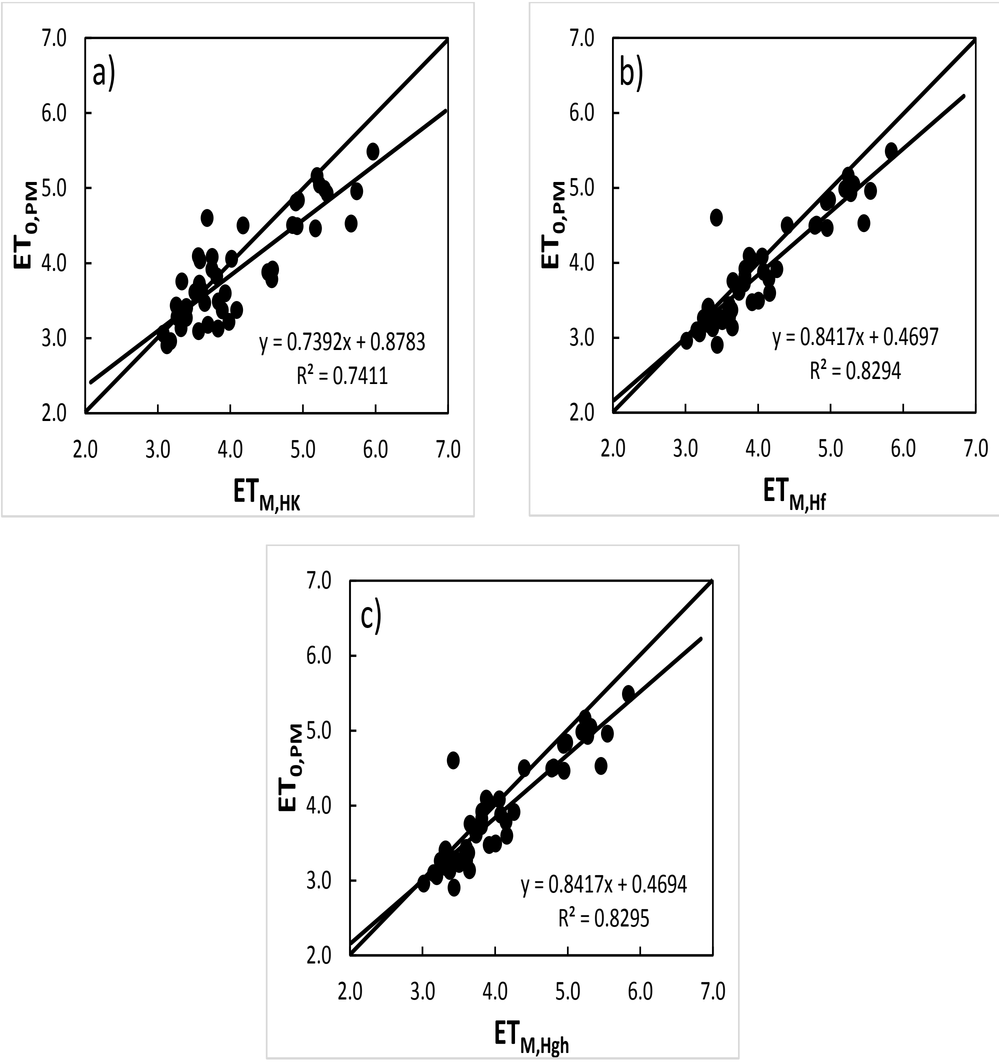


**Figure 4.3: Comparison of estimates by PM equation ($ET_{0,PM}$) with estimates by the a)HG Equation (4.4a) ($ET_{M,HK}$) and b) HG Equation (4.4b) ($ET_{M,Hf}$) c) HG Equation (4.4c) ($ET_{M,Hgh}$) for the validation phase at Davangere station (CD1)**

Table 4.3 shows optimal values of parameters $K_H$ (Equation 4.4a) and g and h (Equation 4.4c) which were obtained by calibration with $ET_0$ estimates by the PM method (Equation 3.1) using the monthly values for the period January 2006 – December 2012 (84 months). For brevity, mean and standard deviation values for the parameters for stations pooled under different agro-climatic zones and for the State are shown therein. It can be seen that the mean value of the parameter $K_H$ was 0.68 with a reasonably low value of the standard deviation of 0.04 for the State as a whole. The range of values of $K_H$ for most of the zones was between 0.64 and 0.68 except for the CO zone where the highest mean value of 0.74 was recorded. The parameter $g_H$

shows high variability ranging from 0.41 in the ED zone to 0.79 in the NED zone. The overall mean value of $g_H$ is 0.56 with a high SD of 0.27 which indicates that local calibration is required for this parameter. The parameter $h_H$ also showed high variability with the lowest value of 0.32 in NED and the highest value of 0.56 in the ED zone. Parameter $h_H$ was also accompanied by high values of standard deviation (Table 4.3) indicating high variability within any given agro-climatic zone. Also, it is interesting to note from Table 4.3 that except for Central Dry (CD) and Eastern Dry (ED) zones where optimized mean $g_H$ values are lower than the optimized mean values of $h_H$, in all other zones and for the State as a whole, the opposite is true. This implies that the weightage assigned to $T_{min}$ (parameter $g_H$) is larger than that assigned to $T_{max}$ (parameter $h_H$) while computing $T_{eff}$ by Equation 4.4c in a large part of the study area. Figure 4.4 depicts the spatial variabilities of the optimized HG model parameters $K_H$, $g_H$, and $h_H$ over the study area obtained by interpolating between station-wise parameter values. Significant clusters with low values and high values of the parameter $K_H$ in certain areas were visible. Variability of parameters $g_H$ and $h_H$ across the state was more or less uniform.

Performance statistics of the HG equations using effective temperature (Eqs. 4.4, 4.4a, and 4.4c) relative to the PM equation (Equation 3.1) during the validation phase of 48 months (2013-2016) are shown in Table 4.1. Again, for brevity minimum and maximum values of statistics $R^2$, RMSE, and MBE for stations pooled under different agro-climatic zones and also for the State as a whole are listed therein. Comparison of $ET_{M,HK}$ values relative to $ET_{0,PM}$ estimates indicate that local calibration of the parameter in Equation 4.4a does not yield many benefits in terms of performance statistics $R^2$, RMSE, and MBE values. Except in very few cases such as the CO and NT zones (Table 4.1), the maximum values of $R^2$ for this method indicate that it fails to match the performance of the modified HG equation. Surprisingly, despite local calibration, the accuracy of $ET_{M,HK}$ estimates do not match even the original HG equation estimates ($ET_{0,H}$). The same conclusion regarding the accuracy of $ET_{M,HK}$ estimates being poorer than $ET_{M,H}$, and $ET_{0,H}$ values in most of the zones, and for the State as a whole may be drawn upon examination of results in Table 4.1. On

**Table 4.3: Mean and standard deviations of optimal parameters of HG equations using effective temperature (Equation 3, 3a, 3c) for stations pooled in each agro-climatic zone**

| Zone | No. of Stations | $K_H$ | | $g_H$ | | $h_H$ | |
|---|---|---|---|---|---|---|---|
| | | Mean | Std. Dev | Mean | Std. Dev | Mean | Std. Dev |
| CD | 6 | 0.67 | 0.06 | 0.42 | 0.25 | 0.55 | 0.17 |
| CO | 5 | 0.74 | 0.05 | 0.60 | 0.14 | 0.43 | 0.10 |
| ED | 4 | 0.69 | 0.05 | 0.41 | 0.40 | 0.56 | 0.27 |
| HL | 5 | 0.66 | 0.04 | 0.63 | 0.14 | 0.43 | 0.08 |
| NED | 7 | 0.70 | 0.01 | 0.79 | 0.67 | 0.32 | 0.43 |
| NET | 5 | 0.64 | 0.04 | 0.51 | 0.03 | 0.49 | 0.02 |
| ND | 17 | 0.68 | 0.02 | 0.51 | 0.04 | 0.49 | 0.03 |
| NT | 5 | 0.67 | 0.03 | 0.68 | 0.21 | 0.39 | 0.13 |
| SD | 4 | 0.67 | 0.04 | 0.62 | 0.13 | 0.42 | 0.08 |
| ST | 9 | 0.67 | 0.02 | 0.53 | 0.08 | 0.48 | 0.05 |
| State | 67 | 0.68 | 0.04 | 0.56 | 0.27 | 0.46 | 0.17 |

the other hand, the performance of the HG equation (Equation 3) with $T_{eff}$ defined by Equation 4.4c (i.e., $ET_{M,Hgh}$) is significantly superior. In terms of $R^2$ values, this approach involves local calibration of parameters and is better than the original HG equation (Equation 4.1) in all zones and better than or on par with the modified HG equation (Equation 4.2) in many zones. Values of RMSE and MBE for $ET_{M,Hgh}$ estimates (Table 4.1) also indicate that this approach provides the lowest errors and bias in several zones and for the State as a whole it performs on par with the modified HG equation (Equation 4.2).

Since the results of the performance evaluation of the four HG models tested in the present study during the validation phase were presented in Table 4.1 by pooling stations in each zone and for the study area as a whole, a simple favourable statistic-based approach was implemented to provide information on station-wise performances. Accordingly, as described in Article 4.2, a score of 1 was assigned to the method which yielded the best value of a particular performance statistic (highest value of $R^2$, lowest values of RMSE, and MBE) at each station. Subsequently, scores were summed for each method under each statistic for all stations pooled in agro-climatic zones and for the State as a whole. For example, at the Davangere station located in the CD zone, $R^2$ values obtained during the validation phase are 0.81, 0.83, 0.74, and 0.83 for $ET_{0,H}$, $ET_{M,H}$, $ET_{M,HK}$ and $ET_{M,Hgh}$ estimates respectively. Accordingly, the modified HG equation (Equation 4.2) with the highest $R^2$ value of 0.83 was assigned a score of 1. However, since $ET_{M,Hgh}$ estimates also yielded the same value of $R^2$, Equation 4.3 with $T_{eff}$ computed using Equation 4.4c was also assigned a score of 1. Next, considering the values of RMSE and MBE at the Davangere station, scores were assigned to the HG equations. Using this procedure, scores were assigned to all four HG equations at all 67 stations considered in the present analysis. Results of this analysis shown in Table 5 are presented in terms of the number of stations with favourable performance yielded by each method during the validation phase in different zones.

The last row in Table 4.4 indicates that the performance of the original HG equation (Equation 4.1) with standard values of parameters was the poorest among all methods considered at the 67 stations located in the State. Although the method yielded the highest $R^2$ and lowest MBE values between $ET_{0,H}$, and $ET_{0,PM}$ estimates at 15 and 12 stations respectively, RMSE values were lowest at only 4 stations. In terms of $R^2$ and MBE values, the best performance of the original HG equation was recorded in the Southern Transition (ST) zone. With local calibration of parameters, the performance of the modified HG equation (Equation 4.2) showed remarkable improvement in performance in terms of all three statistics. $ET_{M,H}$ estimates yield the highest value of $R^2$ at 34 stations (Table 4.4) and the lowest RMSE values at 45 of the 67 stations in the State. MBE values were lowest at 24 stations. It is not only the number of stations at which the modified HG equation performed better but as was pointed out earlier, results shown in Table 4.1 indicate that the magnitude of reduction in error and bias was quite substantial for $ET_{M,H}$ estimates in comparison to $ET_{0,H}$ estimates. The performance of Equation 4.2 with optimized parameters was best in the Northern Dry (ND) zone and also consistently good across all the agro-climatic zones recording the best statistics at more than 50% of the stations in many zones. The performance of the HG equation using $T_{eff}$ in place of $T_{mean}$ (Equation 4.3) with $T_{eff}$ being computed

**Table 4.4: Results of favourable statistic-based performance analysis of the four HG equations for stations pooled in each agro-climatic zone**

| Zone | No. of Stations | $R^2$ | | | | RMSE ($mm\ d^{-1}$) | | | | MBE ($mm\ d^{-1}$) | | | |
|---|---|---|---|---|---|---|---|---|---|---|---|---|---|
| | | $ET_{0,H}$ | $ET_{M,H}$ | $ET_{M,HK}$ | $ET_{M,Hgh}$ | $ET_{0,H}$ | $ET_{M,H}$ | $ET_{M,HK}$ | $ET_{M,Hgh}$ | $ET_{0,H}$ | $ET_{M,H}$ | $ET_{M,HK}$ | $ET_{M,Hgh}$ |
| CD | 6 | 2* | 4 | 1 | 4 | 0* | 3 | 3 | 3 | 1* | 2 | 3 | 1 |
| CO | 5 | 1 | 3 | 3 | 3 | 0 | 4 | 1 | 4 | 1 | 1 | 3 | 2 |
| ED | 4 | 2 | 2 | 0 | 1 | 0 | 3 | 0 | 1 | 1 | 2 | 0 | 1 |
| HL | 5 | 2 | 1 | 1 | 2 | 0 | 2 | 2 | 3 | 0 | 0 | 2 | 3 |
| NED | 7 | 1 | 4 | 1 | 5 | 0 | 4 | 3 | 3 | 0 | 3 | 4 | 2 |
| NET | 5 | 1 | 4 | 0 | 3 | 1 | 4 | 0 | 3 | 1 | 2 | 2 | 1 |
| ND | 17 | 1 | 11 | 4 | 12 | 1 | 13 | 3 | 11 | 1 | 10 | 6 | 10 |
| NT | 5 | 1 | 1 | 0 | 4 | 1 | 2 | 0 | 4 | 1 | 2 | 1 | 2 |
| SD | 4 | 0 | 2 | 0 | 4 | 0 | 3 | 0 | 4 | 2 | 0 | 0 | 2 |
| ST | 9 | 4 | 2 | 4 | 4 | 1 | 7 | 2 | 5 | 4 | 2 | 3 | 2 |
| State | 67 | 15 | 34 | 14 | 42 | 4 | 45 | 14 | 41 | 12 | 24 | 24 | 26 |

. ** Numbers indicate the number of stations where the HG equation yielded the highest value of* $R^2$ *and lowest values of RMSE and MBE in comparison to the other equations.*

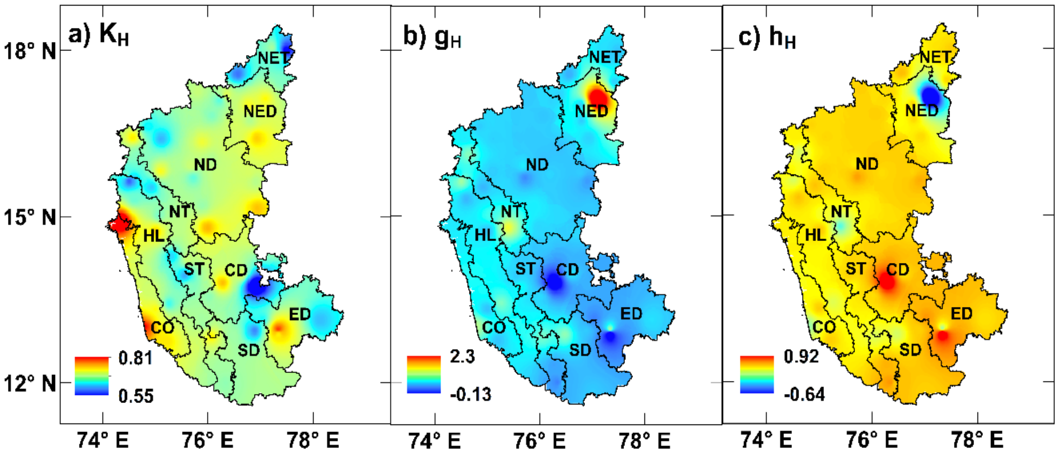


**Figure 4.4: Maps depicting spatial variations of optimized HG model parameters $K_H$, $g_H$, and $h_H$ (Equation 4.4a, 4.4c) over the study area**

by Equation 4.4a ($ET_{M,HK}$ estimates) was superior to the original HG equation ($ET_{0,H}$ estimates) in terms of RMSE and MBE but slightly poorer in terms of $R^2$ (Table 4.1). Given the fact that this approach involved the optimization of an additional parameter (K), its performance was not significantly better across any of the zones either. On the contrary, the other HG equation using $T_{eff}$ in place of $T_{mean}$ (Equation 4.3) with $T_{eff}$ being computed by Equation 4.4c ($ET_{M,Hgh}$ estimates) provided the best comparisons to $ET_{0,PM}$ estimates among all the methods tested in terms of the highest $R^2$ (42 stations) and lowest MBE (26 stations) across 67 stations located in the State (Table 4.1). However, in terms of the number of stations with minimum RMSE, this method was slightly poorer than the modified HG equation ($ET_{M,H}$ estimates). Results shown in Table 4.1 indicate that $ET_{M,Hgh}$ estimates compare favourably with $ET_{0,PM}$ estimates across all agro-climatic zones. But it must be noted that despite having the advantage of error minimization with additional two parameters $ET_{M,Hgh}$ estimates did not yield substantially lower errors nor bias in comparison to $ET_{M,H}$ estimates (Table 4.1).

Therefore, from the overall results of the performance analysis of the four HG equations considered in the present study, it appears that the modified HG equation (Equation 4.2) with the local calibration of three parameters is the most preferred approach to obtain estimates of Equation$ET_0$ with limited data which are closest to those obtained by the more data-intensive PM method (Equation 3.1) in Karnataka State, India. Although replacing mean temperature ($T_{mean}$) with effective mean temperature ($T_{eff}$) defined by Equation 4.4c provides slightly more accurate results (Tables 4.1 and 4.4), this benefit is offset by the need to optimize two additional parameters. The novel 'favourable statistic-based' evaluation approach developed and implemented in this study appears to be extremely useful in extracting precise information on the relative performances of multiple models when they are evaluated using diverse statistical measures using large datasets.

### 4.4.3 Discussion

The main focus of the present study was to evaluate the effect of simultaneous local calibration of all three parameters in the Hargreaves-Samani (HG) $ET_0$ equation on its accuracy in a region subject to significant spatial heterogeneity in climatic conditions. Also, the study considered the effect of replacing the mean air temperature ($T_{mean}$) variable in the HG equation with an effective air temperature ($T_{eff}$) which uses variable weightages for the maximum and minimum air temperature variables. The analysis was carried out using climate records for the 11-year historical period (2006-2016) for 67 stations located in 10 different agro-climatic zones of Karnataka State, India. Comprehensive performance evaluation of the original HG equation with standard parameters modified HG equation with the local calibration of three parameters, and local calibration of three alternative versions of the modified HG equation with the use of $T_{eff}$ (Eqs. 4.3, 4.4a, 4.4b, and 4.4c) was carried out. The accuracy of monthly mean daily $ET_0$ estimates by all five methods was assessed using $ET_0$ estimates by the FAO-56 Penman-Monteith (PM) equation as reference considering stations pooled under different agro-climatic zones and also the entire study area.

Results indicated that the performance of the original HG equation during the validation phase was quite poor as reflected in low values of coefficient of determination ($R^2$) and high values of root mean square error (RMSE) and mean bias error (MBE) values across all zones. Among all the methods evaluated, this approach yielded the best values of performance statistics at the smallest number of stations in the study area. Therefore, it may be deduced that the standard values of the three parameters in Equation 4.1 do not apply to a large number of stations in Karnataka State if $ET_0$ estimates are comparable to those by the PM method ($ET_{0,PM}$) are desired. On the other hand, the results shown in Table 4.1 indicate that when the parameters of the HG equation ($a_H$, $b_H$, and $c_H$) were treated as unknowns (Equation 4.2) and their optimal values were determined at each station by minimizing the sum of squared errors with reference to $ET_{0,PM}$ estimates, the accuracy of $ET_{0,H}$values improved significantly. It was noted that when Equation 4.2 with optimal values of $a_H$, $b_H$, and $c_H$ was independently validated, RMSE values at most stations located across different agro-climatic zones were reduced by more than 50% in comparison to the original HG equation. Although $R^2$ values were quite low at a few stations, MBE values also improved indicating a reduction in bias in $ET_{M,H}$estimates in comparison to $ET_{0,PM}$ estimates. This improvement in the performance of the modified HG equation was on account of the fact that the optimal parameter values were quite different from the standard values. For example, the mean value of the parameter $a_H$ varied over the range 0.0032 to 0.0067 for stations pooled under the ten agro-climatic zones with a mean value of 0.0049 for the 67 stations in the study area indicating a significant departure from the standard value of 0.0023. Parameter $b_H$ indicated much higher variability across the zones ranging from -0.74 to 34.95 with a mean value of 13.3 for the study area as against the standard value of 17.8. Although exhibiting comparatively lower variability, the mean value of the parameter $c_H$ was 0.27 for the study area with a range of 0.20-0.39 across the zones indicating a departure from the standard value of 0.5. Using station-wise values of optimized parameters, maps depicting spatial variabilities of $a_H$, $b_H$, and $c_H$ were generated which will prove useful to researchers/practitioners to select location-specific values in the study area. Although preliminary analysis revealed that parameters $a_H$ and $b_H$ were correlated with station elevations, further studies are needed to explore the effect of other influencing variables before methods for regional parameter estimation can be developed. Results indicated that replacing $T_{mean}$ with $T_{eff}$ defined by Equation 4.4c does offer a small increase in accuracy of $ET_0$ estimates, but this is offset by the need to optimize 2 additional parameters ($g_H$ and $h_H$) in Eqs. 4.3 and 4.4c.

CHAPTER 5

# PERFORMANCE EVALUATION OF SIMPLER $ET_0$ EQUATIONS

## 5.1 GENERAL

The primary objective of the present research was to evaluate the performances of simpler alternative $ET_0$ equations against the PM equation across heterogenous agro-climatic zones in Karnataka state. Accordingly, four simpler alternative equations namely, FAO-24 radiation (RAD), Priestley-Taylor (PT), Turc (TC), and Blaney-Criddle (BC) were considered in the analysis. The climate dataset described in Chapter 2 along with PM $ET_0$ estimates derived in Chapter 3 were used to evaluate the performances of these equations. Review of relevant literature and complete details of the simpler equations and the methodology adopted for performance evaluation are provided in subsequent sections of this chapter.

## 5.2 RELATIVE PERFORMANCE ANALYSIS

Numerous studies have developed and evaluated the performances of these equations under different climatological conditions, with Katul et al. (1992), Amatya et al. (1995), Khandelwal et al. (1999), Mall and Gupta (2002), Jothiprakash et al. (2007,2008), being a few of the important ones. The majority of comparative studies have shown the superiority of combination-type $ET_0$ equations. In particular, the physically-based Penman-Monteith (PM) combination equation has proved to be the best estimator of $ET_0$ across a wide range of climates (Jensen et al. 1990). McMahon et al. (2013) provide a guide for more than 12 methods in finding evaporation as well as ET, it is highly unlikely to incorporate all methods in the study due to limitations in the availability of data, and therefore in the current study globally accepted standard forms of equations with full climatic data and limited climatic data are used.

McKenney and Rosenberg (1993) articulate PM as the only method which is capable of reflecting actual ET rates under conditions of limited soil moisture and results reveal that PM estimates of PET are somewhat less responsive to changes in all climate variables compared to other methods, not surprisingly GCM scenarios indicate for increases in temperature and solar radiation. Temesgen et al. (2005) demonstrate the robustness of the FAO PM method and mention if there is complete input data local calibration may not be required. This study also compared the FAO PM equation, FAO 56 PM, CIMIS Penman equation, Hargreaves, and Radiation equation at daily and hourly time steps across 37 agricultural weather stations across California State reports despite differences in microclimates no visible spatial trends were found between $ET_0$, the observed values showed a difference of 14% (CIMIS v/s ASCE PM) and 25% (CIMIS v/s FAO56 PM).Kisi (2014) evaluated nine different $ET_0$ methods against PM $ET_0$ in the Mediterranean region. The study concluded the performance of Valiantzas equation was best while Hargreaves ranked next. The Turc method was found to be the least-performing method. Kovoor (2006) studied the impact of climate change on CWR and IWR. To derive CWR, firstly $ET_0$ estimates were obtained at four stations across India. Results showed the performance of simpler equations with less error in monthly $ET_0$ estimates. The performance of regression equations against the PM $ET_0$ developed yielded better results than the original equations. Thomas (2000) analyses the time series 1954–1993 of Penman-Monteith evapotranspiration estimates for 65 stations in mainland China and Tibet. The analysis shows that for China as a whole, the PET has decreased in all seasons. Urrea et al. (2006) calculated average daily $ET_0$ by seven methods for semiarid climate from 2000 to 2002 using a continuous weighing lysimeter with precision. FAO-56 Penman-Monteith equation turned out to be the most precise method under semiarid climatic conditions. Nandagiri and Kovoor (2006) evaluate the performances of seven $ET_0$ methods, representing temperature-based, radiation-based, pan evaporation-based, and combination-type equations, which were compared with the FAO-56 PM method using historical climate data from four stations located one each in arid (Jodhpur), semiarid (Hyderabad), subhumid (Bangalore), and humid (Pattambi) climates of India. The novelty of the study was it investigated the reasons for the climate-dependent success of the simpler alternative $ET_0$ equations using multivariate factor analysis techniques. For each climate, datasets comprising FAO-56 PM $ET_0$ estimates. Kundu et al. (2017) projected future ET changes for a period of 40 years (1961-2001) using HADCM3 data by the Hargreaves method with the changes in the pattern of different climate variables. Three major parameters of climate, i.e., rainfall, temperature, and reference evapotranspiration were considered to downscale the future projection of climate by the least-square support vector machine method. The study recommends the use of temperature based-based Hargreaves method as an alternative during the non-availability of complete data for the PM method.

Stockle (2004) used ClimGen, generated datasets: daily $R_s$ and vapour pressure deficit was estimated from temperature data and used to calculate evapotranspiration at five locations, representing tropical, temperate, semi-arid, and arid climates. Weekly analyses showed significant improvement in performance for both $R_s$ and vapour pressure deficit estimations in arid and semi-arid locations. The daily PM $ET_0$ results were poor to acceptable in all locations, but analyses for weekly periods showed the improved performance to acceptable and good levels for arid and semi-arid locations. A non-calibrated version of the Hargreaves method did not work for either daily or weekly periods. The PM $ET_0$ and HG $ET_0$ methods appeared suitable for weekly periods in arid and semi-arid locations provided that at least 2 years of complete weather records were available to calibrate the parameters required.

Jabloun and Sahli (2008) compare $ET_0$ estimates using limited data to those computed with full data sets and revealed that the difference between $ET_0$ obtained from a full and limited data set is small considering the 8 locations studied. Both the mean bias error and RMSE of the comparison were less than 0.6 and 0.8 with a minimum of 0.4 and 0.2 $\mathrm{mm\ d^{-1}}$, respectively, leading to small errors in the $ET_0$ estimates. These deviations were significantly higher when using the Hargreaves equation to calculate $ET_0$. Thus, the use of $T_{dew} = T_{min}$ in the FAO-56 PM equation could be a good alternative to estimate $e_a$ when measured RH values are missed. The use of the average annual wind speed of the location instead of daily records leads to acceptable estimates of $ET_0$, especially for high $ET_0$ rates (>4 $\mathrm{mm\ d^{-1}}$). Results obtained from the comparison of $ET_0$ daily estimates by the Hargreaves equation against FAO-56 PM, throughout Tunisian locations showed a systematic overestimation at inland sites, though in coastal areas, the Hargreaves equation tends to underestimate $ET_0$.

## 5.3 ORIGINAL $ET_0$ EQUATIONS

Five $ET_0$ equations namely, FAO-56 PM Penman-Monteith (PM), FAO-24 radiation (RAD), Priestley-Taylor (PT), Turc (TC), and Blaney-Criddle (BC) in their 'original' form mentioned below were used to calculate daily $ET_0$ ($\mathrm{mm\ d^{-1}}$). Since measured $ET_0$ data was unavailable for the study area, the standard FAO-56 PM was used as a 'reference' method to evaluate the other $ET_0$ methods. In this study, standard recommended procedures laid out in Allen et al. (1998) were used to compute variables and estimate $ET_0$ by all five methods.

### 5.3.1 Blaney-Criddle equation

In this study, Blaney -Criddle equation given by Allen and Pruitt (1986) is used

$$ET_{0,B} = \{a_B + b_B\left[p\left(0.46T_{mean} + d_B\right)\right]\}\left[1 + 0.1\frac{z}{1000}\right] \tag{5.1}$$

where $ET_{0,B}$ is the daily reference evapotranspiration estimated by the BC equation ($\mathrm{mm\ d^{-1}}$), $a_B$, $b_B$ and $d_B$ are the parameters calculated as per Doorenbos and Pruitt (1977) and Frevert et al. (1983), p is the ratio of actual daily day time hours to annual mean daily time hours (%) and $T_{mean}$ is the mean daily air temperature ($^{\circ}C$).

### 5.3.2 Priestley-Taylor equation

In this study, the Priestley-Taylor equation given by Mc. Mahon et al. 2013 is used

$$ET_{0,P} = \alpha\frac{\Delta}{\Delta + \gamma}\left(R_n\right) \tag{5.2}$$

$ET_{0,P}$ is the daily reference crop evapotranspiration estimated by the Priestley-Taylor method ($\mathrm{mm\ d^{-1}}$), α is the Priestley-Taylor constant, $R_n$ is the net radiation at crop surface ($\mathrm{MJm^{-2}day^{-1}}$), and Δ is the slope of saturation vapour pressure versus temperature curve.

### 5.3.3 FAO- 24 Radiation equation

In this study, FAO- 24 Radiation equation given by Doorenbos and Pruitt (1977) is used

$$ET_{0,R} = b_r\left[\frac{\Delta'}{\Delta' + \gamma'}\left(R'_s\right)\right] - 0.3 \tag{5.3}$$

where $ET_{0,R}$ is the daily reference crop evapotranspiration estimated by the FAO-24 radiation method ($\mathrm{mm\ d^{-1}}$), $b_r$ is adjustment factor computed from $\mathrm{RH_{mean}}$ and wind speed; $\Delta'$ is the slope of saturation vapour pressure versus temperature curve ($\mathrm{mm\ d^{-1}}$); $\gamma'$ is the psychrometric constant, and $R_s$ is incoming solar radiation ($\mathrm{mm\ d^{-1}}$).

### 5.3.4 Turc equation

In this study, the Turc equation given by McMahon et al. (2013) is used

$$ET_{0,T} = 0.013\left(\frac{T_{\text{mean}}}{T_{\text{mean}} + 15}\right)(23.8856 * R_s + 50)\left(1 + \frac{50 - RH_{\text{mean}}}{70}\right) \text{ for RH} < 50 \tag{5.4a}$$

$$ET_{0,T} = 0.013\left(\frac{T_{\text{mean}}}{T_{\text{mean}} + 15}\right)(23.8856 * R_s + 50) \text{ for RH} > 50 \tag{5.4b}$$

$ET_{0,T}$ is the daily reference crop evapotranspiration estimated by the Turc method ($\mathrm{mm\ d^{-1}}$), $T_{mean}$ is the mean daily air temperature, $R_s$ is the incoming solar radiation ($\mathrm{MJm^{-2}day^{-1}}$), $\mathrm{RH_{mean}}$ is the mean relative humidity (%).

## 5.4 SPATIO-TEMPORAL VARIATION OF ORIGINAL $ET_0$

For each of 67 stations monthly $ET_0$ values ($\mathrm{mm\ d^{-1}}$) were computed using the original forms of the five methods – PM, BC, PT, RAD and TC (Equations 3.1, and 5.1-5.4b) for the period 2006-2016. Maps showing the spatial distribution of mean $ET_0$ estimates by the five methods for the entire calibration period were derived from station-wise estimates using the inverse distance weightage interpolation (IDW) method and are depicted in Figure 5.1. Also, to provide a picture of the relative magnitudes and seasonal variations of monthly mean $ET_0$ estimates by all five methods, time series plots across different zones are shown in Figure 5.2.

It can be seen from Figure 5.1 $ET_0$ values of all five methods showed significantly higher values in the northern regions but were converse compared to the southern regions' SD zone where $ET_0$ values were significantly less. The overall average $ET_0$ PM for the entire state ranged from 2.68 to 4.58 $\mathrm{mm\ d^{-1}}$ with the highest value at Siruguppa station in the ND zone and lowest at Hunsur in the ST zone. Likewise, the seasonal variability of PM is maximum during pre-monsoon seasons (March to

May). Similarly, the comparisons of the other five $ET_0$ methods showed the RAD method to be maximum at 5.13 $\mathrm{mm\ d^{-1}}$ and of all the methods BC method yielded the lowest $ET_0$ value of 2.1 $\mathrm{mm\ d^{-1}}$ at Hunsur. In the northern region, the overall $ET_0$ was highest but clusters of lower PT values were observed in three zones at NET, NED and ND zones.

Results depicted in Figure 5.1a reveal that the classification of the State into agro-climatic zones based on various criteria (Section 2.2.3) appears valid for the spatial distribution of PM $ET_0$ estimates too. As can be seen, $ET_0$ estimates (and also climate variables, Figure 3.1) are more or less uniformly distributed over each zone except for some clusters of high/low values appearing in some zones which may have resulted on account of spatial interpolation from point values. An examination of SD (not shown here for brevity) and CV values also indicated low temporal variabilities of PM $ET_0$ within most of the agro-climatic zones further confirming the efficacy of classifying the Karnataka State into 10 agro-climatic zones. Since $ET_0$ is an integrated response to prevailing climatic conditions which in turn is affected by various other criteria, the results of this study suggest that patterns in the spatial variability of $ET_0$ may be used to discretize large heterogeneous regions into smaller homogeneous climatic zones.

Figure 5.2 depicts the intra-annual variations in mean $ET_0$ estimates averaged over climate stations located within each agro-climatic zone. Considering the most accurate PM estimates ($ET_{0,PM}$), it can be seen that values steadily rise from January and peak during the month of April. The magnitude of the peak value varies from one zone to another with high values of the order of 5 $\mathrm{mm\ d^{-1}}$ occurring in the northern dry zones (NED, NET, ND, NT) and lower peaks of about 4.5-5 $\mathrm{mm\ d^{-1}}$ in the other zones. With the onset of the monsoon rains in May-June, $ET_0$ values begin to decrease from around 3.5-4 $\mathrm{mm\ d^{-1}}$ in the northern dry zones to 3 $\mathrm{mm\ d^{-1}}$ in the other zones. Extremely low values of $ET_0$ (2.5 $\mathrm{mm\ d^{-1}}$) are witnessed during the peak monsoon months (June-August) in the coastal zone (CO). A small recovery in the magnitude of $ET_0$ during the post-monsoon season (September-October) followed by a reduction to low values of 3 $\mathrm{mm\ d^{-1}}$ during the winter months (November-

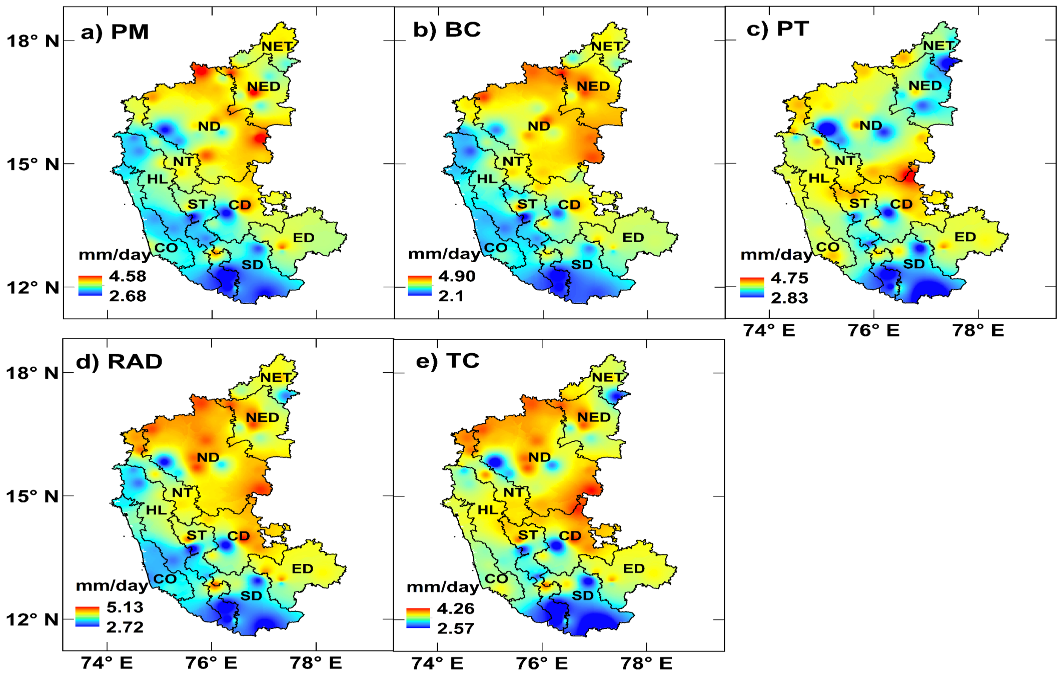


**Figure 5.1: Spatial variability of $ET_0$ estimates obtained using a) Penman-Monteith b) Blaney-Criddle c) Priestley-Taylor d) Radiation e) Turc methods**

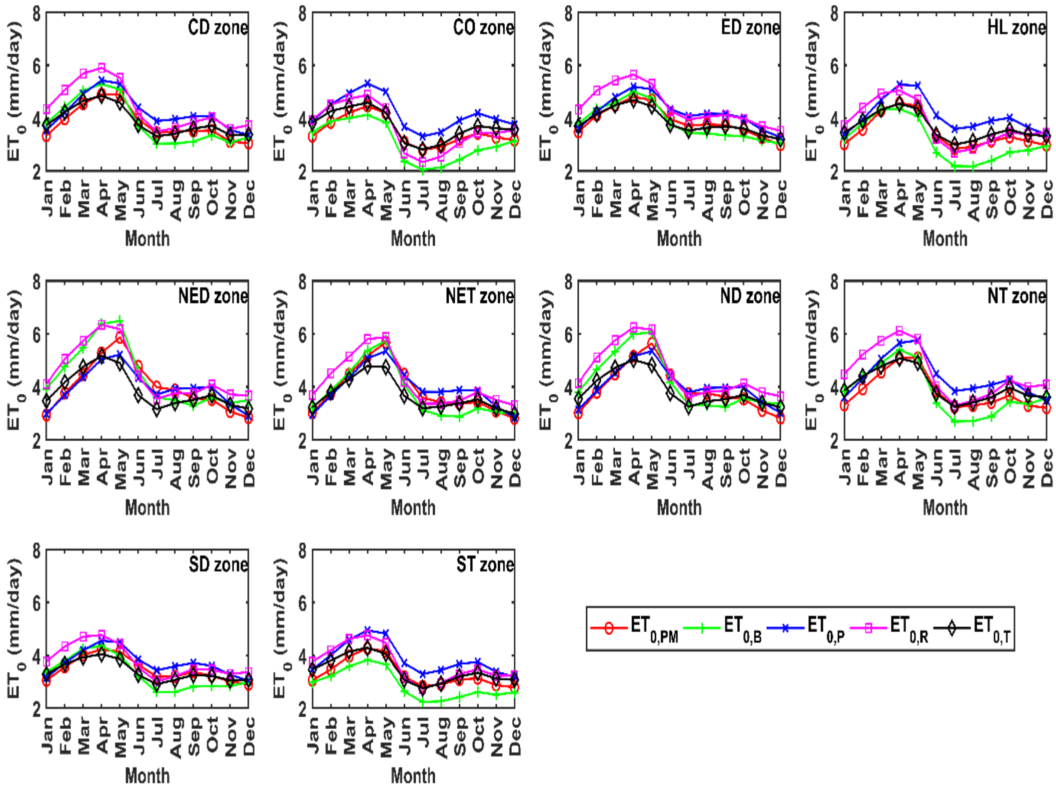


**Figure 5.2: Seasonal variability of $ET_0$ by different methods**

December) is evident in most of the zones (Figure 5.2).

A comparison of the intra-annual variations in $ET_0$ estimates provided by the simpler alternative equations relative to the PM $ET_0$ estimates can be seen in Figure 5.2. The performance of the BC equation ($ET_{0,B}$) is reasonably accurate during the year across most of the zones, except for overestimation during the summer months in the NED and ND zones. The BC equation also exhibits underestimation during the monsoon and winter months in several zones. The Priestley-Taylor estimates ($ET_{0,P}$) appear to be consistently higher than $ET_{0,PM}$ values during most of the months across all zones with the overestimation being more pronounced in the CO and HL zones. The FAO-24 Radiation equation provides the largest estimates ($ET_{0,R}$) during all months in all zones except in the CO and HL zones where the estimates are comparable to $ET_{0,PM}$ estimates. Figure 5.2 indicates that $ET_0$ estimates by the Turc method ($ET_{0,T}$) are most comparable to the PM method across all months and zones with a slight underestimation being seen during the monsoon months in the NED zone.

## 5.5 COMPARISON OF DIFFERENT ORIGINAL $ET_0$ METHODS

Performance statistics defined in Eqs. 4.6-4.8 were computed to assess the accuracy of the simpler alternative $ET_0$ equations (Eqs. 5.1-5.4b) relative to the PM method (Equation 3.1) for the validation period, January 2013-December 2012 (48 months) at each of the 67 stations. However, for the sake of brevity, the mean values of the performance statistics for stations lying within each agro-climatic zone were computed and are presented in Table 5.1.

Considering the original BC equation (Equation 5.1), it can be seen from Table 5.1 that its performance relative to the PM equation was relatively good in most agro-climatic zones as evident from $R^2$ values exceeding 0.68. The best performance of the BC equation was in the NET, NT and ED zones where $R^2$ values ranged from 0.81 to 0.82. The lowest values of RMSE (0.61 $\mathrm{mm\ d^{-1}}$) for the BC equation were recorded in the NET and NT zones. The equation yielded RMSE values ranging between 0.67 – 0.78 $\mathrm{mm\ d^{-1}}$ in the other zones with the highest error being recorded in the SD zone. The BC equation yielded over-estimates in some zones and under-estimates in others as indicated by both positive and negative values of MBE. However, the magnitudes of MBE were relatively low in the CD, CO, ND, NET and NED zones indicating the consistent performance of the BC equation in these zones. Large overestimation was noted in the HL zone. Overall, the performance of this equation proved to be reasonably accurate, especially in the northern dry agroclimatic zones.

The original PT equation (Equation 5.2) provided the best $ET_0$ estimates relative to the PM equation in terms of $R^2$ among all the simpler alternative equations considered in this study. This is evident from the relatively high values of $R^2$ across all the zones (Table 5.1). This equation yielded the highest values of $R^2$ (0.88 – 0.89) in the NT and NET zones and $R^2$ values exceeding 0.70 in all the other zones except the NED zone. However, the PT equation recorded higher values of RMSE than the BC equation in 5 out of the 10 zones. Also, this equation provided significantly higher overestimates in almost all zones as indicated by the MBE statistic (Table 5.1).

The original RAD equation (Equation 5.3) yielded higher $R^2$ values than the BC equation in some zones but its performance was poorer than the PT equation based on this statistic. Also, this equation provided the highest values of RMSE among all the methods considered in almost all the zones again indicating poor performance. Further, the RAD equation consistently overestimated $ET_0$ values by a large magnitude as revealed by the high values of MBE across all zones (Table 5.1).

In terms of $R^2$, the performance of the original TC equation (Eqs. 5.4a and 5.4b) was the poorest among all the methods considered in almost all the zones. However, it yielded the lowest values of RMSE in most of the zones. Also, although this equation provided overestimates in some zones and underestimates in others, MBE values were the lowest in several zones.

Overall, the results shown in Table 5.1 indicate that the original PT equation (Equation 5.2) performed the best among the 4 alternative simpler equations in terms of $R^2$ and RMSE in most of the agroclimatic zones of the study area. However, the equation consistently overestimated $ET_0$ values relative to the PM equation in several of the zones.

**Table 5.1: Comparison of different $ET_0$ with FAO56**

| Zone No. | Zone | Variable | BC | PT | RAD | TC |
|---|---|---|---|---|---|---|
| I | Central Dry | $R^2$ | 0.68 | 0.82 | 0.72 | 0.68 |
| | | RMSE | 0.78 | 0.66 | 0.87 | 0.59 |
| | | MBE | 0.05 | 0.38 | 0.58 | 0.12 |
| II | Coastal | $R^2$ | 0.68 | 0.77 | 0.69 | 0.65 |
| | | RMSE | 0.74 | 0.69 | 0.89 | 0.56 |
| | | MBE | -0.08 | 0.43 | 0.60 | 0.14 |
| III | Eastern Dry | $R^2$ | 0.81 | 0.74 | 0.77 | 0.69 |
| | | RMSE | 0.74 | 0.79 | 0.79 | 0.66 |
| | | MBE | -0.16 | 0.28 | 0.37 | -0.03 |
| IV | Hilly | $R^2$ | 0.77 | 0.73 | 0.72 | 0.64 |
| | | RMSE | 0.69 | 0.53 | 0.77 | 0.61 |
| | | MBE | 0.31 | 0.07 | 0.44 | -0.08 |
| V | North Eastern Dry | $R^2$ | 0.70 | 0.64 | 0.71 | 0.60 |
| | | RMSE | 0.67 | 0.66 | 0.95 | 0.58 |
| | | MBE | 0.12 | 0.31 | 0.71 | 0.05 |
| VI | North Eastern Transition | $R^2$ | 0.82 | 0.89 | 0.83 | 0.80 |
| | | RMSE | 0.61 | 0.63 | 0.68 | 0.45 |
| | | MBE | -0.11 | 0.33 | 0.39 | 0.02 |
| VII | Northern Dry | $R^2$ | 0.76 | 0.73 | 0.71 | 0.65 |
| | | RMSE | 0.68 | 0.69 | 0.76 | 0.62 |
| | | MBE | -0.06 | 0.28 | 0.39 | -0.02 |
| VIII | Northern Transition | $R^2$ | 0.81 | 0.88 | 0.83 | 0.83 |
| | | RMSE | 0.61 | 0.68 | 0.63 | 0.38 |
| | | MBE | -0.23 | 0.48 | 0.36 | 0.10 |
| IX | Southern Dry | $R^2$ | 0.69 | 0.80 | 0.75 | 0.72 |
| | | RMSE | 0.93 | 0.75 | 1.05 | 0.59 |
| | | MBE | 0.24 | 0.58 | 0.84 | 0.34 |
| X | Southern Transition | $R^2$ | 0.72 | 0.57 | 0.63 | 0.57 |
| | | RMSE | 0.72 | 0.89 | 0.87 | 0.82 |
| | | MBE | -0.16 | 0.19 | 0.33 | -0.14 |

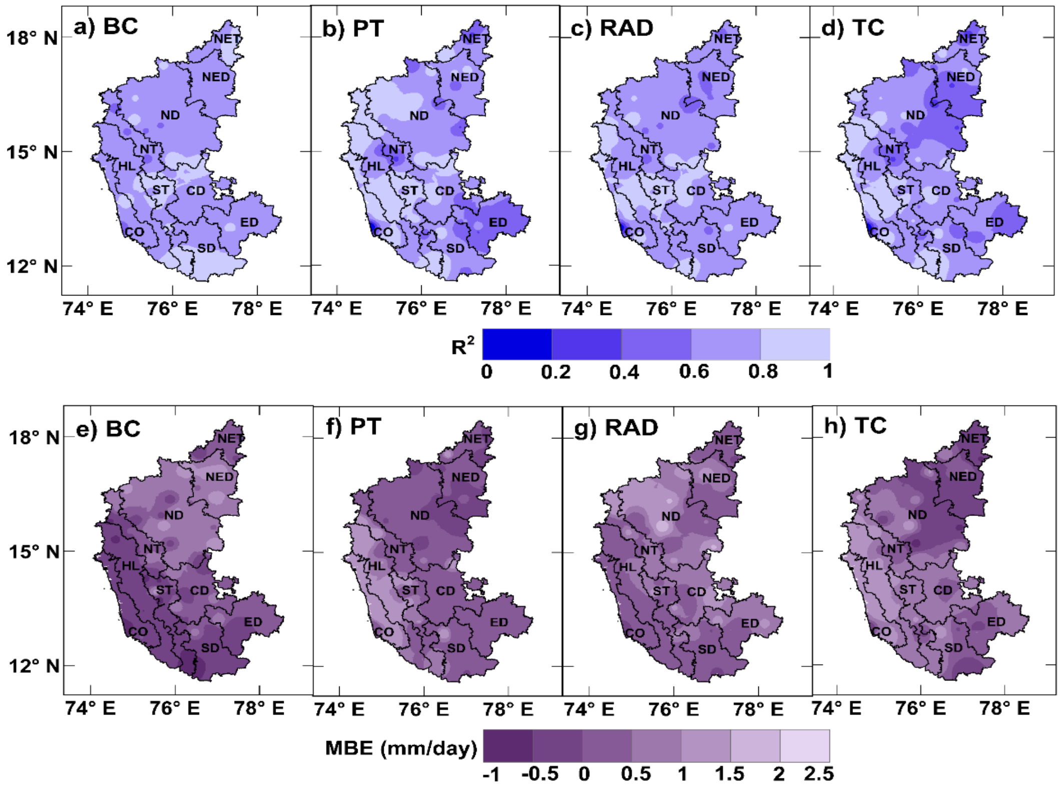


**Figure 5.3: Performance analysis of original and modified methods**

## CHAPTER 6

## LOCAL CALIBRATION OF SIMPLER $ET_0$ EQUATIONS

### 6.1 GENERAL

Quantification of evapotranspiration (ET) is essential in many studies related to hydrology, climate and irrigation engineering. It is a major hydrological process that provides linkages between the land-plant-atmosphere continuum. Given the complexity of the ET process due to the effect of a large number of factors related to climate, vegetation and soil moisture, direct estimation of actual ET from heterogeneous regions/catchments has proved to be difficult. Therefore, procedures to estimate ET rates have been proposed in which a key variable known as ‘Reference Crop Evapotranspiration’ ($ET_0$) (Allen et al. 1998) needs to be computed using historical records of climatic variables pertaining to air temperature, humidity, windspeed, and radiation/sunshine (Goyal 2004; Irmak et al. 2012; Jhajharia and Singh 2011; McVicar et al. 2012). $ET_0$ forms an essential forcing variable in hydrological, agricultural, and climate models (Attorre et al. 2007; Mardikis et al. 2005). The United Nations (UN) Food Agriculture Organization (FAO)’s Penman-Monteith (PM) equation is considered the sole benchmark method for calculating $ET_0$.

Several worldwide studies have shown the $ET_0$ estimates of FAO-56 PM are accurate across different climatic regimes (Bandyopadhyay et al. 2009; Bormann 2011; Garcia et al.2004; Itenfisu et al. 2003; Jhajharia et al. 2012; Masanta and Srinivas 2021; McKenney and Rosenberg 1993; McVicar et al. 2007; Mohan 1991; Verma et al. 2008; Xu and Singh 2002; Zhang et al. 2007). However, a major impediment to the routine use of the FAO-56 PM $ET_0$ equation is the requirement of input data pertaining to a large number of climatic variables. Specifically, the availability of humidity, radiation, and wind speed data is limited in less developed and developing nations, and therefore researchers/practitioners there are unable to use the preferred PM equation at a large number of locations. To overcome this limitation, significant research efforts have been directed toward the development and evaluation of $ET_0$ estimation equations which use a limited number of climatic inputs such as air temperature, radiation and pan evaporation (e.g., Awal et al. 2020; Mohan 1991; Nandagiri and Kovoor 2006; Tabari 2010; Xu and Singh 2002). McMahon et al. (2013) provide an excellent review of worldwide studies focused on the estimation of $ET_0$ using ground-based climate measurements. In general, several studies have shown the use of simpler options can reduce the accuracy of hydrological model output (Bai et al. 2016; Remesan and Holman 2015; Zhao et al. 2013). Despite this, numerous studies worldwide have validated the simpler alternative $ET_0$ methods and have found them to yield fairly accurate results. Some of the popular methods are temperature-based Hargreaves (HG) and Blaney-Criddle (BC) equations, radiation-based FAO-24 Radiation (RAD), Priestley-Taylor (PT) and Turc (TC) equations. These methods are popular since their application is simpler requiring 1-2 input climatic variables, unlike the PM method which requires 5-6 climatic variables (Dinpashoh 2006; Gong et al. 2006; McKenney and Rosenberg 1993; Senbin et al. 2006; Tabari and Talaee 2014; Valiantzas 2015). Nigee (2015) calibrated the modified BC equation against PM $ET_0$ in six stations in Karnataka state. Additionally, the effective temperature method was used to improve BC $ET_0$ estimates. The overall results showed the performance of BC was poor and there was no trend in coefficients a and b. However, it was observed that the modified BC method significantly improved estimates with a visible trend in the coefficients across different stations. Ananya (2019) evaluated the performance of the advection-aridity model in Karnataka state. The study highlights the need for local calibration and thus calibrated the Priestley-Taylor equation to obtain potential, actual and wet environment ET. The study was conducted using climate data from 24 stations across ten agro-climatic zones. The results showed the use of an optimized coefficient yielded better results than the original value of 1.26. Owing to the complexity of the standard FAO-56 PM procedures, numerous studies have been conducted in reducing these complexities and implementing simpler equations at regional scales. Several studies have found that locally calibrated standard equations yield better results compared to the direct application of such equations (McMahon et al. 2013; Mohan 1991; Nandagiri and Kovoor 2006; Xu and Singh

2002). However, few studies have reported spatio-temporal variability of PM $ET_0$ estimates and performance evaluation of simpler $ET_0$ equations over large spatial domains such as a region or a state. Also, few efforts have been made to evaluate the effect of local calibration on the performances of $ET_0$ methods at regional scales. Recently, Niranjan and Nandagiri (2021) evaluated the effect of local calibration on the performance of the FAO-56 Hargreaves $ET_0$ equation relative to the PM equation at 67 climate stations located in Karnataka State, India and showed improvement in prediction accuracy. However, other simpler alternative $ET_0$ equations, in particular the BC, RAD, PT and TC, are popular amongst researchers/practitioners and hence there is a need to assess their performances when calibrated for local conditions.

Therefore, the present study was taken up to develop a comprehensive methodology for the evaluation of the performances of simpler $ET_0$ equations with and without local calibration of parameters. The methodology was implemented using historical climate records from a large number of stations located in Karnataka State, India. The study also seeks to analyze the spatio-temporal variations in climate variables and PM $ET_0$ estimates across a wide variety of climatic conditions that exist in the State.

## 6.2 METHODOLOGY

As demonstrated in Section 4.2, similar steps were carried out in calibrating the four simpler (BC, PT, RAD, TC) equations. The steps followed for this purpose are 1) determination of optimal parameters within each of the modified equations 2) retaining these optimal values of parameters in the other three versions of each equation with $T_{mean}$ replaced by alternate definitions of $T_{eff}$ (Eqs. 4.2, 4.4a, 4.4b, and 4.4c) were calibrated separately with corresponding values of $ET_{0,PM}$ to obtain optimal model parameters for each station.

In all cases of local calibration, optimal model parameters were obtained by minimizing the sum of squared errors (SSE) between PM $ET_0$ estimates and those obtained from each of four simpler equations (BC, PT, RAD, and TC). That is, accuracy assessment of the $ET_0$ equations (Eqs. 6.1-6.4b) relative to the PM equation was accomplished in both calibration and validation phases using the coefficient of determination ($R^2$), root mean square error (RMSE) and mean bias error (MBE) statistics computed as, A convenient method proposed by Niranjan and Nandagiri (2021) for interpreting the overall performance of a given $ET_0$ equation using performance statistics across the stations was used in which a 'score' was computed using the following steps: 1) Considering a particular $ET_0$ equation, one of the statistic, say $R^2$ is selected and the number of stations at which this $ET_0$ equation yielded the highest value of $R^2$ relative to the other equations is noted 2) A similar count is made for the number of stations at which the $ET_0$ equation yielded the lowest RMSE and lowest MBE 3) Next the ratio of the number of stations at which the particular $ET_0$ equation yielded the best values of statistics to the total number of stations is calculated 4) The same steps are applied to all the original and modified $ET_0$ equations whose performance was evaluated to identify the equation which performed best at the largest number of stations in each zone and also in the study area as a whole.

## 6.3 COMPUTATION OF $ET_0$ AND CALIBRATION PROCEDURES

An effort was made in this study to evaluate the performances of the alternative simpler $ET_0$ equations (Eqs. 5.1-5.4b) when the numerical coefficients which appear in them were treated as unknown parameters and calibrated against the PM equation (Equation 3.1) at each of the 67 selected stations. Accordingly, the simpler equations were rewritten as detailed below. It is to be noted that the variables which appear in the modified equations (Eqs. 6.1-6.4b) retain the same definitions as those in the equivalent original equations (Eqs. 5.1-5.4b).

### 6.3.1 Modified FAO-24 Blaney-Criddle equation

The Blaney-Criddle equation is rewritten in the form,

$$ET_{M,B} = \{a_B + b_B\left[p\left(c_B T_{\text{mean}} + d_B\right)\right]\}\left[1 + 0.1\frac{z}{1000}\right] \tag{6.1}$$

$ET_{M,B}$ is the daily reference crop evapotranspiration estimated by the modified BC method ($\mathrm{mm\ d^{-1}}$) and $a_B$, $b_B$, $c_B$ and $d_B$ are the model parameters.

### 6.3.2 Modified Priestley-Taylor equation

$$ET_{M,P} = a_P \frac{\Delta}{\Delta + \gamma}(R_n) \tag{6.2}$$

$ET_{M,P}$ is the daily reference crop evapotranspiration estimated by the modified Priestley-Taylor method ($\mathrm{mm\ d^{-1}}$) and $a_P$ is the model parameter.

### 6.3.3 Modified FAO-24 Radiation equation

$$ET_{M,R} = a_R \left[\frac{\Delta'}{\Delta' + \gamma'}(R'_s)\right] - b_R \tag{6.3}$$

where $ET_{M,R}$ is the daily reference crop evapotranspiration estimated by the modified radiation method ($\mathrm{mm\ d^{-1}}$) and $a_R$ and $b_R$ are model parameters.

### 6.3.4 Modified Turc equation

$$ET_{M,T} = a_T \left(\frac{T_{\text{mean}}}{T_{\text{mean}} + 15}\right)(23.8856 * R_s + 50)\left(1 + \frac{50 - RH_{\text{mean}}}{70}\right) \ \text{for RH} < 50 \tag{6.4a}$$

$$ET_{M,T} = a_T \left(\frac{T_{\text{mean}}}{T_{\text{mean}} + 15}\right)(23.8856 * R_s + 50) \ \text{for RH} > 50 \tag{6.4b}$$

$ET_{M,T}$ is the daily reference crop evapotranspiration estimated by the modified Turc method ($\mathrm{mm\ d^{-1}}$) and $a_T$ is the model parameter

### 6.3.5 Effective air temperature

As demonstrated in Section 4.2, in locally calibrating the Hargreaves method, apart from the original and modified methods, three more versions of each equation were obtained by replacing the mean air temperature ($T_{mean}$) in the original equation with effective air temperature ($T_{eff}$) thus obtaining Equation 4.4a-4.4c. A similar methodology was followed to study the effect of replacement in four simpler alternative equations (BC, PT, RAD and TC) to obtain three more versions of each simpler alternative $ET_0$ equations.

As shown in the original PT and RAD equations (Eqs. 5.2-5.3), $T_{mean}$ doesn't appear directly, hence an indirect approach where $T_{mean}$ in $\Delta$ is the slope of saturation vapour pressure versus the temperature curve term, is replaced with $T_{eff}$. After replacement, while retaining the original optimal parameters (Eqs. 6.1-6.4b) these equations are again calibrated by minimizing the sum of squared errors (SSE) between PM $ET_0$ and those obtained by replacement (BC, PT, RAD and TC) to obtain optimal parameters K, f, g, and h. In effect, the present study uses 5 different versions of each equation for estimating monthly $ET_0$ using monthly mean climate inputs for the period of record. The period of the calibration was from January 2006-December 2012 (84 months) and validation for the period January 2013- December 2016 (48 months). The final versions of each equation which contains the effective temperature term are presented below.

**Blaney Criddle**

$$ET_{M,Beff} = \{a_B + b_B \left[p\left(c_B T_{\text{eff}} + d_B\right)\right]\} \left[1 + 0.1\frac{z}{1000}\right] \tag{6.5}$$

**Priestley-Taylor**

$$ET_{M,Peff} = a_P \frac{\Delta}{\Delta + \gamma}(R_n) \tag{6.6a}$$

$$\Delta = \frac{4098\left[0.6108\exp\left(\frac{17.27\,T_{\text{eff}}}{T_{\text{eff}} + 237.3}\right)\right]}{\left(T_{\text{eff}} - 237.3\right)^2} \tag{6.6b}$$

**FAO-24 Radiation**

$$ET_{M,Reff} = a_R\left[\frac{\Delta'}{\Delta' + \gamma'}\left(R_s'\right)\right] - b_R \tag{6.7}$$

$$\Delta' = \Delta \times 10 \tag{6.8}$$

**Turc**

$$ET_{M,Teff} = a_T \left( \frac{T_{\text{eff}}}{T_{\text{eff}} + 15} \right) (23.8856 * R_s + 50) \left( 1 + \frac{50 - RH_{\text{mean}}}{70} \right) \text{ for RH} < 50 \tag{6.9a}$$

$$ET_{M,Teff} = a_T \left( \frac{T_{\text{mean}}}{T_{\text{mean}} + 15} \right) (23.8856 * R_s + 50) \text{ for RH} > 50 \tag{6.9b}$$

## 6.4 RESULTS AND DISCUSSION

### 6.4.1 Performance of calibrated $ET_0$ equations

At each of 67 stations, modified $ET_0$ equations (Eqs. 6.1-6.4b) were locally calibrated as per the procedure described in Section (4.3) and their performances relative to the PM equation (Equation 3.1) were assessed. Performance evaluation was carried out by comparing the best values of the performance statistics (Eqs. 4.5-4.8) recorded in each agroclimatic zone for the original and calibrated equations during the validation period, January 2013-December 2012 (48 months). Figure 6 shows the results of this analysis for all four simpler alternatives $ET_0$ equations considering the PM $ET_0$ equation as the reference. While this analysis presents an overview of the average relative performances of the original and calibrated equations using performance statistics averaged over stations in each zone, a more detailed analysis of performances at individual stations in each zone is presented subsequently using the favourable statistic-based approach described in Section 4.3.

From Figure 6.1 it can be seen that the original BC equation (Equation 5.1) proved to be more accurate than the modified/calibrated equation (Equation 6.1) yielding higher average $R^2$ values across all the zones. Also, the original equation recorded lower average RMSE values in many zones and equalled the RMSE values of the calibrated equation in some zones. Average MBE values were identical between the two versions of the BC equation in most of the zones. Overall, this analysis revealed that local calibration of the BC equation did not yield any improvement in $ET_0$ estimates indicating that the numerical coefficients in the original BC equation (Equation 5.1) were appropriate for use in the Karnataka State.

On the other hand, Figure 6.1 indicates the benefit of local calibration of the PT equation (Equation 6.2) relative to the original equation (Equation 5.2). Although identical average $R^2$ values were recorded for both versions of the equation, average RMSE values reduced quite substantially in all zones except two on account of local calibration of the single parameter $a_P$. Though not of large magnitude, the calibrated PT equation also yielded lower average MBE values in most of the zones (Figure 6.1). Therefore, it appears that although the original and modified PT equations provided similar patterns of variability in $ET_0$ estimates, calibration resulted in significantly lower prediction errors. Though not as substantial as in the case of the PT equation, local calibration of the RAD equation (Equation 6.3) yielded benefits in terms of reduced average RMSE values in many of the zones and smaller average MBE values in some zones (Figure 6.1). However, average $R^2$ values were identical between the two equations.

With regard to the TC equation, local calibration did not yield any substantial benefit in terms of any of the performance statistics (Figure 6.1) but unlike in the case of the BC equation, calibration did not lead to a reduction in prediction accuracies of this equation.

### 6.4.2 Performance evaluation based on favourable statistics

Performance evaluation of monthly mean daily $ET_0$ estimates provided by the four alternatives $ET_0$ models during the validation phase considering their performances at individual stations was carried out. The objective was to assess station-wise differences in performances of the original equations (Eqs. 5.1-5.4b) and the modified/calibrated equations (Eqs. 6.1-6.4b) relative to the PM equation (Equation 3.1). A simple favourable statistic-based approach proposed by Niranjan and Nandagiri (2021) was used for this purpose by pooling stations in each zone and also for the entire study region. As per this approach (Section 4.3), the better value of a particular performance statistic (higher value of $R^2$, lower values of RMSE and MBE) by either the original or the calibrated equation at each station was given a score of 1. A score of 0 was assigned to the other method which yielded a poorer statistic. Following that, scores for each equation (original or calibrated) and each statistic were pooled for all stations lying in agro-climatic zones and for the entire state. For example, at the Ajekar station located in the CO zone, for the RAD method, $R^2$ values obtained during the validation phase for the original and modified equations were 0.92 and 0.94 relative to PM $ET_0$ estimates. Therefore, a score of 1 was assigned to the modified/calibrated equation and a score of 0 was assigned to the original equation for this station since the $R^2$ value was lower. Results of the favourable performance-statistic approach applied to the four alternatives $ET_0$ equations are shown in Tables 6.1 to 6.8 considering climate stations located in various agro-climatic zones.

Table 6.1 shows the number of stations in each zone where the performance statistic considered ($R^2$, RMSE and MBE) was better when $ET_0$ estimates by the original BC equation (Equation 5.1) ($ET_{0,B}$) and estimates by the modified/calibrated BC equation (Equation 6.1) ($ET_{M,B}$) were compared with the estimates of the PM equation (Equation 3.1) ($ET_{0,PM}$) during the 48-month validation period. It is apparent from Table 6.1 that the original BC equation provided higher $R^2$ values than the modified BC equation in almost all the stations (59) except for a few stations in the NED and ND zones (8). This indicates the fact that the original BC equation was able to explain a larger proportion of the variability in $ET_{0,PM}$ estimates. However, the same clear superiority in performance was not exhibited by the original BC equation when the RMSE and MBE statistics were considered. Although the number of stations where $ET_{0,B}$ estimates yielded lower RMSE values were higher (39), the modified BC equation also yielded lower RMSE values in 28 stations of the State. Table 6.1 also clearly indicates that local calibration results in lower MBE values at a large number of stations across all agro-climatic zones.

The relative performances of the PT equation without ($ET_{0,P}$) (Equation 5.2) and with ($ET_{M,P}$) local calibration (Equation 6.2) are shown in Table 6.2. Similar to the identical nature of zone-average $R^2$ values shown in Figure 6.1, results for station-wise values also indicate that identical values of $R^2$ were recorded for both the original PT and modified equations at all stations considered in this study. However, the effect of local calibration on the PT equation ($ET_{M,P}$) yields a substantial reduction in prediction errors (RMSE) and bias (MBE) in a large number of stations (52 out of 67).

The need for local calibration seems to be more critical in some climatic zones (CD, CO, HL, ST) since all stations located in them yielded lower RMSE and MBE values (Table 6.2).

Table 6.3 compares the performances of the original RAD equation (Equation 5.3) and the modified RAD equation (Equation 6.3) for stations located in different zones using performance statistics computed relative to the PM equation (Equation 3.1) during the validation phase. Unlike in the earlier case of the PT equation, $R^2$ values were different between the two approaches with higher values for more stations being recorded by the original equation in comparison to the modified/calibration equation in some zones and vice versa in other zones. For the State as a whole, the number of stations where the original equation performed better was marginally higher than for the modified equation (Table 6.3). While both approaches yielded identical $R^2$ values in two zones (CD, SD), it is only in the HL zone that local calibration gave higher $R^2$ values at all stations.

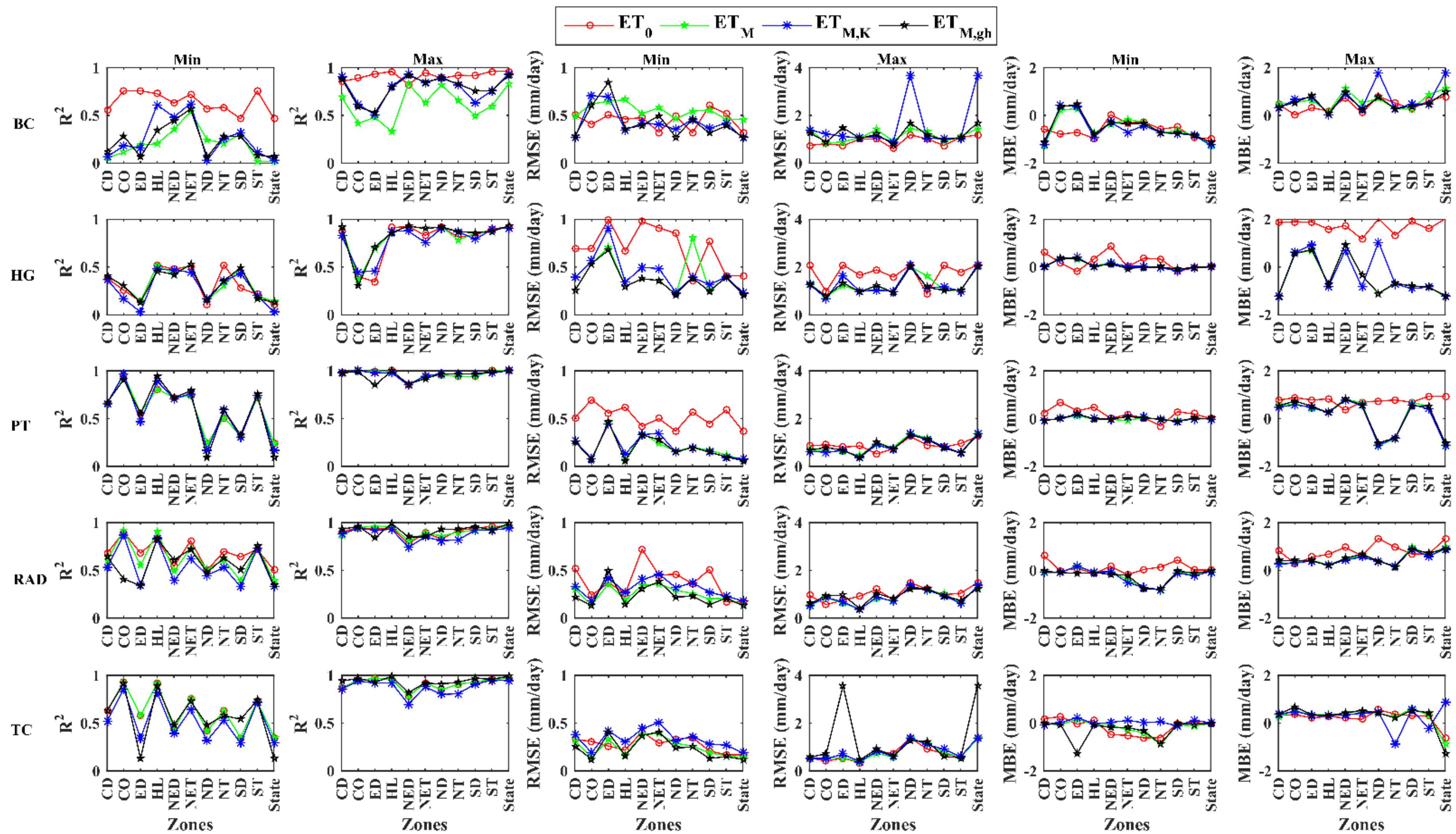


**Figure 6.1: Performance analysis of the original and modified methods**

However, as with the BC and PT equations, local calibration of the RAD equation too yielded lower RMSE and MBE values at a significantly larger number of stations in all zones and the State, except the ST zone.

The performances of the original TC equation (Equation 5.4a and 5.4b) and its modified version (Equation 6.4a and 6.4b) were compared using the favourable statistic-based approach and the results are shown in Table 6.4. While identical values of $R^2$ were obtained by both approaches at all stations, RMSE and MBE values varied across the agroclimatic zones with the original equation performing better in 28 out of 67 stations and the calibrated equation performing better in 39 stations. These results are consistent with results obtained for the other alternative $ET_0$ equations wherein local calibration may not necessarily yield higher $R^2$ values but significant benefit in terms of reduction in prediction error (RMSE) and bias (MBE) can be achieved in a large number of diverse agroclimatic conditions.

### 6.4.3 Optimal model parameters

Values of the parameters/coefficients of the modified versions of the four alternatives $ET_0$ equations (Eqs. 6.1-6.4b) were obtained at each climate station by minimizing the SSE (Equation 4.5) relative to the PM $ET_0$ equation (Equation 3.1) during the calibration period January 2006-December 2012 (84 months). The mean and standard deviation (SD) of these optimal parameters computed by pooling stations in each agro-climatic zone and for the State as a whole are listed in Table 6.5.

As indicated by Equation 6.1, the modified BC equation comprises 4 parameters $a_B$, $b_B$, $c_B$ and $d_B$ and a comparison with Equation 5.1 indicates that in the original BC equation, the first two parameters are climate-dependent while $c_B$ and $d_B$ have constant values of 0.46 and 8.13 respectively. Therefore, from the results shown in Table 6.5, the deviation of $a_B$ and $b_B$ from the original equation cannot be assessed but the same is possible for the other two parameters. In any case, it can be seen that the optimized value of parameter $a_B$ varies over a reasonably narrow range of -2.26 to -3.25 across the zones and its value is -3.02 for the State. SD values for this parameter indicate reasonably large variability in some zones implying its sensitivity to local rather than zonal climatic conditions. On the other hand, the parameter $b_B$ exhibits

**Table 6.1: Results of favourable statistic-based performance analysis of the BC $ET_0$ equation for stations pooled in each agro-climatic zone**

| Zone | No. of stations | $R^2$ | | RMSE (mm $d^{-1}$) | | MBE (mm $d^{-1}$) | |
|---|---|---|---|---|---|---|---|
| | | $ET_{0,B}$ | $ET_{M,B}$ | $ET_{0,B}$ | $ET_{M,B}$ | $ET_{0,B}$ | $ET_{ETM,B}$ |
| CD | 6 | 6 | 0 | 3 | 3 | 3 | 3 |
| CO | 5 | 5 | 0 | 4 | 1 | 3 | 2 |
| ED | 4 | 4 | 0 | 4 | 0 | 2 | 2 |
| HL | 5 | 5 | 0 | 3 | 2 | 1 | 4 |
| NED | 7 | 4 | 3 | 2 | 5 | 3 | 4 |
| NET | 5 | 5 | 0 | 4 | 1 | 3 | 2 |
| ND | 17 | 13 | 5 | 10 | 7 | 5 | 12 |
| NT | 5 | 5 | 0 | 3 | 2 | 3 | 2 |
| SD | 4 | 4 | 0 | 2 | 2 | 3 | 1 |
| ST | 9 | 9 | 0 | 4 | 5 | 1 | 8 |
| State | 67 | 59 | 8 | 39 | 28 | 27 | 40 |

**Table 6.2: Results of favourable statistic-based performance analysis of the PT $ET_0$ equation for stations pooled in each agro-climatic zone**

| Zone | No. of stations | $R^2$ | | RMSE (mm $d^{-1}$) | | MBE (mm $d^{-1}$) | |
|---|---|---|---|---|---|---|---|
| | | $ET_{0,P}$ | $ET_{M,P}$ | $ET_{0,P}$ | $ET_{M,P}$ | $ET_{0,P}$ | $ET_{M,P}$ |
| CD | 6 | 6 | 6 | 0 | 6 | 0 | 6 |
| CO | 5 | 5 | 5 | 0 | 5 | 0 | 5 |
| ED | 4 | 4 | 4 | 1 | 3 | 0 | 4 |
| HL | 5 | 5 | 5 | 0 | 5 | 0 | 5 |
| NED | 7 | 7 | 7 | 5 | 4 | 5 | 3 |
| NET | 5 | 5 | 5 | 3 | 2 | 3 | 2 |
| ND | 17 | 17 | 17 | 6 | 11 | 6 | 11 |
| NT | 5 | 5 | 5 | 1 | 4 | 1 | 4 |
| SD | 4 | 4 | 4 | 1 | 3 | 1 | 3 |
| ST | 9 | 9 | 9 | 0 | 9 | 0 | 9 |
| State | 67 | 67 | 67 | 17 | 52 | 16 | 52 |

**Table 6.3: Results of favourable statistic-based performance analysis of the RAD $ET_0$ equation for stations pooled in each agro-climatic zone**

| Zone | No. of stations | $R^2$ | | RMSE (mm $d^{-1}$) | | MBE (mm $d^{-1}$) | |
|---|---|---|---|---|---|---|---|
| | | $ET_{0,R}$ | $ET_{M,R}$ | $ET_{0,R}$ | $ET_{M,R}$ | $ET_{0,R}$ | $ET_{M,R}$ |
| CD | 6 | 3 | 3 | 0 | 6 | 0 | 6 |
| CO | 5 | 1 | 4 | 1 | 4 | 1 | 4 |
| ED | 4 | 3 | 1 | 1 | 3 | 1 | 3 |
| HL | 5 | 0 | 5 | 0 | 5 | 1 | 4 |
| NED | 7 | 6 | 1 | 0 | 7 | 1 | 6 |
| NET | 5 | 4 | 1 | 2 | 4 | 1 | 4 |
| ND | 17 | 10 | 8 | 5 | 12 | 3 | 14 |
| NT | 5 | 2 | 3 | 1 | 4 | 1 | 4 |
| SD | 4 | 2 | 2 | 1 | 3 | 1 | 3 |
| ST | 9 | 5 | 4 | 4 | 5 | 4 | 5 |
| State | 67 | 36 | 32 | 15 | 53 | 14 | 53 |

**Table 6.4: Results of favourable statistic-based performance analysis of the TC $ET_0$ equation for stations pooled in each agro-climatic zone**

| Zone | No. of stations | $R^2$ | | RMSE (mm $d^{-1}$) | | MBE (mm $d^{-1}$) | |
|---|---|---|---|---|---|---|---|
| | | $ET_{0,T}$ | $ET_{M,T}$ | $ET_{0,T}$ | $ET_{M,T}$ | $ET_{0,T}$ | $ET_{M,T}$ |
| CD | 6 | 6 | 6 | 3 | 3 | 3 | 3 |
| CO | 5 | 5 | 5 | 1 | 4 | 1 | 4 |
| ED | 4 | 4 | 4 | 3 | 1 | 3 | 1 |
| HL | 5 | 5 | 5 | 1 | 4 | 1 | 4 |
| NED | 7 | 7 | 7 | 4 | 3 | 4 | 3 |
| NET | 5 | 5 | 5 | 3 | 2 | 3 | 2 |
| ND | 17 | 17 | 17 | 6 | 11 | 6 | 11 |
| NT | 5 | 5 | 5 | 2 | 3 | 2 | 3 |
| SD | 4 | 4 | 4 | 3 | 1 | 3 | 1 |
| ST | 9 | 9 | 9 | 2 | 7 | 2 | 7 |
| State | 67 | 67 | 67 | 28 | 39 | 28 | 39 |

more uniform across the zones and less variable behaviour within the stations in the zones. An average value close to 1.0 seems to be appropriate for the zones/state, except for the CO zone where a low value was obtained. Table 6.5 shows that the optimal values of parameters $c_B$ and $d_B$ were also quite different for the CO zone in comparison to the other zones. Also, it can be seen that optimal values of these two parameters although exhibiting relatively low values of SD in most zones, deviated significantly from the standard values in the original BC equation, indicating the need for a local optimization to achieve smaller values of MBE in $ET_0$ estimates by this method (Table 6.1).

The single parameter $a_P$ in the modified PT equation (Equation 6.2) varied over quite a narrow range of 1.06 to 1.30 across the zones as compared to the standard value of 1.26 used in the original PT equation (Equation 5.2). For the State as a whole, a value of 1.18 can be recommended based on the present analysis. Also, this parameter displayed small values of SD in all zones. However, as the results are shown in Table 6.2 indicate, the value of $a_P$ did not influence the ability of the PT equation to explain the variability in PM $ET_0$ estimates (identical values of $R^2$), using locally calibrated values did seem to significantly influence predictive error and bias in $ET_0$ estimates.

As with the BC equation, the parameter $a_R$ in the original RAD equation (Equation 5.3) is a function of $\mathrm{RH}_{\mathrm{mean}}$ and windspeed whereas the parameter $b_R$ has a constant value of -0.3. Optimized values of these parameters for the modified RAD equation (Equation 6.3) are shown in Table 6.1 from which the dynamic nature of the parameter $a_R$ across zones can be seen (range of 0.45 to 0.81). SD values are low in some zones and moderate in other zones. Among all the parameters optimized, $b_R$ varies over the largest range, even taking on positive values in the NED and ND zones while in a few zones, the optimal parameter value is close to the standard value of -0.3. High variability for $b_R$ values were evident for stations within zones (Table 6.1).

The single parameter in the modified TC equation (Equation 6.4a and 6.4b) upon optimization remains close (0.012 – 0.014) to the constant value of 0.013 in the original equation (Equation 5.4a and 5.4b) across all the zones (Table 6.1). Extremely low SD values are also evident for this parameter indicating that the original TC equation can be used without local calibration in the study area without much difference in its predictive capabilities.

### 6.4.4 Spatial maps of optimal parameters

Optimal values of parameters/coefficients of the modified $ET_0$ equations (Eqs. 6.1-6.4b) obtained at each of the 67 climate stations were used to prepare maps showing their spatial variabilities across the Karnataka State using inverse distance interpolation. Maps for parameters $a_B$, $b_B$, $c_B$ and $d_B$ of the BC equation, $a_P$ for the PT equation, $a_R$ and $b_R$ for the RAD equation and $a_T$ for the TC equation are shown in Figure 6.2(a-h). While Table 6.1 shows only the mean values of the optimal parameters for each agro-climatic zone, the maps depict their variations across individual stations. Figure 6.2a shows that the BC parameter $a_B$ exhibits lower values towards the southern part of the State whereas moderate values towards the southeast and high values towards the west and northern parts are evident. High values of $b_B$ towards the southern part and low values along the west coast region are evident in Figure 6.2b. Both $c_B$ and $d_B$ parameters show uniform variations across the entire study area with two clusters of high values (Figure 6.2c and 6.2d). The single parameter $a_P$ of the PT equation shows low values close to 1.00 in all zones located towards the west and higher values (up to 1.44) in the northern dry zones (Figure 6.2e). Both parameters of the RAD equation ($a_R$ and $b_R$) show almost identical patterns of spatial variations (Figures 6.2f and 6.2g) across the State taking on low values in the southern part and high values in the northern part. Parameter $a_T$ of the TC equation exhibits lower values towards the western part of the State and increases towards the eastern and northern parts with a few clusters of high values (Figure 6.2h).

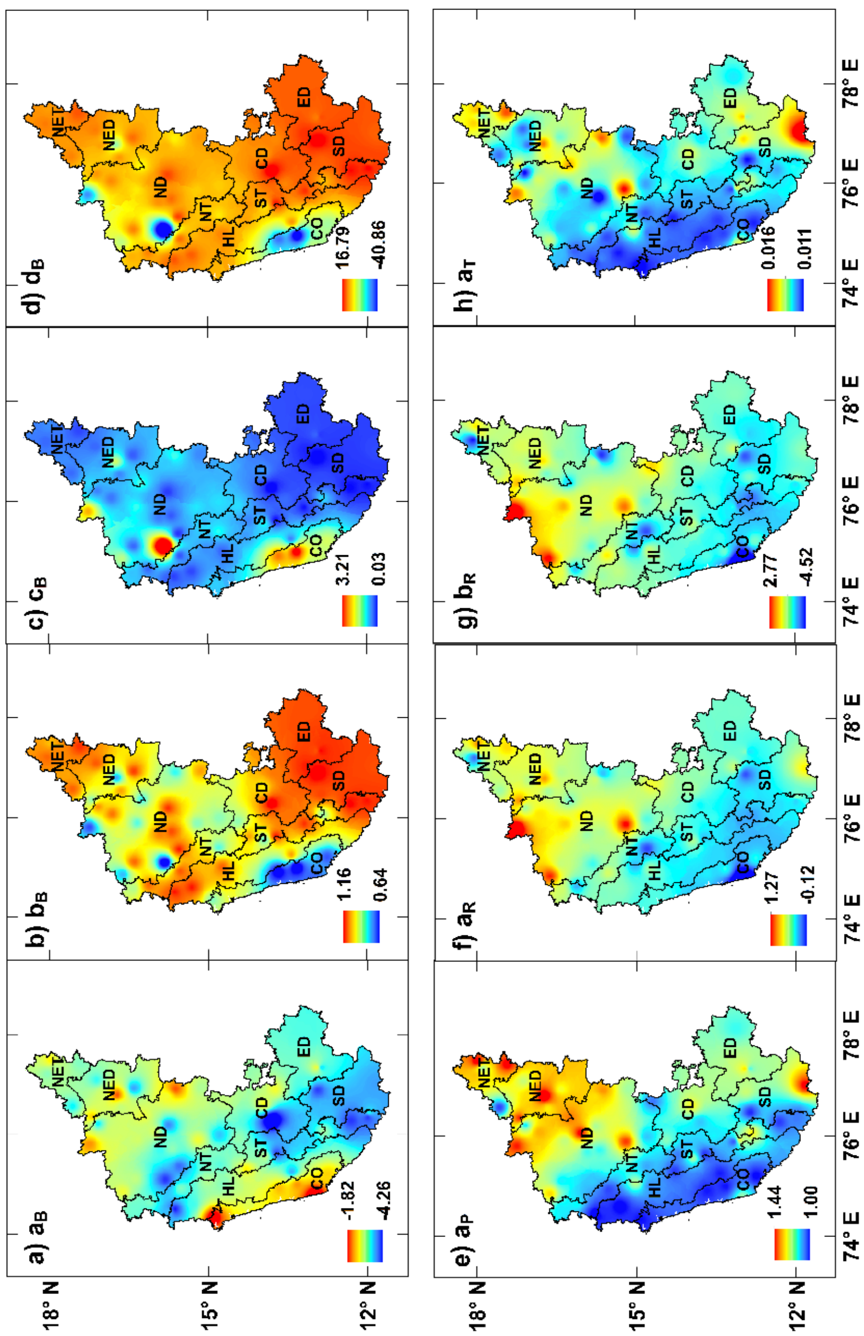


**Figure 6.2: Maps depicting spatial variabilities of optimal model parameters of the modified BC, PT, RAD and TC $ET_0$ equations**

**Table 6.5: Mean and standard deviation (SD) values of optimal parameters of the four modified $ET_0$ equations for stations pooled in each agro-climatic zone**

| Zone | Stats | CD | CO | ED | HL | NED | NET | ND | NT | SD | ST | State |
|---|---|---|---|---|---|---|---|---|---|---|---|---|
| $a_B$ | Mean | -3.16 | -2.26 | -3.07 | -3.24 | -2.85 | -2.99 | -2.98 | -3.14 | -3.33 | -3.25 | -3.02 |
| | SD | 0.53 | 0.32 | 0.19 | 0.26 | 0.34 | 0.18 | 0.36 | 0.10 | 0.23 | 0.32 | 0.41 |
| $b_B$ | Mean | 1.03 | 0.75 | 1.12 | 1.09 | 0.98 | 1.09 | 0.96 | 1.02 | 1.07 | 1.08 | 1.01 |
| | SD | 0.09 | 0.09 | 0.01 | 0.04 | 0.11 | 0.03 | 0.14 | 0.10 | 0.10 | 0.08 | 0.14 |
| $c_B$ | Mean | 0.38 | 1.28 | 0.23 | 0.32 | 0.56 | 0.33 | 0.70 | 0.43 | 0.28 | 0.27 | 0.51 |
| | SD | 0.18 | 0.50 | 0.06 | 0.08 | 0.26 | 0.07 | 0.70 | 0.17 | 0.21 | 0.19 | 0.49 |
| $d_B$ | Mean | 9.68 | -7.20 | 11.84 | 10.03 | 6.09 | 9.83 | 3.62 | 8.53 | 11.27 | 11.26 | 6.90 |
| | SD | 3.36 | 10.98 | 1.32 | 1.53 | 4.73 | 1.26 | 12.62 | 2.38 | 3.49 | 3.26 | 8.99 |
| $a_P$ | Mean | 1.16 | 1.06 | 1.19 | 1.07 | 1.30 | 1.26 | 1.22 | 1.09 | 1.22 | 1.10 | 1.18 |
| | SD | 0.06 | 0.07 | 0.06 | 0.08 | 0.08 | 0.15 | 0.09 | 0.06 | 0.14 | 0.07 | 0.11 |
| $a_R$ | Mean | 0.68 | 0.45 | 0.65 | 0.61 | 0.79 | 0.76 | 0.81 | 0.62 | 0.58 | 0.57 | 0.68 |
| | SD | 0.09 | 0.32 | 0.08 | 0.08 | 0.14 | 0.21 | 0.20 | 0.17 | 0.20 | 0.07 | 0.20 |
| $b_R$ | Mean | -0.09 | -1.19 | -0.39 | -0.35 | 0.12 | -0.11 | 0.41 | -0.25 | -0.91 | -0.56 | -0.19 |
| | SD | 0.56 | 1.87 | 0.50 | 0.60 | 0.69 | 1.07 | 1.07 | 1.02 | 0.75 | 0.41 | 1.00 |
| $a_T$ | Mean | 0.013 | 0.012 | 0.013 | 0.012 | 0.014 | 0.014 | 0.013 | 0.012 | 0.014 | 0.013 | 0.013 |
| | SD | 0.0005 | 0.0009 | 0.0007 | 0.0008 | 0.001 | 0.0011 | 0.0011 | 0.0003 | 0.0018 | 0.0006 | 0.001 |

### 6.4.5 Performance of equations with effective temperature

Considering the BC equation, the results obtained by the replacement of mean temperature with effective temperature did not lead to significant improvement in $ET_0$ estimates compared to the modified equation $ET_{M,B}$ (Equation 6.1). The results shown in Figure 6.1 indicate estimates by $ET_{M,B}$ and $ET_{M,Bgh}$ yielded equivalent estimates as $ET_{M,B}$. Also, using the effective method did not improve $R^2$ values and significant error reduction of RMSE and MBE values was also not observed. In fact, RMSE values at the ND station obtained using $ET_{M,K}$ were highest in comparison to all the methods. Therefore, as stated in Section 6.4.1 use of the original BC equation with its numerical coefficients in Karnataka is more appropriate than the use of the effective temperature method.

The effect of replacement with $T_{eff}$ in the PT equation method yielded equivalent estimates in terms of $R^2$ values by $ET_{M,PK}$ and $ET_{M,Pgh}$ method as shown in the Figure 6.1. The optimal parameters ($K_P$, $g_P$ and $h_P$) variability are shown in Figure 6.3(i) to 6.3(j) across all the agroclimatic zones. The northern regions show high values with an overall average $K_P$ = 1.04 which was accompanied by higher RMSE and MBE values. The overall average $K_P$= 1.04 with an SD of 0.08 indicates less variability compared to $g_P$ and $h_P$ where the SD was about 1.11 and 0.73 indicating a high departure from the average values. The h values were found high to be in mountainous regions such as ED, HL, and SD zones. The overall spatial range of $K_P$ ranged from 0.92 to 1.02, $g_P$ ranged from -2.85 to 3.96, and $h_P$ from -1.97 to -2.72.

It is clearly visible from Figure 6.3(J) that $K_P$ varies uniformly, with lower in the coastal to higher values in northern zones (ND, NED, NET). However, the zones falling on the eastern side showed minimum variability in $K_P$ values. The $g_P$ values are mostly clustered with lower values in northern, ED, and HL zones and uniform values in the plains. Since the weights of g and h are equal, the values obtained from the CO zone departed from this observation where both the $g_P$ and $h_P$ were different from each other. The validation score statistics (Table 6.7) $R^2$ values showed similar scores of $ET_{0,P}$ and $ET_{M,P}$ and $ET_{M,PK}$. The scores of $ET_{M,Pgh}$ were high in more than 45% of stations. However, the RMSE and MBE indicate the departure from these predictions where in the case of RMSE $ET_{M,Pgh}$ were better at 30 stations whereas in terms of MBE maximum $ET_{M,PK}$ was better at 27/97 stations. Therefore, from the overall statistics, it is found that using the effective temperature method improved the $ET_0$ results by reducing the errors in the values. For the state as a whole, the $ET_{M,Rgh}$ method yielded the maximum values across different zones. The RMSE and MBE values are high in the dry and plain areas such NED and low in HL, and CO zones. The original equations yielded high RMSE and MBE values indicating the need for calibration. The use of a modified and effective temperature method contributed to the improvement in $ET_0$ estimates. Spatial maps (Figure 6.3(j)-(l)) show the uniform variability of $K_R$ values ranging from 0.55 to 0.81 with a lower SD of 0.04. Significant variability was observed in the pooled values of $g_R$ and $h_R$ values with the highest value of 3.36 in the NED zone accompanied by higher SD values of more than 1.5. Prominent lower clustered values were observed in the coastal values. The overall average was about 0.001 in $h_R$ values and 1.37 for $g_R$ values. The overall RAD score statistics (Table 6.8) show the performance of the $ET_{M,Rgh}$ method to be better by all the statistics such as $R^2$, RMSE, and MBE. In more than 50% of the cases, the gh method yielded better results than the original method. Whereas the modified methods in terms of $R^2$ performed better at only 8 stations. Significant error reduction was observed using modified and effective temperature by the K method. For example in the ND zone, RMSE and MBE reduced errors at 10 stations each. Considering the TC method, as shown in Figure 6.1 the use of effective temperature seems to yield better $R^2$ values where a significant increase in maximum $R^2$ can be observed while using the $ET_{M,Tgh}$ method. Except in the ED and SD zone, the $R^2$ values in all zones were more than 0.3 indicating the overall performance of TC equations to better across the state. Additionally, RMSE and MBE values indicate high values of 3.57 $\mathrm{mm\ d^{-1}}$ with maximum MBE by $ET_{M,Tgh}$, and MBE of -1.27 was found for the state. The $ET_{M,T}$seems to show a lower MBE value in comparison to $ET_{M,Tgh}$. Table 6.9 shows the overall favourable statistics, where $ET_{M,Tgh}$ yielded improvements has nearly 70% of show the performance of the statistics better in comparison to other methods. The performance was found to be maximum in the ND zone. The overall error reduction in terms of RMSE and MBE was visible to 40% of the stations using the effective temperature method.

### 6.4.6 Discussion

The main focus of the present study was to evaluate the effect of local calibration on the performances of four simpler $ET_0$ estimation methods namely; BC, PT, RAD and TC relative to the PM method. A comprehensive comparison of the performances of these equations without and with local calibration revealed that significant improvement in prediction accuracies (RMSE) and bias (MBE) could be achieved especially for the PT and RAD equations with the use of parameters derived through local calibration. With local calibration, these equations outperformed the original equations at a large number of stations located in different agroclimatic zones. This is on account of the fact that the optimal parameter values for these equations were not only different from the values in the original equations but also varied from one climate station to another. Although regionalization of the optimal parameters through the establishment of relationships with climatic or terrain features was beyond the scope of the present study, the derived zonal/State means and spatial maps may be used to estimate optimal parameters for any location within the study area.

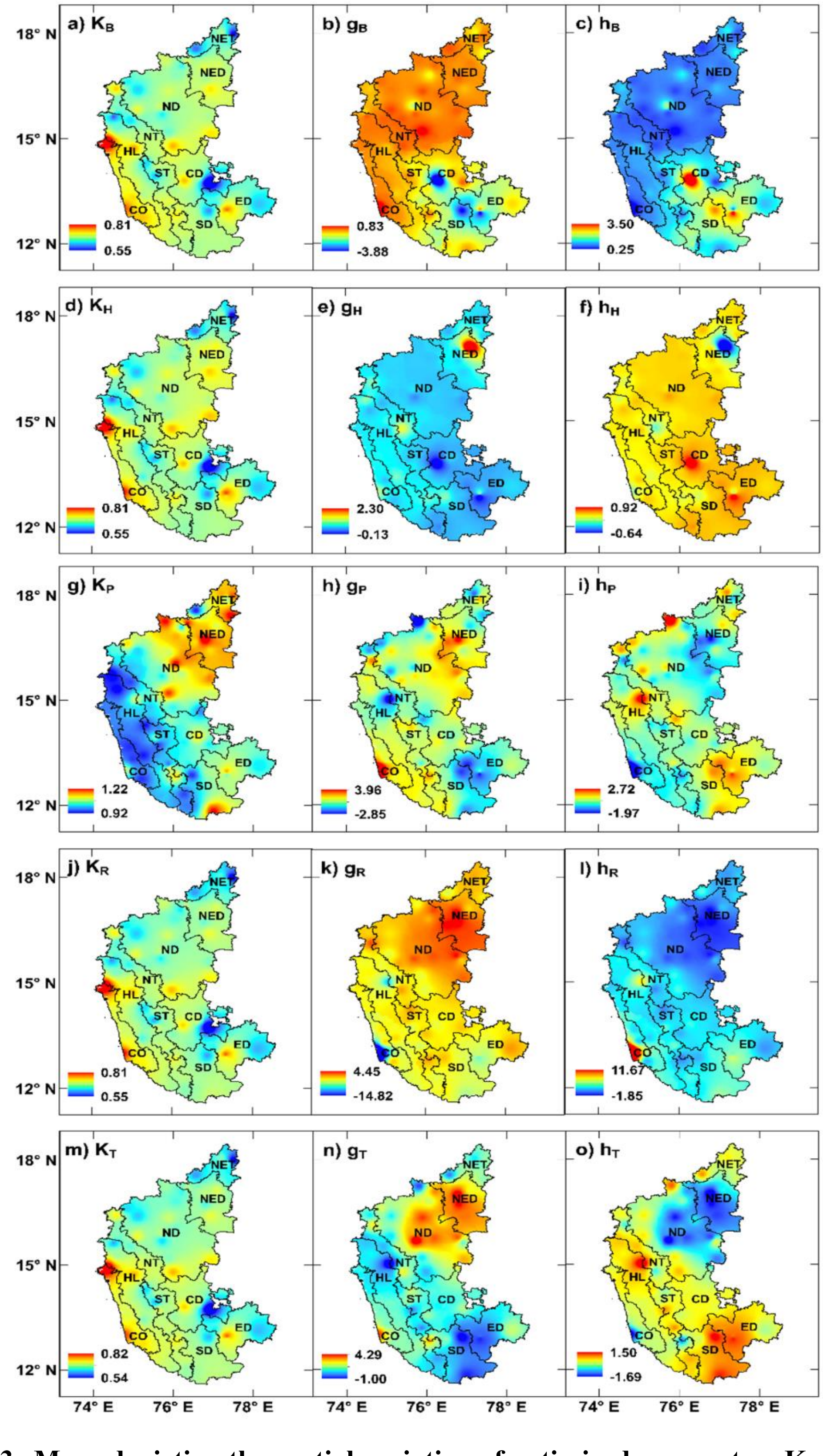


**Figure 6.3: Maps depicting the spatial variation of optimized parameters K, g, and H (Eqs. 6.5-6.8b) derived for each simpler $ET_0$ equations (BC, HG, PT, RAD, TC) over the study area**

**Table 6.6: Mean and standard deviations of optimal parameters of simpler $ET_{0,T}$ equations using effective temperature for stations pooled in each agro-climatic zone**

| Zone | No. of | $K_P$ | | $g_P$ | | $h_P$ | | $K_R$ | | $g_R$ | | $h_R$ | | $K_T$ | | $g_T$ | | $h_T$ | |
|---|---|---|---|---|---|---|---|---|---|---|---|---|---|---|---|---|---|---|---|
| | stations | Mean | SD | Mean | SD | Mean | SD | Mean | SD | Mean | SD | Mean | SD | Mean | SD | Mean | SD | Mean | SD |
| **CD** | 6 | 1.03 | 0.06 | -0.10 | 0.72 | 0.88 | 0.48 | 0.67 | 0.06 | 1.40 | 0.51 | -0.02 | 0.29 | 0.67 | 0.06 | 1.30 | 0.32 | 0.03 | 0.16 |
| **CO** | 5 | 0.97 | 0.07 | 0.84 | 1.76 | 0.26 | 1.26 | 0.74 | 0.05 | -1.81 | 7.28 | 2.22 | 5.29 | 0.75 | 0.05 | 1.70 | 0.98 | -0.32 | 0.68 |
| **ED** | 4 | 1.05 | 0.06 | -1.11 | 1.05 | 1.52 | 0.65 | 0.69 | 0.05 | 0.43 | 1.58 | 0.60 | 0.95 | 0.69 | 0.05 | 0.58 | 0.86 | 0.48 | 0.50 |
| **HL** | 5 | 0.97 | 0.08 | -0.50 | 1.34 | 1.19 | 0.93 | 0.68 | 0.04 | 0.34 | 1.58 | 0.64 | 1.04 | 0.68 | 0.04 | 0.53 | 0.90 | 0.51 | 0.58 |
| **NED** | 7 | 1.14 | 0.08 | 0.55 | 1.06 | 0.48 | 0.68 | 0.68 | 0.02 | 3.36 | 1.03 | -1.29 | 0.62 | 0.77 | 0.08 | 2.99 | 0.69 | -1.05 | 0.42 |
| **NET** | 5 | 1.09 | 0.15 | -0.31 | 1.04 | 1.00 | 0.67 | 0.64 | 0.04 | 1.43 | 0.70 | -0.03 | 0.42 | 0.67 | 0.03 | 1.09 | 0.47 | 0.17 | 0.25 |
| **ND** | 17 | 1.08 | 0.09 | -0.10 | 1.08 | 0.89 | 0.70 | 0.68 | 0.02 | 2.14 | 1.13 | -0.49 | 0.69 | 0.72 | 0.05 | 2.09 | 1.19 | -0.46 | 0.71 |
| **NT** | 5 | 0.98 | 0.06 | -0.05 | 0.97 | 0.87 | 0.64 | 0.68 | 0.02 | 1.77 | 1.09 | -0.27 | 0.64 | 0.70 | 0.02 | 1.36 | 0.82 | -0.03 | 0.49 |
| **SD** | 4 | 1.07 | 0.14 | -0.62 | 1.32 | 1.16 | 0.80 | 0.68 | 0.03 | 1.06 | 1.29 | 0.14 | 0.82 | 0.69 | 0.04 | 0.82 | 1.56 | 0.27 | 0.97 |
| **ST** | 9 | 0.98 | 0.07 | 0.25 | 0.51 | 0.66 | 0.32 | 0.67 | 0.02 | 1.00 | 0.77 | 0.20 | 0.47 | 0.68 | 0.02 | 0.92 | 0.51 | 0.25 | 0.30 |
| **State** | 67 | 1.04 | 0.08 | -0.05 | 1.11 | 0.85 | 0.73 | 0.68 | 0.04 | 1.37 | 2.38 | 0.001 | 1.65 | 0.71 | 0.05 | 1.52 | 1.13 | -0.12 | 0.70 |

**Table 6.7: Results of favourable statistic-based performance analysis of the four PT equations for stations pooled in each agro-climatic zone**

| Zone | No.of | $R^2$ | | | | RMSE ($mm\ d^{-1}$) | | | | MBE ($mm\ d^{-1}$) | | | |
|---|---|---|---|---|---|---|---|---|---|---|---|---|---|
| | stations | $ET_{0,P}$ | $ET_{M,P}$ | $ET_{M,PK}$ | $ET_{M,Pgh}$ | $ET_{0,P}$ | $ET_{M,P}$ | $ET_{M,PK}$ | $ET_{M,Pgh}$ | $ET_{0,P}$ | $ET_{M,P}$ | $ET_{M,PK}$ | $ET_{M,Pgh}$ |
| CD | 6 | 4 | 4 | 2 | 5 | 0 | 4 | 1 | 3 | 0 | 4 | 3 | 3 |
| CO | 5 | 4 | 4 | 5 | 4 | 0 | 1 | 2 | 4 | 0 | 3 | 4 | 1 |
| ED | 4 | 2 | 2 | 1 | 1 | 0 | 2 | 1 | 1 | 1 | 3 | 0 | 1 |
| HL | 5 | 2 | 2 | 2 | 3 | 0 | 0 | 2 | 3 | 0 | 1 | 3 | 2 |
| NED | 7 | 5 | 5 | 1 | 6 | 4 | 2 | 1 | 2 | 4 | 1 | 3 | 0 |
| NET | 5 | 1 | 2 | 2 | 2 | 3 | 1 | 0 | 1 | 2 | 1 | 0 | 2 |
| ND | 17 | 8 | 6 | 9 | 9 | 5 | 4 | 2 | 10 | 6 | 2 | 7 | 4 |
| NT | 5 | 2 | 2 | 2 | 3 | 1 | 2 | 1 | 1 | 1 | 1 | 1 | 2 |
| SD | 4 | 0 | 0 | 3 | 2 | 1 | 0 | 1 | 3 | 1 | 1 | 0 | 2 |
| ST | 9 | 4 | 4 | 4 | 6 | 0 | 2 | 5 | 2 | 0 | 3 | 6 | 0 |
| State | 67 | 32 | 31 | 31 | 41 | 14 | 18 | 16 | 30 | 15 | 20 | 27 | 17 |

**Table 6.8: Results of favourable statistic-based performance analysis of the four RAD equations for stations pooled in each agro-climatic zone**

| Zone | No.of | $R^2$ | | | | RMSE (mm $d^{-1}$) | | | | MBE (mm $d^{-1}$) | | | |
|---|---|---|---|---|---|---|---|---|---|---|---|---|---|
| | stations | $ET_{0,R}$ | $ET_{M,R}$ | $ET_{M,RK}$ | $ET_{M,Rgh}$ | $ET_{0,R}$ | $ET_{M,R}$ | $ET_{M,RK}$ | $ET_{M,Rgh}$ | $ET_{0,R}$ | $ET_{M,R}$ | $ET_{M,RK}$ | $ET_{M,Rgh}$ |
| CD | 6 | 2 | 0 | 3 | 0 | 2 | 1 | 4 | 0 | 0 | 3 | 3 | 3 |
| CO | 5 | 1 | 2 | 4 | 1 | 0 | 0 | 4 | 1 | 0 | 2 | 2 | 1 |
| ED | 4 | 3 | 1 | 0 | 1 | 2 | 1 | 1 | 1 | 1 | 1 | 2 | 1 |
| HL | 5 | 0 | 1 | 4 | 0 | 1 | 1 | 3 | 1 | 1 | 2 | 1 | 2 |
| NED | 7 | 2 | 0 | 5 | 0 | 2 | 0 | 5 | 1 | 2 | 3 | 2 | 0 |
| NET | 5 | 4 | 1 | 0 | 2 | 2 | 1 | 3 | 0 | 2 | 2 | 1 | 2 |
| ND | 17 | 10 | 1 | 8 | 5 | 3 | 1 | 10 | 2 | 3 | 10 | 5 | 4 |
| NT | 5 | 1 | 0 | 4 | 1 | 0 | 0 | 4 | 1 | 2 | 0 | 2 | 2 |
| SD | 4 | 2 | 0 | 2 | 1 | 0 | 0 | 3 | 1 | 0 | 1 | 2 | 2 |
| ST | 9 | 3 | 2 | 3 | 3 | 1 | 2 | 4 | 2 | 0 | 4 | 3 | 0 |
| State | 67 | 28 | 8 | 33 | 14 | 13 | 7 | 41 | 10 | 11 | 28 | 23 | 17 |

**Table 6.9: Results of favourable statistic-based performance analysis of the four TC equations for stations pooled in each agro-climatic zone**

| Zone | No.of stations | $R^2$ | | | | RMSE ($mm\ d^{-1}$) | | | | MBE ($mm\ d^{-1}$) | | | |
|---|---|---|---|---|---|---|---|---|---|---|---|---|---|
| | | $ET_{0,T}$ | $ET_{M,T}$ | $ET_{M,TK}$ | $ET_{M,Tgh}$ | $ET_{0,T}$ | $ET_{M,T}$ | $ET_{M,TK}$ | $ET_{M,Tgh}$ | $ET_{0,T}$ | $ET_{M,T}$ | $ET_{M,TK}$ | $ET_{M,Tgh}$ |
| CD | 6 | 1 | 0 | 2 | 4 | 1 | 1 | 1 | 3 | 2 | 0 | 2 | 2 |
| CO | 5 | 1 | 0 | 0 | 4 | 1 | 0 | 0 | 4 | 1 | 0 | 1 | 3 |
| ED | 4 | 2 | 3 | 1 | 1 | 3 | 1 | 1 | 0 | 3 | 1 | 0 | 0 |
| HL | 5 | 0 | 1 | 0 | 4 | 1 | 1 | 0 | 3 | 1 | 2 | 1 | 1 |
| NED | 7 | 1 | 0 | 1 | 5 | 2 | 1 | 1 | 3 | 3 | 2 | 2 | 0 |
| NET | 5 | 4 | 0 | 0 | 3 | 3 | 0 | 0 | 2 | 3 | 0 | 1 | 1 |
| ND | 17 | 7 | 1 | 3 | 10 | 4 | 1 | 1 | 12 | 4 | 4 | 5 | 5 |
| NT | 5 | 0 | 0 | 1 | 4 | 1 | 0 | 0 | 4 | 2 | 0 | 2 | 1 |
| SD | 4 | 1 | 1 | 1 | 1 | 2 | 0 | 0 | 2 | 3 | 0 | 0 | 1 |
| ST | 9 | 3 | 5 | 0 | 6 | 1 | 4 | 0 | 5 | 2 | 3 | 1 | 3 |
| State | 67 | 20 | 11 | 9 | 42 | 19 | 9 | 4 | 38 | 24 | 12 | 15 | 17 |

CHAPTER 7

# SPATIAL INTERPOLATION OF $ET_0$

## 7.1 GENERAL

Spatial interpolation of $ET_0$ at unsampled locations is essential for deriving inputs to hydrological models, developing spatial maps, and other hydro-climatological analyses. Globally several large scale-studies have contributed to the development of gridded $ET_0$ datasets (Harris et al. 2020, Zomer et al. 2022). Global $ET_0$ products such as Climate Research Unit gridded Time Series (CRU TS), MODIS evapotranspiration and TerraClimate are widely used. Studies have identified that primarily the accuracy of such a derived dataset is dependent on the density of the climatic network and the nature of the interpolation techniques used (Hobeichi 2018). Based on these criteria, the traditional approach to the development of gridded products consists of interpolating station-based variables to obtain values at unsampled locations. However, owing to the non-availability of input climatic variables and the data-intensive nature of the PM method, several studies rely on multiple gridded or remotely-sensed data to obtain gridded $ET_0$ (McCabe 2016). Therefore, such estimates are prone to significant bias, and hence bias correction is a necessary step before application thus making the process tedious.

In India, gridded products have been largely limited to rainfall and temperature variables (Pai et al. 2014; Rajeevan and Bhate 2014; Srivastava 2009). Despite the importance of evapotranspiration estimates and their requirements across multiple uses, there has been no previous attempt in India to develop gridded $ET_0$ products at a regional scale using only station data. Therefore, the present study was taken up to develop a gridded product of daily PM $ET_0$ for Karnataka State, India for the historical period 2006-2016. To the best of our knowledge, this is the first attempt to develop a comprehensive historical regional gridded $ET_0$ dataset at this scale. In the Chapter, the methodology adopted in estimating $ET_0$ at unsampled locations following performance analysis of different spatial interpolation techniques is presented.

## 7.2 SPATIAL INTERPOLATION TECHNIQUES

Spatial interpolation refers to the exercise of using observed data of a variable at a sampled location to estimate the variable at an unsampled location in the region. Over the past several decades, techniques for spatial interpolation of a wide variety of climate and environmental variables have been proposed by previous researchers. Likewise, there have been several attempts in developing gridded products of reference crop evapotranspiration ($ET_0$) using different spatial interpolation techniques. With recent advances in computational geospatial technologies and geostatistics, several sophisticated methods such as; Inverse Distance Weighted (IDW) averaging, Splining, Kriging, Trend Surface interpolation and Regression modelling are routinely employed for hydrological variable interpolations (Aalto et al. 2016; Handcock et al.1994; Hodam et al. 2017; Jeffrey 2001; Laslett 1994; Martinez-Cob 1996; Yanto 2017). Li and Heap (2011) provide a review of 53 comparative studies adopting different interpolation techniques such as IDW, and Kriging with various forms of kriging. The study observed data variability significantly affected the performances. Contrary to other studies it was seen that sampling density had an insignificant effect on the performance of different methods. Also, irregularly spaced sampling might increase accuracy. Hartkamp et al. (1999) provide a useful comparison of the characteristics of popular interpolation techniques.

Several studies have evaluated the relative performances of different interpolation methods with common datasets (Ambha 2005; Attorre et al. 2007; Livneh et al. 2015; Mardikis et al. 2005; Phillips et al. 1992; Rigden and Salvucci 2015; Sharma and Irmak 2012; Tabios and Salas 1985; Vicente-Serrano et al. 2003, 2017). Dalezios (2002) studied the spatial variability of the FAO-modified Penman method in Greece using geostatistics employing a kriging-based approach. The study suggests for use of geostatistics of $ET_0$ mapping across agroclimatic maps over large regions with complex terrain. Zimmerman 1999 found the performance of kriging to be superior over IDW across varying attributes. These studies have shown that there is no single preferred method for rainfall data interpolation. Different approaches lead to a large assortment of distinct solutions (Englund 1990). Burrough and McDonnell (1998) noted that when data are abundant most interpolation techniques give similar results. Since the magnitude of a variable between data points can be interpolated only by fitting some plausible model of variation to magnitudes between the data points, all interpolation techniques use simplifying models in the analysis. Daly (2006) studied the relationship between scale and spatial climate-forcing factors and provided the background for assessing the suitability of data sets. The study also provides insights into the relative performances of various interpolation techniques such as IDW, kriging, DAYMET, PRISM and the use of regional regression for spatial interpolation.

Most studies developing gridded $ET_0$ products are largely point-based wherein the data at an unsampled location is derived solely from the network of input climate station data (Hodam et al. 2017; Tomas-Burguera 2019). However, one of the primary challenges to this approach is fulfilling the requirement of input climate data. During inadequate data-requirement studies rely on other ancillary datasets such as remote-sensing and climate-based reanalysis models to derive estimates at unsampled locations (Alves 2013). Singer et al. (2005) derived FAO56 PM daily global potential evapotranspiration data called dPET at 0.1 degrees using ERA5-Land reanalysis climatic data for the period 1981-present. The developed dPET dataset was validated with other available global $ET_0$ gridded products and concluded the performance of dPET was better than other products. The study also highlights different avenues for the application of the developed gridded $ET_0$ product. Purnadurga et al. (2019) evaluated $ET_0$ obtained from IMD climate station data and two reanalysis data. The performance results showed an underestimation of reanalysis during different seasons. Among the two-reanalysis data, the performance of CRU ET was better in comparison to ERA.

There exist several global gridded $ET_0$ products, and each of the available products varies with the way of the methodology and formulation involved in developing these products. Hence prior to application, assessment and error correction is a necessary step (Pelosi 2020; Purnadurga et al. 2019). Among many available methods, reanalysis models are frequently used to develop global gridded products. A few of the popular $ET_0$ data are mentioned here: CRU TS (Harris et al. 2020), DOLCE (Hobeichi et al. 2018), ERA5 (Hersbach et al. 2020), GLEAM (Martens et al. 2017), TerraClimate (Abatzoglou 2018), WorldClim (Fick and Hijmans 2017).

However, there have been fewer attempts in developing regional $ET_0$ gridded products. Sperna Weiland (2012) developed global gridded calibrated Hargreaves $ET_0$ data. The dataset was developed after performance comparisons were made against three other methods (PM, BC, HG). Tanguy et al. 2017 developed historical gridded $ET_0$ data for the United Kingdom. The methodology of data development comprised five stages, first two stages comprised of identifying the best performing method. The third and fourth stages comprised spatio-temporal evaluation of the $ET_0$ methods. Finally, the catchment averaged and CHESS PM $ET_0$ data were regridded at 5 km resolution. Burguera et al. (2019) developed a gridded climatic database for Spain and Balearic Islands which was in turn used to calculate PM $ET_0$ at these grid locations. The study employed kriging to generate climatic grids at various temporal periods. Althoff et al. (2020) developed daily gridded PM $ET_0$ for Brazil over a period of 2000-2018 using both station-based data and reanalysis data. However, the study used machine algorithms to generate the $ET_0$ grids. Huerta et al. 2022 developed PM $ET_0$ gridded data for the Peru region at 0.01° resolution. The overall framework of the development of the dataset comprised of 1) the use of a gridded dataset and remotely measured input climatic data required for the $ET_0$ dataset and 2) the use of climatologically aided interpolation for developing the dataset. Validation was carried out against the existing global gridded products such as CRU, Terraclimate and ERA5-Land $ET_0$ data.

Pirinen et al. (2022) developed gridded PM $ET_0$ data for Finland for the period 1981–2020 at a resolution of 1 km $\times$ 1 km. The methodology for the construction of data involved two steps, firstly using the input station-based climate data to generate a 1 km grid using kriging with external drift and secondly using this input to develop PM PM $ET_0$ for Finland. The results show the close estimation of the developed product with station-based $ET_0$ estimates. The comparisons between gridded $ET_0$ and pan-evaporation estimates were inconsistent with each other. Overall the vital outcome from most of these regional studies through performance analysis revealed the superiority of the developed gridded dataset over the global products.

## 7.3 METHODOLOGY

Spatial interpolation was carried out using three methods to determine $ET_0$ values at unsampled grid points at a spatial resolution of 0.25×0.25 using daily PM $ET_0$ estimates derived for 67 climate stations over the historical period from 2006 to 2016. The three different interpolation techniques used are Inverse distance weightage (IDW), Kriging and P-BSHADE. These methods were validated using the cross-validation technique. Thus, the method producing the least errors was used to obtain gridded $ET_0$ estimates for the state of Karnataka. Finally, the obtained daily gridded $ET_0$ dataset was examined for its efficiency at ten stations, one in each agroclimatic zone.

Figure 7.1 shows the overall methodology adopted for performing spatial interpolation. It was carried out in two steps: determination of optimal input parameters and statistical validation to identify the best approach. Finally, the most accurate method was chosen to develop gridded data $ET_0$ at 0.25×0.25 resolution. IDW and Kriging interpolation was carried out by using the *ArcGIS*® model builder. P-BSHADE was implemented using the graphical user interface application developed by Wang et al. (2011).

## 7.4 INVERSE DISTANCE WEIGHTAGE (IDW)

Based on the findings of the review of the literature and the content of the available dataset, the simple yet popular Inverse Distance Weighted (IDW) spatial interpolation method (Shepard, 1968) was used in the present study. According to this method,

$$Y_i = \sum_{j=1}^{N} w_i Y_j \tag{7.1}$$

$$w_j = \frac{d_{ij}^{-n}}{\sum_{j=1}^{N} d_{ij}^{-n}} 1 \leq j \leq N \tag{7.2}$$

where $Y_i$ is the interpolated value at location i, $Y_j$ is the measured variable at station j, $w_j$ is the associated station weight, N represents the number of surrounding stations

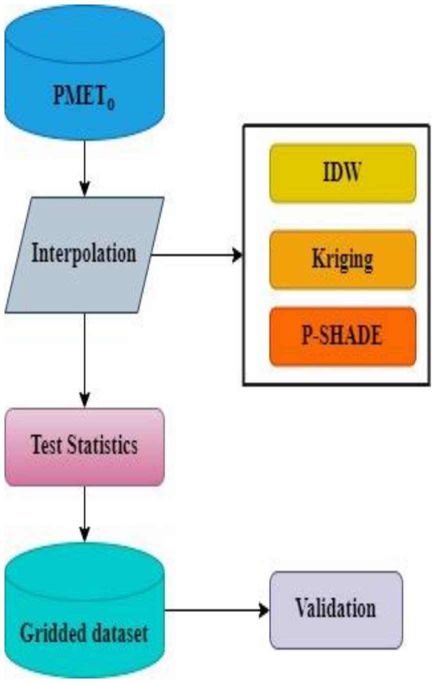


**Figure 7.1: Methodology adopted in the development of the gridded $ET_0$ dataset**

considered, $d_{ij}$ is the distance from the unsampled location i to measurement location j and n is the power exponent. Figure 7.2 provides a conceptual representation of the IDW method.

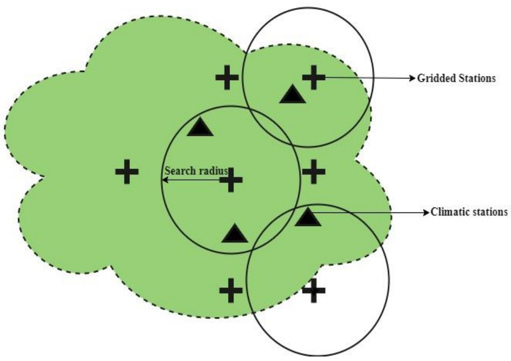


**Figure 7.2: Concept of IDW spatial interpolation**

## 7.5 KRIGING

Kriging works on the principle of measured degree of spatial dependence among the known points in terms of semivariance given by (Goovaerts 2000, Mancosu et al.

2014):

$$\gamma(h) = \frac{1}{2N(h)} \sum_{j=1}^{N(h)} \left[ Z(x_j) - Z(x_j + h)^2 \right] \tag{7.3}$$

γ(h) is the estimated semivariance at a separation distance or lag h, N(h) is the number of pairs for lag h, $z(x_j)$-$z(x_j + h)$ are the observed values at the point $x_j$ and $x_j + h$, separated by h. Therefore, semivariance is half of the variance, and it expresses the degree of similarity of the variable Z in two points separated by distance h.

$$Z = \sum_{j=1}^{N} \lambda_j Z_j \tag{7.4}$$

The objective of the Ordinary Kriging method is to estimate the value at the Z point through the sum of the product of available observations $z_j$ and the weight found in semivariance analysis ($\lambda_j$), where the sum is equal to 1. The semivariogram can be fitted by different models such as spherical, circular, exponential, gaussian and linear.

## 7.6 P-BSHADE

Xu et al. (2013) proposed a modified version of the original Biased Sentinel Hospitals-Based Area Disease Estimation model (BSHADE) and called it the P-BSHADE model. The P-BSHADE technique can be used to estimate any given variable at unsampled locations considering non-homogeneity in the spatial distribution of the variable. The estimate at the unsampled location is obtained as a weighted sum of observed data at surrounding stations. By imposing two conditions on the estimate – unbiasedness and minimum mean square estimation error, the method ensures that it is the best linear unbiased estimate (BLUE). In deriving station weights, both the ratio and covariance of the variable between stations are considered. A concise description of the P-BSHADE method is given below. Xu et al. (2013) provide a detailed description of the theory and governing equations of the method. The estimate of the variable at the target location $(\hat{y}_0)$ is given by (Xu et al., 2013),

$$\hat{y}_0 = \sum_{i=1}^{n} w_i y_i \tag{7.5}$$

where $(y_i)$ is the observed value at the ith station and $w_i$ is the associated station weight. Assuming that $y_0$ is the true but unknown value of the variable to be estimated at a target location 0, the condition of unbiasedness will lead to,

$$E(y_0) = E(\hat{y}_0) \tag{7.6}$$

The condition of minimum estimation error (or variance) will give,

$$\min_{w} \left[ \sigma^2_{\hat{y}_0} = E(\hat{y}_0 - y_0)^2 \right] \tag{7.7}$$

Combining Eqs. 7.5 and 7.6, we get (Xu et al. 2013),

$$E(y_0) = \sum_{i=1}^{n} w_i y_i \tag{7.8}$$

where E denotes statistical expectation. In order to account for heterogeneity in the spatial distribution of the variable under consideration, Xu et al. (2013) consider the ratio of the variable between the target station (0) and observation station (i) as an index and accordingly propose the relationship,

$$b_i E y_0 = E y_i \tag{7.9}$$

where $b_i$ is the ratio of the variable. Combination of Eqs. 7.5 and 7.9 gives,

$$\sum_{i=1}^{n} w_i b_i = 1 \tag{7.10}$$

Therefore, the problem reduces to one of determination of the weights $(w_i)$ for which the condition of minimization of mean estimation variance subject to unbiasedness is used. This results in a standard-constrained optimization problem involving the minimization of the following objective function (Wang et al. 2013),

$$\begin{aligned}\sigma_{\hat{y}_0}^2 =& \sigma_{y_0}^2 + \sum_{i=1}^{n}\sum_{j=1}^{n} w_i w_j C\left(w_i w_j\right) - \\ & 2\sum_{i=1}^{n} w_i C\left(y_i y_0\right) + 2\mu\left(\sum_{i=1}^{n} w_i b_i - 1\right)\end{aligned} \tag{7.11}$$

where μ is the Lagrange multiplier and C is the statistical covariance between the variable at two locations. Minimization of $\sigma_{\hat{y}_0}^2$ is carried out by considering its partial derivatives with respect to $(w_i)$ and μ and setting them to zero. While minimization with respect to μ satisfies the condition of unbiasedness, minimization with respect to weights $(w_i)(i = 1 \ldots. n)$ leads to (Xu et al. 2013),

$$\begin{aligned}\partial\sigma_{\hat{y}_0}^2/\partial w_i = 0 &\Rightarrow 2\sum_{j=1}^{n} w_j C\left(y_i y_j\right) - 2C\left(y_i y_0\right) + 2\mu b_i = 0 \\ &\Rightarrow \sum_{j=1}^{n} w_j C\left(y_i y_j\right) + \mu b_i = C\left(y_i y_0\right)\end{aligned} \tag{7.12}$$

By combining Eq. 7.12 with Eq. 7.10, we obtain n+1 simultaneous equations which can be solved to obtain the station weights $(w_i)$.

## 7.7 DETERMINATION OF OPTIMAL INPUT PARAMETERS

The three spatial interpolation methods evaluated in this study require certain parameters to be determined prior to application. For instance, the IDW method requires the specification of two parameters in Eqs. 7.1 and 7.2 – the value of the power exponent (n) and the number of surrounding stations to be considered (N). The Kriging method (Eqs. 7.3 and 7.4) requires the selection of the type of model for the experimental semivariogram and its shape parameters and also the separation distance or lag (h). Similarly, the P-BSHADE method requires the specification of the number of surrounding observation stations (n). Since there are no specific rules for determining these parameters, they have to be determined for the given dataset using a trial procedure.

In the present study, the input parameters for each of the interpolation methods were determined through a limited sampling approach which involved the following procedure: 1) two agroclimatic zones, one with the largest number of climate stations and the other with the smallest number of stations were selected. Accordingly, the hilly zone (HL) with 5 stations and the northern dry zone (ND) with 17 stations were chosen 2) for each of these zones two validation climate stations were selected such that one station was located within the zone and the other was located in an adjacent zone. Accordingly, the HL zone validation stations selected were HL5 and NT5 for the ND zone the ND3 and NED1 were selected (Figure 7.3) 3) in each of these zones, using historical daily PM $ET_0$ estimates at the identified surrounding stations, the three interpolation methods were implemented considering the validation stations to be unsampled/target locations by varying the values of the input parameters 4) the accuracy of the interpolation in each case was evaluated by comparing the estimated $ET_0$ values with observed values of $ET_0$ at the validation stations for the period 2006-2016 5) the optimal values of input parameters were selected on the basis of $R^2$, RMSE and MBE values computed at the validation stations.

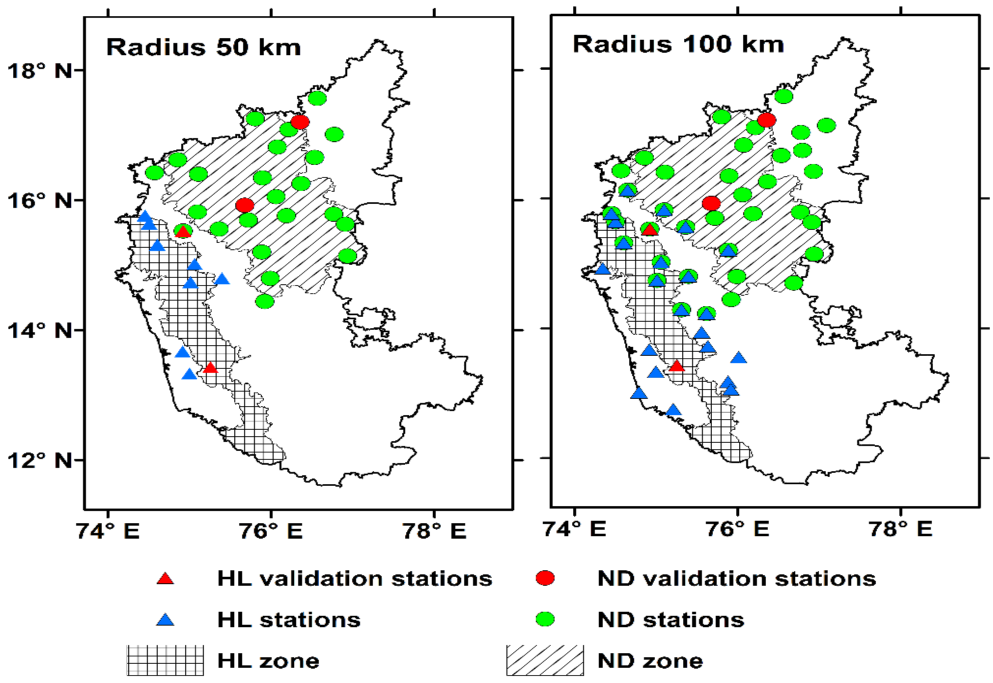


**Figure 7.3: Validation stations to determine optimal search radius**

### 7.7.1 IDW

For IDW, in applying Eqs. 7.1 and 7.2, a value of power function n=2 was used and search radius values of 50 and 100 km were used to determine the optimum number of surrounding stations (N) to be used. For deriving $ET_0$ estimates for the Sringeri target station (HL5), the number of surrounding stations (N) considered were 2 and 11 for 50 km and 100 km radius respectively while the corresponding number of surrounding stations for the Walmi station (NT5) were 4 and 13 respectively. Similarly, for the Badami station (ND3) 50 km radius yielded 2 surrounding stations and a 100 km radius yielded 10 stations while for the Afzalpur station (NED1) the corresponding number of stations was 3 and 8 for a 50 km and 100 km radius. At each of the target/validation stations, daily values of $ET_0$ were obtained through IDW interpolation considering $ET_0$ values computed from the PM equation at the N surrounding stations for the period 1st January 2006 to 31st December 2016. Subsequently, interpolated $ET_0$ values were compared with those computed at the target stations using the PM equation. The results of this comparison for the HL and ND zones for search radius values of 50 km and 100 km are depicted in scatter plots shown in Figures 7.4 (a)-(d). The accuracy of interpolation was assessed using the $R^2$ values (shown in Figures 7.4 (a)-(d)) obtained between station PM $ET_0$ values and those obtained through IDW interpolation at the 4 target/validation stations. From the results shown in Figure 7.4, it is evident that the IDW method provides reasonably accurate estimates at both the station located within the HL zone (Sringeri – HL5) ($R^2$ = 0.5501) and also the station located in the adjacent NT zone (Walmi – NT5) ($R^2$ = 0.5808) for a search radius of 50 km. However, at the Sringeri target station, interpolated $ET_0$ values seem to be significantly underestimated especially for high values of station $ET_0$. An increase in the search radius to 100 km and the associated increase in the number of surrounding stations leads to an improvement in the accuracy of interpolation at the Sringeri station ($R^2$ = 0.6114) but yields poorer estimates at the Walmi station ($R^2$ = 0.3727) (Figure 7.4). Figures 7.4 (c) and 7.4 (d) indicate that IDW interpolation leads to the underestimation of high values of station $ET_0$ at the Afzalpur target station and the overestimation of low values at the Badami station.

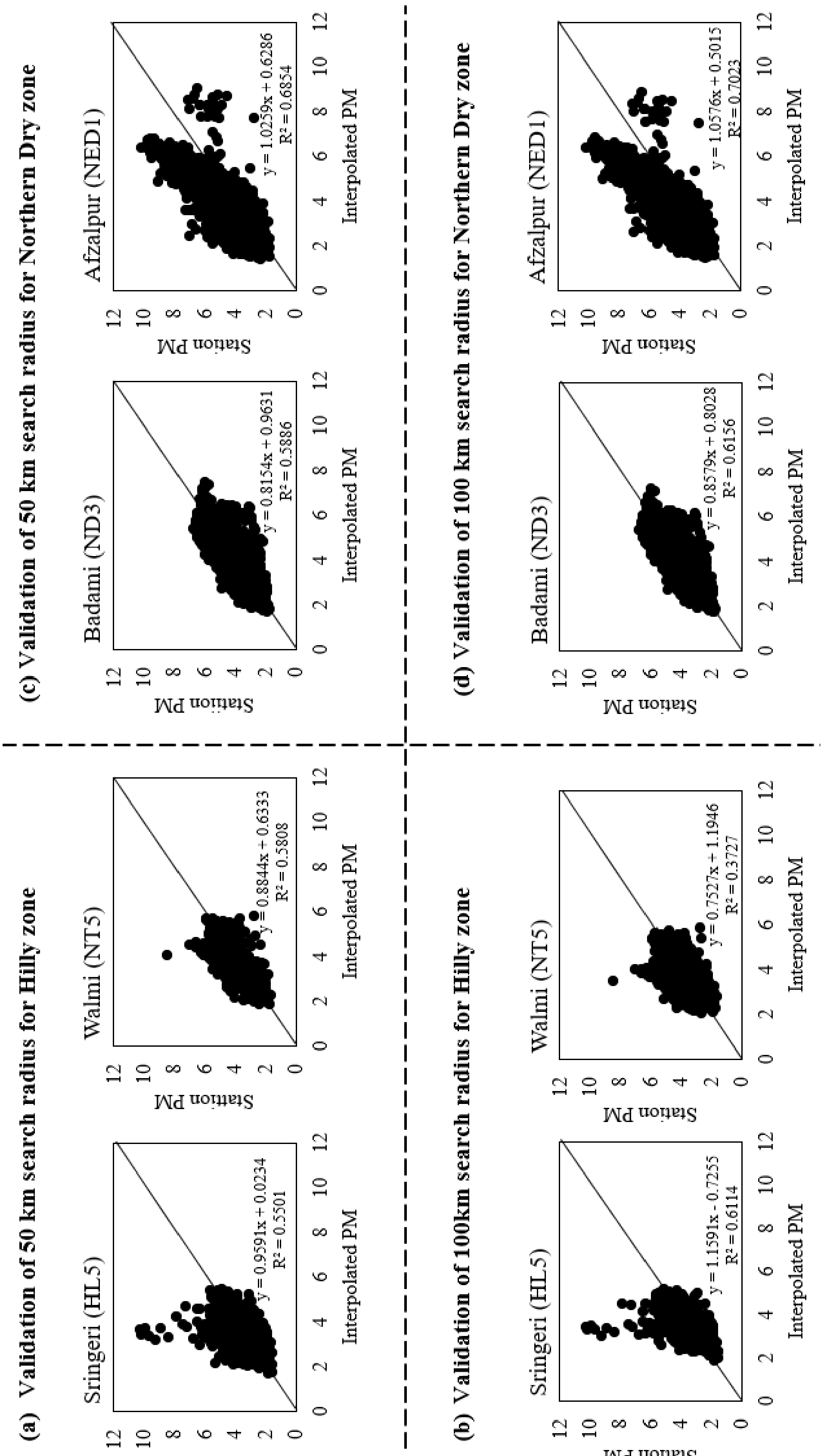


**Figure 7.4: Comparison of different search radius in HL and ND zones**

Also, an increased search radius of 100 km does not seem to provide any significant improvement in the accuracy of interpolation at both target stations (Figure 7.4). Based on the above analysis, it was decided to select a search radius of 50 km for implementing the IDW method since this seemed to provide reasonably accurate estimates and also resulted in the use of a smaller number of surrounding stations in the implementation of Eqs. 7.1 and 7.2.

### 7.7.2 KRIGING

Mean daily $ET_0$ values for the period 2006-2016 at each of the 67 stations were used to fit the experimental semivariogram model in *ArcGIS*10.3®. Although the software offers the choice of different semivariogram models, in the study the spherical model was chosen because of its superior accuracy (Moncosu et al. 2014, Hodam et al. 2017). Many simulations were carried out to determine the optimum semivariogram parameters such as lag, sill and nugget considering the 4 target stations – HL5, NT5, NED1 and ND3. For the 12, 15 and 20 nearest neighbours, the parameters were determined through optimization (Naganna and Deka 2018). It was found that at all these target stations, the experimental variogram with 12 lags performed better with a lag size of 0.3247, nugget of 0.1388 and sill of 0.0724. Using these parameters, the option of fixing a predetermined search radius of 50 km was used to implement Equation 7.4 on a 0.25×0.25 km grid.

### 7.7.3 P-BSHADE

Implementation of the P-BSHADE interpolation algorithm (Eqs. 7.5 – 7.12) requires specification of the number of neighbouring stations. This was determined using a trial procedure at the two target/validation stations Sringeri and Walmi. Considering a 100 km search radius around each of them, the algorithm was implemented by successively increasing the number of neighbouring stations to be used in the interpolation. The reduction in estimation variance between observed and interpolated daily $ET_0$ values during the period of record was tracked as the number of neighbouring stations increased. Figure 7.5 depicts the results obtained in this manner from which it can be seen that at both stations there is a sharp drop in the variance up to 5 neighbouring stations and a more moderate decrease thereafter. Based on these results, it was decided to use a uniform value of 15 neighbouring stations for all target grid

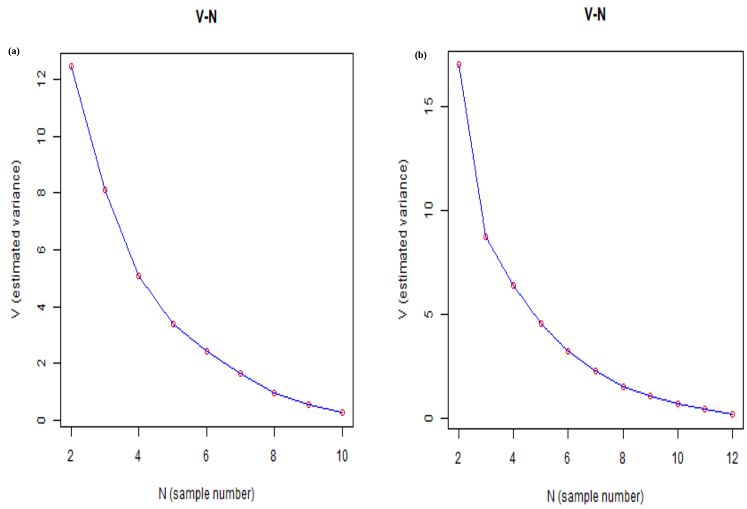


**Figure 7.5: Variation of estimated variance by P-BSHADE for an increasing number of neighbouring stations located within a search radius of 100 km at (a) Sringeri and (b) Walmi stations**

points while implementing the P-BSHADE method.

## 7.8 RESULTS AND DISCUSSION

### 7.8.1 Performance evaluation of interpolation methods

After the determination of the optimal values of input parameters for the 3 interpolation methods considered, their performance was evaluated by considering one target station in each of the 10 agroclimatic zones. Daily $ET_0$ values obtained for the period 2006-2016 through interpolation were compared with the station values of PM $ET_0$. The performances of the IDW, Kriging and P-BSHADE methods were assessed by computing the mean and CV of interpolated $ET_0$ values for the period 2006-2016 and comparing them with the corresponding values of these statistics for the station PM $ET_0$ values. Table 7.1 shows the results of this comparison from which it can be seen that all three interpolation methods provide $ET_0$ estimates with mean and CV quite close to those computed at all stations across different agroclimatic zones. It appears that the mean $ET_0$ values obtained by interpolation for the period of record are not very different between the IDW, Kriging and P-BSHADE methods. While CV values are also similar for the three methods, the IDW method seems to provide more variable estimates in some zones. In comparison to the station means, all

**Table 7.1: Comparison of mean and CV (2006-2016) of daily station PM $ET_0$ and interpolated $ET_0$ in different agroclimatic zones**

| Zone | Station | Station $ET_0$ | | Interpolated $ET_0$ | | | | | |
|---|---|---|---|---|---|---|---|---|---|
| | | Mean (mm $d^{-1}$) | CV | IDW | | Kriging | | P-BSHADE | |
| | | | | Mean (mm $d^{-1}$) | CV | Mean (mm $d^{-1}$) | CV | Mean (mm $d^{-1}$) | CV |
| CD | Hiriyur | 4.40 | 0.13 | 3.68 | 0.19 | 3.72 | 0.19 | 3.69 | 0.21 |
| CO | Hosangadi | 3.28 | 0.12 | 3.59 | 0.19 | 3.56 | 0.18 | 3.55 | 0.20 |
| ED | Thippagondanahalli | 4.35 | 0.14 | 3.57 | 0.27 | 3.60 | 0.20 | 3.60 | 0.20 |
| HL | Sringeri | 3.27 | 0.18 | 3.52 | 0.19 | 3.54 | 0.18 | 3.51 | 0.19 |
| NED | Bheemarayanagudi | 2.94 | 0.17 | 3.78 | 0.27 | 3.87 | 0.26 | 3.86 | 0.26 |
| NET | Halhalli | 3.81 | 0.07 | 3.96 | 0.33 | 3.79 | 0.26 | 3.94 | 0.22 |
| ND | Hungund | 4.17 | 0.20 | 3.79 | 0.23 | 3.85 | 0.23 | 3.86 | 0.25 |
| NT | Walmi | 3.73 | 0.20 | 3.53 | 0.20 | 3.60 | 0.20 | 3.59 | 0.20 |
| SD | Marconahalli | 3.07 | 0.15 | 3.68 | 0.20 | 3.56 | 0.19 | 3.72 | 0.18 |
| ST | Belur | 3.97 | 0.19 | 3.47 | 0.21 | 3.52 | 0.18 | 3.48 | 0.19 |

three interpolation methods provide overestimates in some zones and underestimate in other zones. The underestimation is particularly high in the CD, ED and ND zones while significant overestimation can be seen at the stations located in the NED and SD zones.

The performances of the interpolation methods were further evaluated by computing $R^2$, RMSE, and MBE values between station $ET_0$ and interpolated $ET_0$ at the 10 stations located in different agroclimatic zones (Table 7.1). The magnitude and so also the relative differences in these statistics for the IDW, Kriging and P-BSHADE can be assessed from the results shown in Figure 7.6. Again, it is evident that there appears to be very little difference in the performances of the three interpolation methods across all stations with the performance being either good or poor being the same for all of them. Figure 7.6 shows that $R^2$ values very extremely low for the ED and SD zones whereas the highest $R^2$ of more than 0.8 was recorded for the station in the ND zone. For the other 8 zones, $R^2$ ranged between 0.5 – 0.6 for all the methods indicating acceptable performance for practical applications (Sharma and Irmak 2012). In terms of RMSE, it can be seen from Figure 7.6 that high values (1.0 – 1.5 mm $d^{-1}$) were recorded for the CD, ED, NED and SD zones whereas it was between 0.5 - 1.0 mm $d^{-1}$ for the other zones indicating reasonably accurate performance by all

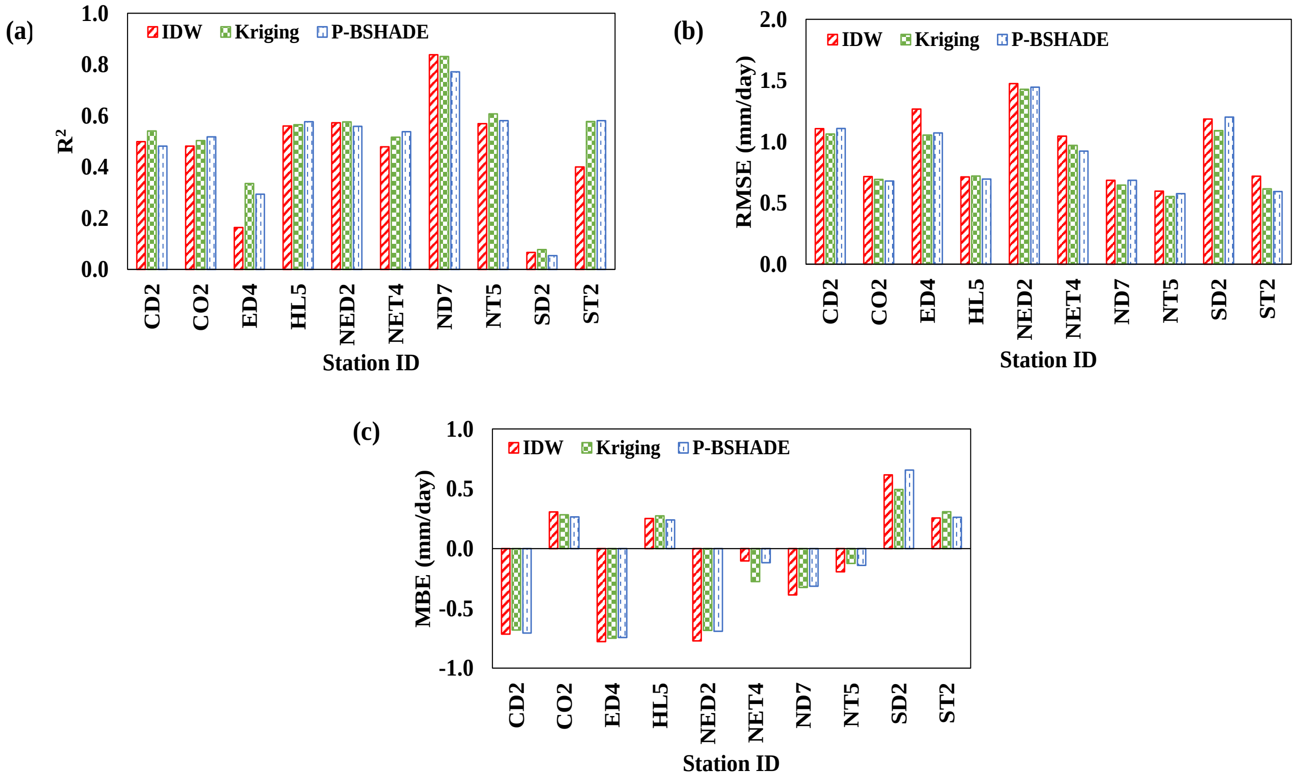


**Figure 7.6: Performance statistics for the interpolation methods at stations located in different agroclimatic zones**

three interpolation methods. MBE values exhibited a large range of variation across the zones (-0.4 – 0.6 mm $d^{-1}$) indicating a high bias in interpolations by all methods. In only 5 out of the 10 zones, acceptable values of MBE of less than ±0.5 mm $d^{-1}$ (Figure 7.6) were obtained.

Overall results of the performance evaluation of the IDW, Kriging and P-BSHADE interpolation methods indicate that there was very little difference in the accuracy of interpolations obtained from them. Also, all three methods performed poorly in 2-3 zones (Table 7.1 and Figure 7.6) probably because the number of neighbouring stations selected within the specified search radius was low. In the remaining zones, all three methods yielded interpolated $ET_0$ estimates which compared reasonably well with the station-computed PM $ET_0$ values. Based on these results, it was decided to select the IDW method for deriving the gridded $ET_0$ product since it is conceptually and computationally simpler than the other two methods.

### 7.8.2 WEB-GIS and GOOGLE EARTH ENGINE data

The validated IDW method with optimal input parameters was used to derive a daily $ET_0$ gridded product covering the Karnataka State. For this purpose, a $0.25 \times 0.25$ spatial resolution was adopted resulting in a total of 260 grid points for the study area. Using daily PM $ET_0$ estimates obtained at the 67 climate stations for the period 1st January 2006 to 31st December 2016, the IDW method was implemented to derive daily $ET_0$ estimates at the grid points. Post-processing of the point data involved converting it to vector files having position, day of data, and value format.

Access to the gridded data was provided separately for local users in the National Institute of Technology Karnataka, Surathkal who possessed an official email id and for the general public. Local users can access these vector files through the web service on the Mapstore platform inter-linked with Geoserver and Apache Tomcat.

Public users can access the data on the Google Earth Engine platform (Gorelick et al. 2017) using the following link: https://sites.google.com/nitk.edu.in/karnatakaet data/home

https://code.earthengine.google.com/?asset=projects/ee-niranjan/assets/karetdata

### 7.8.3 Comparison of gridded data product with global $ET_0$ products

An effort was made to compare the accuracy of the daily $ET_0$ gridded data product developed in this study with other global $ET_0$ data products available in the public domain. Three products namely, ERA5 (Hersbach et al., 2020), GLEAM (Martens et al., 2017) and dPET (Singer et al., 2021) were selected for this purpose. Table 7.2 provides details of the source website/reference, spatial and temporal resolutions and data period available for each of these $ET_0$ products. The dPET product provides $ET_0$ estimates by the PM method whereas GLEAM is based on the PT method. The ERA5 $ET_0$ reanalysis product uses a surface energy balance approach to estimate potential evaporation.

For the comparative analysis, 10 climate stations located in each of the agroclimatic zones were selected (Table 7.3) and daily station $ET_0$ values were derived using the PM method was extracted for the period 1 January 2006 to 31 December 2016 for each of them. Daily $ET_0$ values for this period for the grid points located closest to

**Table 7.2: Details of the global $ET_0$ data products considered in the comparative analysis**

| Dataset | Spatial Resolution | Temporal Resolution | Period | Data Source |
|---|---|---|---|---|
| ERA5 (https://cds.climate.copernicus.eu/cdsapp#!/dataset/reanalysis-era5-single-levels?tab=overview) | 0.25° | Hourly | 1959 to present | Hersbach et al. 2020 |
| GLEAM v3.6a PET (GLEAM) (https://www.gleam.eu/) | 0.25° | Daily | 1981 to present | Martens et al. 2017 |
| dPET (https://doi.org/10.5523/bris.qb8ujazzda0s2aykkv0oq0ctp) | 0.1° | Daily | 1981 to present | Singer et al. 2021 |

**Table 7.3: Details of the validation stations considered in the comparative analysis of each agro-climatic zone**

| Zone | Station ID | Station |
|---|---|---|
| CD | CD2 | Hiriyur |
| CO | CO2 | Hosangadi |
| ED | ED1 | Hebbur |
| HL | HL5 | Sringeri |
| NED | NED5 | Jewargi |
| NET | NET4 | Halhalli |
| ND | ND7 | Hungund |
| NT | NT3 | Hidkal |
| SD | SD3 | Shravanabelgola |
| ST | ST2 | Belur |

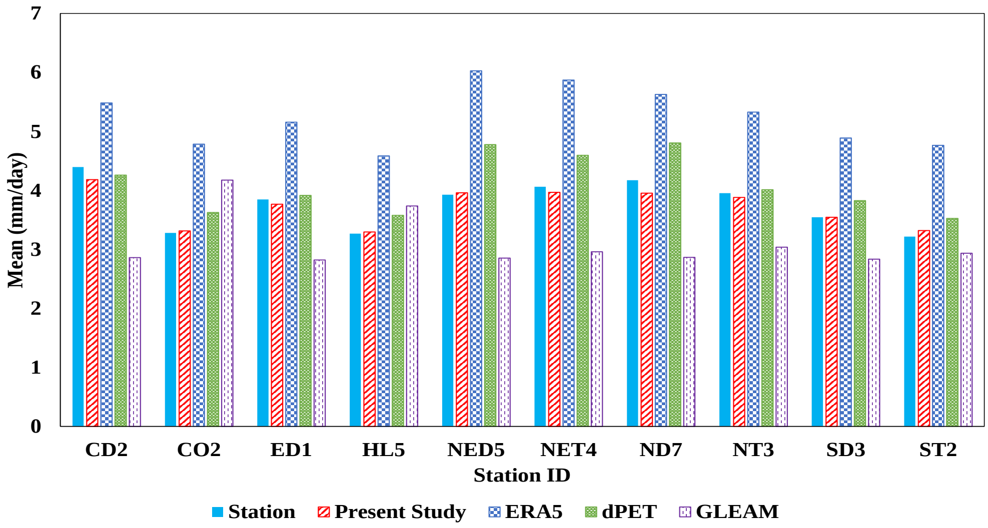


**Figure 7.7: Comparison of station mean $ET_0$ values with those obtained from the 4 gridded data products for 2006-2016 at the 10 climate stations**

these stations were extracted from the data product developed in the present study and also from the 3 global data products listed in Table 7.2. For the ERA5 product, hourly estimates of potential evaporation were aggregated to daily values.

At each station, the mean and CV of station $ET_0$ estimates for the period of record (2006-2016) were computed and compared with the corresponding mean and CV values for the nearest grid point $ET_0$ estimates by the 4 data products (present study, ERA5, GLEAM and dPET). Results of this comparative analysis are shown for mean $ET_0$ values (Figure 7.7) and CV of $ET_0$ (Figure 7.8).

Figure 7.7 indicates that the IDW-derived mean $ET_0$ values of the present study closely match the station-computed mean $ET_0$ values at all stations located in different agroclimatic zones. Mean $ET_0$ values from the ERA5 data product are significantly larger than station means in all the zones while the GLEAM estimates are underestimated except in the CO and HL zones. In comparison to these two products, the dPET product estimates appear to be closer to the station means at most stations except in the northern dry zones where slight overestimation was evident (Figure 7.7). The variability in daily $ET_0$ estimates at the 10 stations over the period 2006-2016 by the 4 gridded data products were compared with the variability of station computed values using the coefficient of variation (CV). As Figure 7.8 depicts, the gridded data product developed in the present study yielded CV values closest to

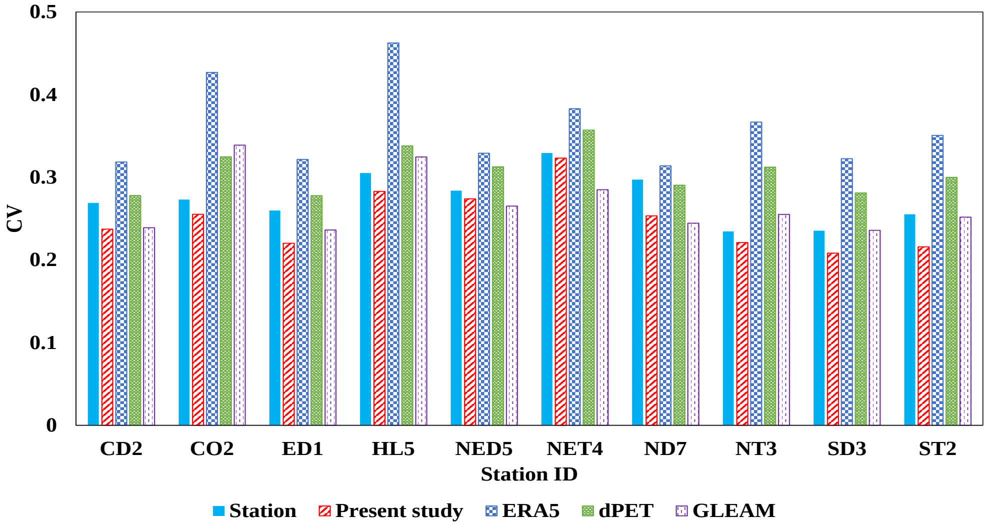


**Figure 7.8: Comparison of CV values of station $ET_0$ with those obtained from the 4 gridded data products for 2006-2016 at the 10 climate stations**

the station values albeit with smaller variabilities. Interestingly, the GLEAM product which underestimated mean $ET_0$ estimates (Figure 7.7), produced CV values comparable to the station values across most of the stations. The ERA5 yielded significantly large values of CV across all the zones while the dPET estimates also yielded larger CV values than the station CV values but of smaller magnitude. Overall, it is apparent that the gridded data product developed in this study was the best in terms of estimating mean $ET_0$ values and capturing their temporal variabilities across all the agroclimatic zones of Karnataka State. The dPET product proved to be the second best.

The comparison between the accuracies of the 4 gridded $ET_0$ products was further investigated by computing $R^2$, RMSE and MBE values for each of them relative to the daily station $ET_0$ values for the period 2006-2016 at the selected 10 validation climate stations. Figure 7.9 shows the comparison of $R^2$ values from which it is evident that the grid $ET_0$ estimates obtained by the product developed in the present study were superior to all the other products yielding $R^2$>0.9 at all the stations except the station in the NET zone where it performed on par with the others. $R^2$ values for the ERA5 and dPET were almost the same across all the stations and varied between 0.4 to 0.6 except for the station in the ED zone where their performance was poor. The GLEAM estimates exhibited mixed performance, being extremely poor in some

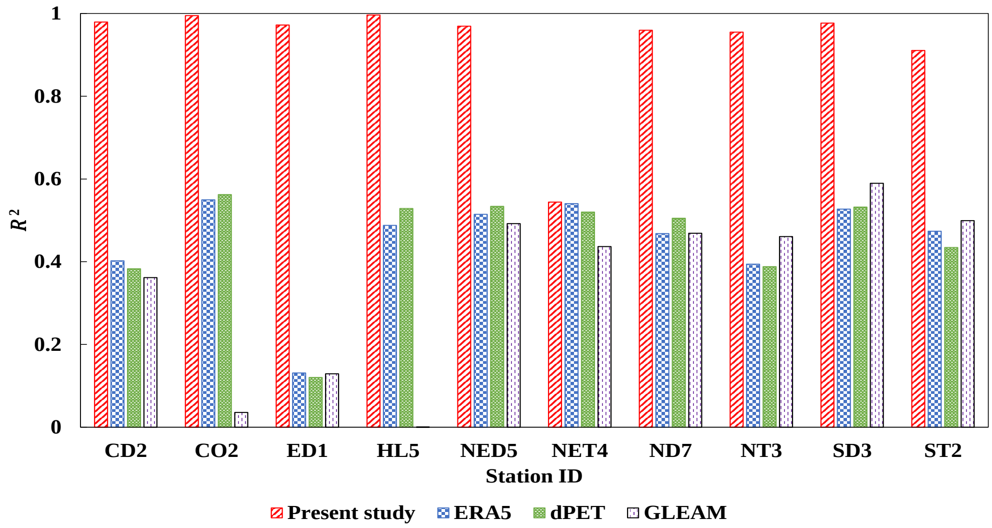


**Figure 7.9: Comparison of coefficient of determination ($R^2$) values obtained between daily $ET_0$ estimates by the 4 gridded products and PM $ET_0$ values computed at the 10 selected climate stations for the period 2006-2016**

zones (CO, ED, HL) and being either on par or slightly better than the ERA5 and dPET products in some zones (Figure 7.9). Figure 7.10 also indicates the superiority of the $ET_0$ product developed in the present study which yielded the lowest values of RMSE in all zones in comparison to the other 3 products. On the other hand, the ER5 product recorded the highest errors in almost all the agroclimatic zones with RMSE values in excess of 1.5 mm $d^{-1}$ while the dPET product performance was reasonably better with RMSE values being close to 1.0 mm $d^{-1}$ across the zones. The GLEAM product yielded errors which were greater than for the dPET product but less than the ERA5 product (Figure 7.10).

A relative comparison of the MBE values for the 4 products is depicted in Figure 7.11 from which it is evident that the product developed in the present study yielded $ET_0$ estimates with the least bias relative to the station $ET_0$ values across all the zones. The ERA5 product consistently overestimated $ET_0$ by a significant magnitude while the GLEAM product provided a large negative bias in most of the zones. The performance of the dPET product was significantly better than the ERA5 and GLEAM products in most of the zones and in terms of MBE was even better than the product of the present study in the CD and NT zones (Figure 7.11).

From this analysis, it can be concluded that the daily PM $ET_0$ gridded data product

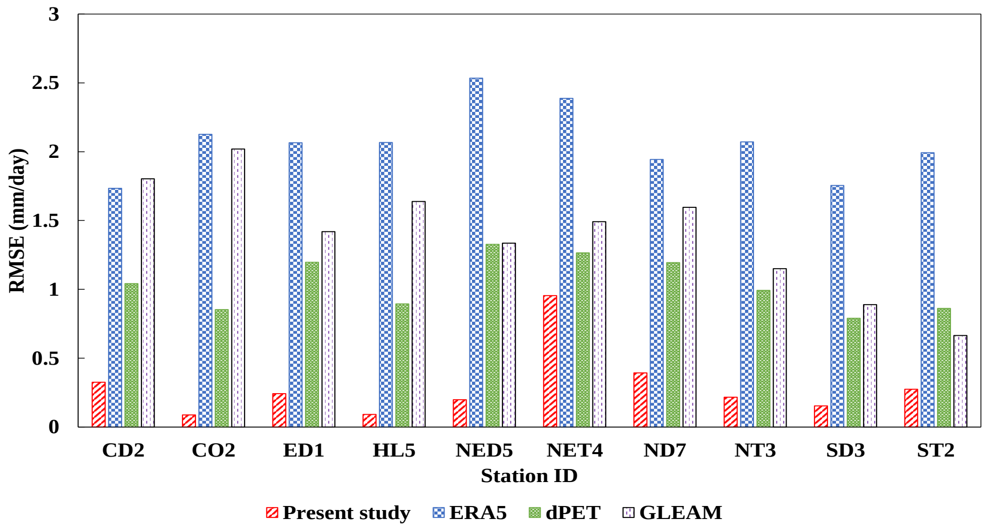


**Figure 7.10: Comparison of root mean square error (RMSE) values obtained between daily $ET_0$ estimates by the 4 gridded products and PM $ET_0$ values computed at the 10 selected climate stations for the period 2006-2016**

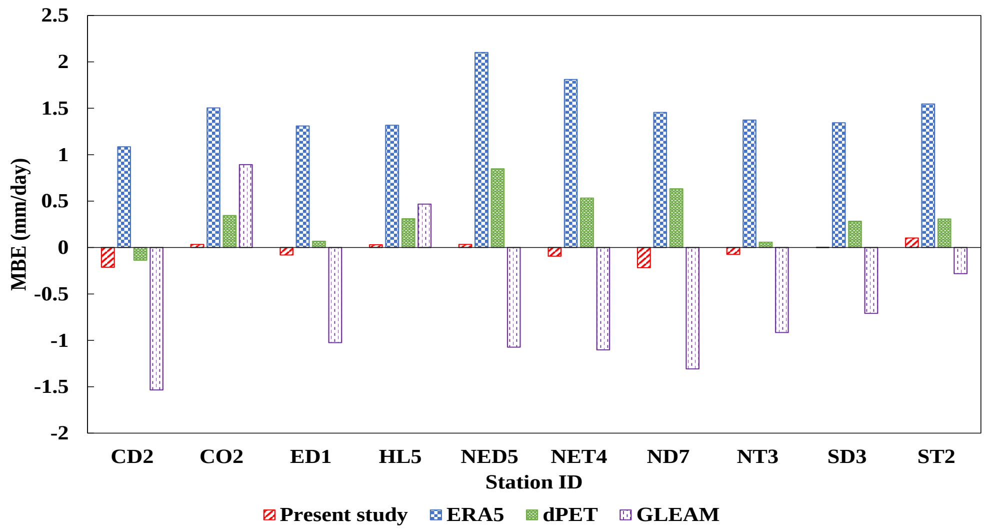


**Figure 7.11: Comparison of mean bias error (MBE) values obtained between daily $ET_0$ estimates by the 4 gridded products and PM $ET_0$ values computed at the 10 selected climate stations for the period 2006-2016**

developed in this study yielded the most accurate grid point estimates in comparison to other global gridded $ET_0$ products available in the public domain. The reason for the success of the data product of the present study is on account of the fact that it was developed using $ET_0$ estimates obtained from climate records of stations located in the same region. On the other hand, the ERA5 and dPET global products have been developed using a reanalysis of climate data. Also, the products not only differ in the spatial and temporal resolutions but also use different methods to compute $ET_0$ – PM in the present study and dPET, PT in GLEAM and surface energy balance in the ERA5. All these factors would have resulted in different levels of performance of the global data products in this particular comparative analysis.

However, the comparative analysis brings into focus the importance of verifying the accuracies of global data $ET_0$ products using regional-scale data products of the type developed in the present study and implementing bias correction so as to improve the accuracies of gridded $ET_0$ estimates.

## 7.9 CLOSURE

This chapter presented a comprehensive methodology for the development of gridded reference crop evapotranspiration ($ET_0$) at a daily temporal scale for the data period of 1st January 2006 to 31st December 2016 covering Karnataka State, India. Prior to this, three spatial interpolation methods namely, IDW, Kriging and P-BSHADE, were evaluated for their prediction accuracy using a limited sample of climate stations. Accordingly, the conceptually and computationally simpler IDW method was selected since the prediction accuracies were more or less the same for all the methods.

Web links for the gridded data product have been created in an effort to share the data on $ET_0$ which is a critical input in a variety of studies in earth sciences. It is hoped that researchers and practitioners will benefit from this effort.

# CHAPTER 8

# SUMMARY AND CONCLUSIONS

## 8.1 GENERAL

The present study was taken up with four key objectives in mind: 1) Assessment of spatio-temporal variations of climatic variables associated with the calculation of reference crop evapotranspiration ($ET_0$) over Karnataka State, India for the historical period 2006-2016 2) Assessment of spatio-temporal variations of Penman-Monteith (PM) $ET_0$ for the study area for the same historical period 3) Performance evaluation of simpler alternative $ET_0$ equations relative to PM $ET_0$ with and without local calibration of parameters and 4) Development of a gridded PM $ET_0$ product for Karnataka State. Historical datasets used various methodologies developed and applied to achieve these objectives and the results obtained thereof are discussed in the previous chapters of this thesis. In this final chapter, the major conclusions from the research carried out are summarized. Also, the limitations of the study and recommendations for future research are enumerated.

## 8.2 SPATIO-TEMPORAL VARIABILITY OF CLIMATE VARIABLES AND PM $ET_0$

Analysis of the spatio-temporal variations of climatic variables over the Karnataka State clearly demonstrated the prevalence of distinct climatic regimes ranging from humid to arid. In particular, the spatial variations in mean PM $ET_0$ values across the study area and the seasonal variability of $ET_0$ in different agroclimatic zones clearly establish the existence of climate heterogeneity. Therefore, any attempt to model regional evapotranspiration rates in the State must necessarily consider this factor and use appropriate spatially discretized units for improved prediction accuracies in $ET_0$. In this context, the present analysis confirms that the agroclimatic classification proposed by Ramachandra et al. (2004) and KSDA, Government of Karnataka (2018) appears appropriate and can be adopted in similar studies which are focused on climate and evapotranspiration analyses. Further refinements in demarcating agroclimatic zones in Karnataka and agroclimatic classifications in other regions may consider $ET_0$ as key criteria.

The overall characterization of climate variables indicates the northern agroclimatic zones (ND, NED, and NT) exhibited high temperature, low humidity, and high sunshine values. Similarly, the southern region is characterized by low temperature and high humidity. On the other hand, windspeed was less in CO and HL zones and clusters of high windspeed in the northern part were observed. Since the climate of Karnataka State is largely influenced by the monsoon phenomenon, distinct variations in climatic variables arise on its account.

A similar influence of the monsoon was seen in the intra-annual variations of mean $ET_0$ estimates. It was seen that $ET_0$ values peak during the month of April (4.5-5 $\mathrm{mm\ d^{-1}}$) and with the onset of the monsoon rains in May-June and begin to decrease to around 3.0-4 $\mathrm{mm\ d^{-1}}$. The spatial variability of $ET_0$ across the Karnataka State indicates lower values in the southern, coastal, and hilly regions in comparison to northern regions. This difference is caused probably on account of the topographical effect created by the Western Ghat mountains which are located in the western part of the State.

## 8.3 LOCAL CALIBRATION OF THE HARGREAVES (HG) EQUATION

Overall results of this analysis lead to three important conclusions: 1) use of the original HG equation with standard values of parameters may yield $ET_0$ estimates that are quite different from those obtained by the FAO-56 recommended PM equation and therefore local calibration of the HG equation is strongly recommended for the sake of accuracy 2) the optimized parameters of the modified HG equations considered in this study showed significant variations between the 67 climate stations. Elevation seemed to explain about 60% of this variability for two of the parameters. Mean values of HG model parameters for different agro-climatic zones in the study area and also maps showing spatial variability of the parameters were developed for the benefit of practitioners who wish to obtain estimates of $ET_0$ comparable to the PM method using only air temperature data 3) the original HG equation appears to adequately represent the most important variables, since replacing the $T_{\mathrm{mean}}$ term (with equal weightage for $T_{min}$ and $T_{min}$) with an alternative $T_{eff}$ with variable weightages for these variables did not lead to any substantial improvement in the accuracy of $ET_0$ estimates.

## 8.4 PERFORMANCE EVALUATION OF SIMPLER $ET_0$ EQUATIONS

The performances of four popular $ET_0$ estimation methods – Blaney-Criddle (BC), Priestley-Taylor (PT), FAO-24 Radiation (RAD) and Turc (TC), which use limited climate inputs were evaluated relative to the FAO-56 Penman-Monteith (PM) method across heterogeneous climatic conditions prevailing in Karnataka State, India. The analysis was carried out at a monthly time step using climate records for the 11-year historical period (2006-2016) for 67 stations located in 10 different agro-climatic zones of the State. Results obtained in terms of the coefficient of determination ($R^2$), root mean square error (RMSE) and mean bias error (MBE) relative to PM $ET_0$ estimates indicated that the BC and PT equations performed reasonably well in several of the agroclimatic zones in the State.

Considering the original BC equation its performance relative to the PM equation was relatively good in most agroclimatic zones as evident from $R^2$ values exceeding 0.68. The lowest values of RMSE (0.61 $\mathrm{mm\ d^{-1}}$) for the BC equation were recorded in the NET and NT zones. The equation yielded RMSE values ranging between 0.67 – 0.78 $\mathrm{mm\ d^{-1}}$ in the other zones with the highest error being recorded in the SD zone. The BC equation yielded over-estimates in some zones and under-estimates in others as indicated by both positive and negative values of MBE. Overall, the performance of this equation proved to be reasonably accurate, especially in the northern dry agroclimatic zones.

The original PT equation provided the best $ET_0$ estimates relative to the PM equation in terms of $R^2$ among all the simpler alternative equations considered in this study. This is evident from the relatively high values of $R^2$ across all the zones (Table 2). However, the PT equation recorded higher values of RMSE than the BC equation in 5 out of the 10 zones. Also, this equation provided significantly higher over-estimates in almost all zones as indicated by the MBE statistic. The original RAD equation yielded higher $R^2$ values than the BC equation in some zones but its performance was poorer than the PT equation based on this statistic. Also, this equation provided the highest values of RMSE and MBE among all the methods considered in almost all the zones again indicating poor performance. In terms of $R^2$, the performance of the original TC equation was the poorest among all the methods considered in almost all the zones. However, it yielded the lowest values of RMSE in most of the zones and MBE values were the lowest in several zones.

Overall, results indicate that the original PT equation performed the best among the 4 alternative simpler equations in terms of $R^2$ and RMSE in most of the agroclimatic zones of the study area. However, the equation consistently over-estimated $ET_0$ values relative to the PM equation in several of the zones.

## 8.5 LOCAL CALIBRATION OF SIMPLER $ET_0$ METHODS

The performances of four popular $ET_0$ estimation methods – Blaney-Criddle (BC), Priestley-Taylor (PT), FAO-24 Radiation (RAD) and Turc (TC), which use limited climate inputs were locally calibrated with the FAO-56 Penman-Monteith (PM) method across heterogeneous climatic conditions prevailing in Karnataka State, India. The analysis was carried out at a monthly time step using climate records for the 11-year historical period (2006-2016) for 67 stations located in 10 different agro-climatic zones of the State. Performance of the calibrated equations was assessed using the coefficient of determination ($R^2$), root mean square error (RMSE) and mean bias error (MBE) relative to PM $ET_0$ estimates. With the use of optimal parameters/coefficients obtained through calibration, the performances of all the equations showed improvement in several of the agroclimatic zones.

In particular, the PT equation showed a significant reduction in RMSE and MBE values at a large number of stations on account of the fact that the value of the parameter aP which is set to 1.26 in the original equation, varied over the range of 1.00 to 1.44 when calibrated at different stations. However, calibration did not lead to any improvement in the $R^2$ values indicating that the proportion of variability explained in the PM $ET_0$ estimates remained the same. The RAD equation also showed reduced prediction errors and bias with local calibration. The performance of the calibrated BC equation did not improve significantly probably because the optimization of 4 model parameter values resulted in an over-fit.

The optimal value of the single parameter in the TC equation did not vary much from the standard value and as a consequence, there was only limited improvement in its performance. The original equations appear to adequately represent the most important variables, since replacing the $T_{mean}$ term (with equal weightage for $T_{max}$ and $T_{min}$) with an alternative $T_{eff}$ with variable weightages for these variables did not lead to any substantial improvement in the accuracy of $ET_0$ estimates. However, the overall results of this study demonstrate that local calibration of empirical to semi-empirical $ET_0$ estimation equations which are routinely used in place of the preferred PM method in data-short situations will result in reduced prediction errors and bias in most if not all, types of climates. Therefore, their use with optimal model parameters/coefficients estimated from spatial maps of the kind derived in this study is recommended for a more accurate estimation of $ET_0$ with limited climate inputs.

## 8.6 DEVELOPMENT OF GRIDDED DATASET

This chapter presented a comprehensive methodology for the development of (0.25 $\times$ 0.25 degree) gridded reference crop evapotranspiration ($ET_0$) at a daily temporal scale for the data period of 1st January 2006 to 31st December 2016 covering Karnataka State, India. Prior to this, three spatial interpolation methods namely, IDW, Kriging and P-BSHADE, were evaluated for their prediction accuracy using a limited sample of climate stations. Accordingly, the conceptually and computationally simpler IDW method was selected since the prediction accuracies were more or less the same for all the methods.

The accuracy of the gridded data product developed in this study was compared with three other global $ET_0$ data products available in the public domain. Results indicated that the gridded product developed in this study provided the most accurate estimates of $ET_0$ in all the agroclimatic zones of Karnataka State.

Web links for the gridded data product have been created in an effort to share the data on $ET_0$ which is a critical input in a variety of studies in earth sciences. It is hoped that researchers and practitioners will benefit from this effort.

## 8.7 LIMITATIONS OF THE STUDY

- The limitation of the study was the equations were calibrated with respect to PM $ET_0$ estimates and not with measured $ET_0$ values since they were unavailable.

- Also, relationships between optimal parameters and other terrain variables could not be established due to the limited spatial extent of the study area. However, the overall methodology developed in this study may be extended to other hydro-climatic regions to derive accurate estimates of $ET_0$ using minimal data inputs.

- Local calibration was performed only using a monthly time step since the analysis performed using a daily time step did not yield satisfactory results probably on account of too much noise in the data.

- During optimization, various parameters in the modified equations were determined using the GRG non-linear method. Other more sophisticated optimization techniques may have yielded more accurate results.

- Due to limited climate network density, validation of the $ET_0$ gridded data product was carried out in fewer stations.

## 8.8 RECOMMENDATIONS FOR FUTURE RESEARCH

- In the study, different $ET_0$ equations were validated against the standard FAO-56 $ET_0$ equation. To obtain the precise performance of these models these $ET_0$ models have to be validated using field-measured data.

- Further studies may focus on sensitivity analysis to determine the variability of $ET_0$ against each climate variable.

- The use of the derived locally calibrated parameters from the study can be tested across different environments. Further, the derived methodology for $ET_0$ equation modification can be applied in other states in India.

- Increasing dependence on simulated (reanalysis) climate and $ET_0$ datasets such as CFSR necessitates studies for validation of these datasets at the regional scale. Hence studies can focus on validating these products across different spatio-temporal scales and climatic regions. Methods for bias correction of global datasets may be developed.

- There is an urgent need to establish a regional-hydrological database providing all required data for hydrological analysis. Since the present overall study was data-driven, the spatio-temporal analysis could be performed only for a shorter time period. Future studies' scope can be broadened by including a large spatio-temporal dataset which will aid in investigating historical and temporal aspects of climatic variables, especially $ET_0$ not only in Karnataka state but across other regions in India.

# REFERENCES


Aalto, J., Pirinen, P., and Jylha, K. (2016). "New gridded daily climatology of Finland: permutation-based uncertainty estimates and temporal trends in climate." *J. Geophys. Res.: Atmos.*, 121(8), 3807-3823.

Abatzoglou, J. T., Dobrowski, S. Z., Parks, S. A., and Hegewisch, K. C. (2018). "TerraClimate, a high-resolution global dataset of monthly climate and climatic water balance from 1958–2015." *Sci. Data*, 5(1), 1-12.

Allen, R. G., and Pruitt, W. O. (1986). "Rational use of the FAO Blaney-Criddle formula." *J. Irrig. Drain. Eng., 112(2),* 139-155.

Allen, R. G. (1996). "Assessing integrity of weather data for reference evapotranspiration estimation." *J. Irrig. Drain. Eng., 122(2)*, 97-106.

Allen, R. G., Pereira, L. S., Raes, D., and Smith, M. (1998). "Crop evapotranspiration-guidelines for computing crop water requirements." Food and Agricultural Organization of the United Nations (FAO) Irrig. Drain. Paper No. 56, Rome.

Allen, R. G., Tasumi, M., and Trezza, R. (2007). "Satellite-based energy balance for mapping evapotranspiration with internalized calibration (METRIC)—Model." *J. Irrig. Drain. Eng.*, 133(4), 380-394.

Almorox, J., Quej, V.H. and Marti, P. (2015). "Global performance ranking of temperature-based approaches for evapotranspiration estimation considering Köppen climate classes." *J. Hydrol.*, 528, 514-522.

Althoff, D., Dias, S. H. B., Filgueiras, R., and Rodrigues, L. N. (2020). "ETo-Brazil: a daily gridded reference evapotranspiration data set for Brazil (2000–2018)." *Water Resourc. Res.*, 56(7), e2020WR027562.

Alves, M. D. C., Carvalho, L. G. C., Vianello, R. L., Sediyama, G. C., Oliveira, M. S. D., and Junior, A. S. D. (2013). "Geostatistical improvements of evapotranspiration spatial information using satellite land surface and weather stations data." *Theor. Appl. Climatol.*, 113(1), 155-174.

Ambha (2005). "Spatial hydrological modelling using remote sensing and GIS." Ph.D. thesis, N.I.T.K., Surathkal, Mangaluru, Karnataka, India.

Ananya S. G. (2019). "Modeling actual evapotranspiration using the advection-aridity model in Karnataka State, India." M.Tech. thesis, N.I.T.K., Surathkal, Mangaluru, Karnataka, India.

Attorre, F., Alfo', M., De Sanctis, M., Francesconi, F., and Bruno, F. (2007). "Comparison of interpolation methods for mapping climatic and bioclimatic variables at regional scale." *Int. J. Climatol.*, 27(13), 1825-1843.

Awal, R., Habibi, H., Fares, A., and Deb, S. (2020). "Estimating reference crop evapotranspiration under limited climate data in West Texas." *J. Hydrol.: Rgnl. Stud.*, 28, 100677.

Bai, P., Liu, X., Yang, T., Li, F., Liang, K., Hu, S., and Liu, C. (2016). "Assessment of the influences of different potential evapotranspiration inputs on the performance of monthly hydrological models under different climatic conditions." *J. Hydrometeorol.*, 17(8), 2259-2274.

Bandyopadhyay, A., Bhadra, A., Raghuwanshi, N. S., and Singh, R. (2009). "Temporal trends in estimates of reference evapotranspiration over India." *J. Hydrol. Eng.*, 14(5), 508-515.

Bangalore Climate Change Initiative – Karnataka (BCCI-K) (2011). Karnataka Climate Change Action Plan. Karnataka, India.

Berti, A., Tardivo, G., Chiaudani, A., Rech, F. and Borin, M. (2014). "Assessing reference evapotranspiration by the Hargreaves method in north-eastern Italy." *Agric. Water Manag.*, 140, 622 20-25.

Blaney, H. F., and Criddle, W. D. (1962). "Determining consumptive use and irrigation water requirements." USDA Tech. Bull. 1275, U.S. Dept. of Agric.

Bormann, H. (2011). "Sensitivity analysis of 18 different potential evapotranspiration models to observed climatic change at German climate stations." *Clim. Chg.*, 104(3), 729-753.

Brugnara, Y., Good, E., Squintu, A. A.,Schrier, V. D. G., and Bronnimann, S. (2019). "The EUSTACE global land station daily air temperature dataset." *Geosci. Data J.*, 6(2), 189-204.

Burrough, P.A., and McDonnell R.A. (1998). "Principles of geographic information systems." Oxford University Press.

Chattopadhyay, N., and Hulme, M. (1997). “Evaporation and potential evapotranspiration in India under conditions of recent and future climate change.” *Agric. Forest Meteorol.*, 87(1), 55-73.

Dalezios, N. R., Loukas, A., and Bampzelis, D. (2002). “Spatial variability of reference evapotranspiration in Greece.” *Phy. Chem. Earth, Parts A/B/C*, 27(23-24), 1031-1038.

Daly, C. (2006). “Guidelines for assessing the suitability of spatial climate data sets.” *Int. J. Climatol.*, 26(6), 707-721.

Debnath, G. C., and Samui, R. P. (1998). “Oscillation of potential evapotranspiration in India and its significance on seasonal potential water requirement of crops.” *Mausam*, 49, 387-394.

Dinpashoh, Y. (2006). “Study of reference crop evapotranspiration in IR of Iran.” *Agric. Water Manag.*, 84(1-2), 123-129.

Doorenbos, J. and Pruitt, W. O. (1977). “Guidelines for predicting crop water requirements.” FAO Irrig. Drain. Paper No. 24. Rome, Italy.

Englund, E.J. (1990). “A variance of geostatisticians.” *Math. Geol.*, 22, 417-455.

Espadafor, M., Lorite, I.J., Gavilan, P. and Berengena, J. (2011). “An analysis of the tendency of reference evapotranspiration estimates and other climate variables during the last 45 years in Southern Spain.” *Agric. Water Manag.*, 98(6), 1045-1061.

Fick, S. E., and Hijmans, R. J. (2017). “WorldClim 2: new 1−km spatial resolution climate surfaces for global land areas.” *Int. J. Climatol.*, 37(12), 4302-4315.

Fisher, J. B., Lee, B., Purdy, A. J., Halverson, G. H., Dohlen, M. B., Nicholson, C. K., ... and Hook, S. (2020). “ECOSTRESS: NASA’s next generation mission to measure evapotranspiration from the international space station.” *Water Resour. Res.*, 56(4), e2019WR026058.

Fooladmand, H.R. and Ahmadi, S.H., (2009). “Monthly spatial calibration of Blaney–Criddle equation for calculating monthly ETo in south of Iran.” *Irrig. Drain.*, 58(2), 234-245.

Fooladmand, H.R., (2011). “Evaluation of Blaney-Criddle equation for estimating evapotranspiration in south of Iran.” *African J. Agric. Res.*, 6(13), 3103-3109.

Frevert, D. K., Hill, R. W., and Braaten, B. C. (1983). “Estimation of FAO evapotranspiration coefficients.” *J. Irrig. Drain. Eng.*, 109(2), 265-270.

Garcia, M., Raes, D., Allen, R., and Herbas, C. (2004). “Dynamics of reference evapotranspiration in the Bolivian highlands (Altiplano).” *Agric. Forest Meteorol.*, 125(1), 67-82.

Gavilan, P., Lorite, I.J., Tornero, S. and Berengena, J. (2006). “Regional calibration of Hargreaves equation for estimating reference ET in a semiarid environment.” *Agric. Water Manag.*, 81(3), 257-281.

George, B. A., and Raghuwanshi, N. S. (2012). “Inter-comparison of reference evapotranspiration estimated using six methods with data from four climatological stations in India.” *J. Indian Water Resour. Soc.*, 32(3− 4), 15-22.

Globalweather (2018). NCEP Climate Forecast System Reanalysis (CFSR). Available from: http://globalweather.tamu.edu/ (accessed October 2018).

Gong, L., Xu, C. Y., Chen, D., Halldin, S., and Chen, Y. D. (2006). “Sensitivity of the Penman–Monteith reference evapotranspiration to key climatic variables in the Changjiang (Yangtze River) basin.” *J. Hydrol.*, 329(3-4), 620-629.

Goovaerts, P. (2000). ”Geostatistical approaches for incorporating elevation into the spatial interpolation of rainfall.” *J. Hydrol.*, 228(1-2), 113-129.

Gorelick, N., Hancher, M., Dixon, M., Ilyushchenko, S., Thau, D., and Moore, R. (2017). “Google Earth Engine: Planetary-scale geospatial analysis for everyone.” *Remote Sens. Env.,* 202, 18-27.

Goyal, R. K. (2004). “Sensitivity of evapotranspiration to global warming: a case study of arid zone of Rajasthan (India).” *Agric. Water Manag.,* 69(1), 1-11.

Guhathakurta, P., Sanap, S., Menon, P., Prasad, A.S., Sable, S.T., and Advani, S.C. (2020). Observed Rainfall Variability and Changes Over Karnataka State, Met Monograph No.: ESSO/IMD/HS/Rainfall Variability/13(2020)/37; India Meteorological Department, Ministry of Earth Sciences, Government of India: New Delhi, India, 2020.

Gundalia, M., and Dholakia, M. (2017). “Modeling daily reference evapotranspiration in middle south Saurashtra region of India for monsoon season using most dominant meteorological variables and the FAO-56 Penman-Monteith method.” *Mausam,* 68(1), 1-8.

Handcock, M. S., Meier, K., and Nychka, D. (1994). “Kriging and splines: An empirical comparison of their predictive performance in some applications: Comment.” *J. Amer. Stats. Assoc.,* 89(426), 401-403.

Hargreaves, G.H., and Samani, Z.A. (1985). “Reference crop evapotranspiration from temperature.” *Appl. Eng. Agric.,* 1(2), 96-99.

Harris, I., Osborn, T. J., Jones, P., and Lister, D. (2020). “Version 4 of the CRU TS monthly high-resolution gridded multivariate climate dataset.” *Sci. Data, 7(1),* 1-18.

Hartkamp, A. D., De Beurs, K., Stein, A., White, J. W. (1999). “Interpolation techniques for climate variables.” NRG-GIS Series 99-01, Mexico, D. F.: CIMMYT.

Hersbach, H., Bell, B., Berrisford, P., Hirahara, S., Horányi, A., Sabater, M. J., ... and Thepaut, J. N. (2020). “The ERA5 global reanalysis.” *Qr. J. Royal Meteorol. Soc.,* 146(730), 1999-2049.

Hobeichi, S., Abramowitz, G., Evans, J., and Ukkola, A. (2018). “Derived Optimal Linear Combination Evapotranspiration (DOLCE): a global gridded synthesis ET estimate.” *Hydrol. Earth Syst. Sci.,* 22(2), 1317-1336.

Hodam, S., Sarkar, S., Marak, A. G., Bandyopadhyay, A., and Bhadra, A. (2017). “Spatial interpolation of reference evapotranspiration in India: comparison of IDW and Kriging Methods.” *J. Inst. Eng. (India): Series A,* 98(4), 511-524.

Huerta, A., Bonnesoeur, V., Adriazola, C. J., Gutierrez, L., Ochoa-Tocachi, B. F., Roman-Danobeytia, F., and Lavado-Casimiro, W. (2022). “PISCOeo_pm, a reference evapotranspiration gridded database based on FAO Penman-Monteith in Peru.” *Sci. Data,* 9(1), 1-18.

India Meteorological Department (IMD) (2022). Agromet Observatories. Available from: https://www.imdagrimet.gov.in/ (accessed August 2022).

Indian Meteorological Society (IMS) (2017). ”IMS Vision 2030.”IMS, New-Delhi, India.

Irmak, S., Kabenge, I., Skaggs, K. E., and Mutiibwa, D. (2012). “Trend and magnitude of changes in climate variables and reference evapotranspiration over 116-yr period in the Platte River Basin, central Nebraska–USA.” *J. Hydrol.,* 420, 228-244.

Itenfisu, D., Elliott, R. L., Allen, R. G., and Walter, I. A. (2003). “Comparison of reference evapotranspiration calculations as part of the ASCE standardization effort.” *J. Irrig. Drain. Eng.,* 129(6), 440-448.

Jabloun, M.D. and Sahli, A. (2008). “Evaluation of FAO-56 methodology for estimating reference evapotranspiration using limited climatic data: Application to Tunisia.” *Agric. Water Manag.,* 95(6), 707-715.

Jaswal, A. K., and Rao, G. S. P. (2010). “Recent trends in meteorological parameters over Jammu and Kashmir.” *Mausam,* 61(3), 369-382.

Jaswal, A. K., Rao, G. P., and De, U. S. (2008). “Spatial and temporal characteristics of evaporation trends over India during 1971-2000.” *Mausam,* 59(2), 149.

Jeffrey, S. J., Carter, J. O., Moodie, K. B., and Beswick, A. R. (2001). “Using spatial interpolation to construct a comprehensive archive of Australian climate data.” *Environ. Model. Soft.,* 16(4), 309-330.

Jensen, M. E., Robb, D. C., and Franzoy, C. E. (1970). “Scheduling irrigations using climate-crop-soil data.” Proceedings of the American Society of Civil Engineers, *J. Irrig. Drain. Division,* 96(IRI), 25-38.

Jensen, M. E., Burman, R. D. and Allen, R. G. (1990). “Evapotranspiration and Irrigation water Requirements.” ASCE Manuals and Rep. on Eng., Pract. No. 70, ASCE, New York, N.Y.

Jensen, D.T., Hargreaves, G.H., Temesgen, B. and Allen, R.G. (1997). “Computation of ETo under nonideal conditions.” *J. Irrig. Drain. Eng.,* 123(5), 394-400.

Jhajharia, D., and Singh, V. P. (2011). “Trends in temperature, diurnal temperature range and sunshine duration in Northeast India.” *Int. J. Climatol.,* 31(9), 1353-1367.

Jhajharia, D., Dinpashoh, Y., Kahya, E., Singh, V. P., and Fard, F. A. (2012). “Trends in reference evapotranspiration in the humid region of northeast India.” *Hydrol. Proc.,* 26(3), 421-435.

Jothiprakash, V., Devamane, M.G., and Sasireka, K. (2008). ”Inter-comparison of radiation-based reference crop evapotranspiration methods.” *J. Inst. Engrs (India)*, 89 Dec(AG), 22-27.

Jothiprakash, V., Devamane, M.G., and Sasireka, K. (2007). ”Intercomparison of temperature-based reference crop evapotranspiration methods.” *J. Inst. Engrs (India)*, 88 Dec (AG), 19-26.

Khandelwal, M. K., Shekh, A. M., Pandey, V. and Zaman, M. S. (1999). “Selection of appropriate method for computation of potential evapotranspiration and assessment of rainwater harvesting potential for middle Gujarat.” *J. Agrometeorol.,* 1 (2), 163-166.

Karnataka State Department of Agriculture (KSDA), Government of Karnataka 2018 Agro-climatic zones of Karnataka.
Available from: http://raitamitra.kar.nic.in/stat/kacz.htm (accessed October 2018).

Karthikeyan, L., Chawla, I., and Mishra, A. K. (2020). “A review of remote sensing applications in agriculture for food security: Crop growth and yield, irrigation, and crop losses.” *J. Hydrol.,* 586, 124905.

Katul, G. G., Cuenca, R. H., Grebet, P., Wright, J. L. and Pruitt, W. O. (1992). “Analysis of evaporative flux data for various climates.” *J. Irrig. Drain. Eng..,* 118 (4), 601-618.

Khan, M. S., Baik, J., and Choi, M. (2020). “Inter-comparison of evapotranspiration datasets over heterogeneous landscapes across Australia.” *Adv. Space Res.,* 66(3), 533-545.

Kisi, O. (2014). “Comparison of different empirical methods for estimating daily reference evapotranspiration in Mediterranean climate.” *J. Irrig. Drain. Eng.,* 140(1): 04013002.

Kovoor, G. M. (2006). “Modelling Impacts of Climate Change on Irrigated Agriculture in India.” Ph.D. thesis, N.I.T.K., Surathkal, Mangalore, Karnataka, India.

Kundu, S., Mondal, A., Khare, D., Hain, C., and Lakshmi, V. (2018). “Projecting climate and land use change impacts on actual evapotranspiration for the Narmada river basin in central India in the future.” *Remote Sens.,* 10(4), 578.

Laslett, G. M. (1994). “Kriging and splines: an empirical comparison of their predictive performance in some applications.” *J. Amer. Stats. Assoc.,* 89(426), 391-400.

Li, J., and Heap, A. D. (2011). "A review of comparative studies of spatial interpolation methods in environmental sciences: Performance and impact factors." *Ecol Inform.,* 6(3-4), 228-241.

Livneh, B., Bohn, T. J., Pierce, D. W., Arriola, M. F., Nijssen, B., Vose, R., ... and Brekke, L. (2015). "A spatially comprehensive, hydrometeorological data set for Mexico, the US, and Southern Canada 1950–2013." *Sci. Data,* 2(1), 1-12.

Ma, Y., and Guttorp, P. (2013). "Estimating daily mean temperature from synoptic climate observations." *Int. J. Climatol.,* 33 (5), 1264–1269.

Mall, R. K., and Gupta, B. R. D. (2002). "Comparison of evapotranspiration models." *Mausam,* 53(2), 119-126.

Mancosu, N., Snyder, R. L., and Spano, D. (2014). "Procedures to develop a standardized reference evapotranspiration zone map." *J. Irrig. Drain. Eng.,* 140(9), A4014004.

Mardikis, M. G., Kalivas, D. P., and Kollias, V. J. (2005). "Comparison of interpolation methods for the prediction of reference evapotranspiration-an application in Greece." *Water Resourc. Manag.,* 19(3), 251-278.

Martens, B. et al. (2017). "GLEAM v3: satellite-based land evaporation and root-zone soil moisture." *Geosci. Model Dev.,* 10, 1903–1925.

Martinez-Cob, A. (1996). "Multivariate geostatistical analysis of evapotranspiration and precipitation in mountainous terrain." *J. Hydrol.,* 174(1-2), 19-35.

Martınez-Cob, A., and Tejero-Juste, M. (2004). A wind-based qualitative calibration of the Hargreaves ET0 estimation equation in semiarid regions. *Agric. Water Manag.,* 64(3), 251-264.

Masanta, S. K., and Srinivas, V. V. (2021). "Regionalization of evapotranspiration in India using fuzzy dynamic clustering approach. Part 2: Applications of regions." *Int. J. Climatol.,* 41, E1371-E1395.

McCabe, M. F., Houborg, R., and Lucieer, A. (2016). "High-resolution sensing for precision agriculture: from Earth-observing satellites to unmanned aerial vehicles." In Remote Sensing for Agriculture, Ecosystems, and Hydrology XVIII (Vol. 9998, pp. 346-355). SPIE.

McKenney, M. S., and Rosenberg, N. J. (1993). "Sensitivity of some potential evapotranspiration estimation methods to climate change." *Agric. Forest Meteorol.,* 64(1-2), 81-110.

McMahon, T. A., Peel, M. C., Lowe, L., Srikanthan, R., and McVicar, T. R. (2013). "Estimating actual, potential, reference crop and pan evaporation using standard meteorological data: a pragmatic synthesis." *Hydrol. Earth Syst. Sci.,* 17(4), 1331-1363.

McVicar, T. R., Roderick, M. L., Donohue, R. J., Li, L. T., Van Niel, T. G., Thomas, A., ... and Dinpashoh, Y. (2012). "Global review and synthesis of trends in observed terrestrial near-surface wind speeds: Implications for evaporation." *J. Hydrol.,* 416, 182-205.

McVicar, T. R., Van Niel, T. G., Li, L., Hutchinson, M. F., Mu, X., and Liu, Z. (2007). "Spatially distributing monthly reference evapotranspiration and pan evaporation considering topographic influences." *J. Hydrol.,* 338(3-4), 196-220.

Mendicino, G. and Senatore, A. (2013). "Regionalization of the Hargreaves coefficient for the assessment of distributed reference evapotranspiration in Southern Italy." *J. Irrig. Drain. Eng.,* 139(5), 349-362.

Mohan, S. (1991). "Intercomparison of evapotranspiration estimates." *Hydrol. Sci. J.,* 36(5), 447-460.

Nandagiri, L. and Kovoor, G.M., (2006). "Performance evaluation of reference evapotranspiration equations across a range of Indian climates." *J. Irrig. Drain. Eng.,* 132(3), 238-249.

National Remote Sensing Cnetre (2021). Actual Evapotranspiration, Geospatial hydro products developed by National Remote Sensing Centre under National Hydrology Project, https://bhuvan.nrsc.gov.in/nhp.(accessed August 2022).

Nigee K, (2015). "Calibration of modified Blaney-Criddle equation to compute reference evapotranspiration at selected locations in Karnataka state, India." M.Tech. thesis, N.I.T.K., Surathkal, Mangalore, Karnataka, India.

Niranjan, S., and Nandagiri, L. (2021). "Effect of local calibration on the performance of the Hargreaves reference crop evapotranspiration equation." *J. Water Clim. Chg.,* 12(6), 2654-2673.

Pai, D. S., Sridhar, L., Rajeevan, M., Sreejith, O. P., Satbhai, N. S., and Mukhopadhyay, B. (2014). “Development of a new high spatial resolution ($0.25 \times 0.25$) long period (1901–2010) daily gridded rainfall data set over India and its comparison with existing data sets over the region.” *Mausam,* 65(1), 1-18.

Pandey, V., Pandey, P.K. and Mahanta, A.P. (2014). “Calibration and performance verification of Hargreaves Samani equation in a humid region.” *Irrig. Drain.,* 63(5), 659-667.

Patel, J., Patel, H., and Bhatt, C. (2015). “Modified Hargreaves equation for accurate estimation of evapotranspiration of diverse climate locations in India.” *Proc. Natl. Acad. Sci., India Sect. B: Biological Sci.,* 85(1), 161-166.

Pelosi, A., Terribile, F., Urso, D. G., and Chirico, G. B. (2020). “Comparison of ERA5-Land and UERRA MESCAN-SURFEX reanalysis data with spatially interpolated weather observations for the regional assessment of reference evapotranspiration.” *Water,* 12(6), 1669.

Pereira, A.R., and Pruitt, W.O. (2004). “Adaptation of the Thornthwaite scheme for estimating daily reference evapotranspiration.” *Agric. Water Manag.,* 66(3), 251-257.

Philips, D.L., Dolph, J., Marks, D. (1992). “A comparison of geostatistical procedures for spatial analysis of precipitation in mountainous terrain.” *Agric. Forest Meteorol.,* 58,119- 141.

Pirinen, P., Lehtonen, I., Heikkinen, R. K., Aapala, K., and Aalto, J (2022). “Daily gridded evapotranspiration data for Finland for 1981–2020.” *FMI’s Clim. Bull.: Res. Lett.,* 4(2), 35–37.

Priestley, C. H. B., and Taylor, R. J. (1972). “On the assessment of surface heat flux and evaporation using large-scale parameters.” *Mon. Weath. Rev., 100(2),* 81-92.

Priya, A., Nema, A., Islam, A., and Sikka, A. K. (2015). Assessing sensitivity of reference evapotranspiration to changes in climatic variables: A case study of Akola, India. *Mausam,* 66(4), 777-784.

Purnadurga, G., Kumar, T. L., Rao, K. K., Barbosa, H., and Mall, R. K. (2019). “Evaluation of evapotranspiration estimates from observed and reanalysis data sets over Indian region.” *Int. J. Climatol.,* 39(15), 5791-5800.

Ramachandra, T. V., Kamakshi, G., and Shruthi, B. V. (2004). "Bioresource status in Karnataka." *Ren. Sustain. Ener. Rev.,* 8(1), 1-47.

Remesan, R., and Holman, I. P. (2015). "Effect of baseline meteorological data selection on hydrological modelling of climate change scenarios." *J. Hydrol,* 528, 631-642.

Rigden, A. J., and Salvucci, G. D. (2015). "Evapotranspiration based on equilibrated relative humidity (ETRHEQ): Evaluation over the continental US." *Water Resourc. Res.,* 51(4), 2951-2973.

Sentelhas, P.C., Gillespie, T.J. and Santos, E.A. (2010). "Evaluation of FAO Penman–Monteith and alternative methods for estimating reference evapotranspiration with missing data in Southern Ontario, Canada." *Agric. Water Manag.,* 97(5), 635-644.

Shahidian, S., Serralheiro, R.P., Serrano, J. and Teixeira, J.L. (2013). "Parametric calibration of the Hargreaves–Samani equation for use at new locations." *Hydrol. Proc.,* 27(4), 605-616.

Sharma, V., and Irmak, S. (2012). "Mapping spatially interpolated precipitation, reference evapotranspiration, actual crop evapotranspiration, and net irrigation requirements in Nebraska: Part I. Precipitation and reference evapotranspiration." *Trans. ASABE,* 55(3), 907-921.

Singer, M. B., Asfaw, D. T., Rosolem, R., Cuthbert, M. O., Miralles, D. G., MacLeod, D., ... and Michaelides, K. (2021). "Hourly potential evapotranspiration at 0.1° resolution for the global land surface from 1981-present." *Sci. Data,* 8(1), 1-13.

Singh, V. P., 1989, "Hydrologic systems", Vol. 2, Prentice-Hall, Englewood Cliffs, N. J., USA.

Sperna Weiland, F. C., Tisseuil, C., Dürr, H. H., Vrac, M., and Van Beek, L. P. H. (2012). "Selecting the optimal method to calculate daily global reference potential evaporation from CFSR reanalysis data for application in a hydrological model study." *Hydrol. Earth Syst. Sci.,* 16(3), 983-1000.

Subburayan, S., Murugappan, A., and Mohan, S. (2011). "Modified Hargreaves equation for estimation of ET0 in a hot and humid location in Tamilnadu State, India." *Int. J. Eng. Sci. Tech.,* 3(1), 592-600.

Tabari, H. (2010). “Evaluation of reference crop evapotranspiration equations in various climates.” *Water Resourc. Manag.,* 24(10), 2311-2337.

Tabari, H., and Talaee, P.H. (2011). “Local calibration of the Hargreaves and Priestley-Taylor equations for estimating reference evapotranspiration in arid and cold climates of Iran based on the Penman-Monteith model.” *J. Hydrol. Eng.,* 16(10), 837-845.

Tabari, H., and Talaee, P. H. (2014). “Sensitivity of evapotranspiration to climatic change in different climates.” *Global Planet. Chg.,* 115, 16-23.

Tanguy, M., Prudhomme, C., Smith, K., and Hannaford, J. (2018). “Historical gridded reconstruction of potential evapotranspiration for the UK.” *Earth Syst. Sci. Data,* 10(2), 951-968.

Temesgen, B., Eching, S., Davidoff, B. and Frame, K. (2005). “Comparison of some reference evapotranspiration equations for California.” *J. Irrig. Drain. Eng.,* 131(1), 73-84.

Thomas, A. (2000). “Spatial and temporal characteristics of potential evapotranspiration trends over China.” *Int. J. Climatol.,* 20(4), 381-396.

Thornthwaite, C. W. (1948). “An approach toward a rational classification of climate.” *Geog. Rev.,* 38(1), 55-94.

Tomas-Burguera, M., Vicente-Serrano, S. M., Beguería, S., Reig, F., and Latorre, B. (2019). “Reference crop evapotranspiration database in Spain (1961–2014).” *Earth Syst. Sci. Data,* 11(4), 1917-1930.

Trajkovic, S. (2007). “Hargreaves versus Penman-Monteith under humid conditions.” *J. Irrig. Drain. Eng.,* 133(1), 38-42.

United Nations Educational, Scientific and Cultural Organization - United Nations World Water Development Report No. 4 (UN,WWDR) (2012). “Managing Water under Uncertainty and Risk.”, UNESCO, Paris, France.

Urrea, L. R., Olalla, S. D. F. M., Fabeiro, C., and Moratalla, A. (2006). “Testing evapotranspiration equations using lysimeter observations in a semiarid climate.” *Agric. Water Manag.,* 85(1-2), 15-26.

Valero, J.F.M., Alvarez, V.M. and Real, M.M.G. (2013). “Regionalization of the Hargreaves coefficient to estimate long-term reference evapotranspiration series in SE Spain.” *Spanish J. Agric. Res.,* (4), 1137-1152.

Valiantzas, J.D. (2013). "Simplified forms for the standardized FAO-56 Penman–Monteith reference evapotranspiration using limited weather data." *J. Hydrol.,* 505, 13-23.

Valiantzas, J. D. (2015). "Simplified limited data Penman's ET0 formulas adapted for humid locations." *J. Hydrol.,* 524, 701-707.

Vanderlinden, K., Giraldez, J.V. and Meirvenne, V. M. (2004). "Assessing reference evapotranspiration by the Hargreaves method in southern Spain." *J. Irrig. Drain. Eng.,* 130(3), 184-191.

Verma, I. J., Jadhav, V. N., and Erande, R. S. (2008). "Recent variations and trends in potential evapotranspiration (PET) over India." *Mausam,* 59(1), 119-128.

Vicente-Serrano, S. M., Sanchez, S. M. A., and Cuadrat, J. M. (2003). "Comparative analysis of interpolation methods in the middle Ebro Valley (Spain): application to annual precipitation and temperature." *Clim. Res.,* 24(2), 161-180.

Vicente-Serrano, S. M., Tomas-Burguera, M., Begueria, S., Reig, F., Latorre, B., Peña-Gallardo, M., ... and González-Hidalgo, J. C. (2017). "A high resolution dataset of drought indices for Spain." *Sci. Data,* 2(3), 22.

Xu, C.Y., and Singh, V.P. (2002). "Cross comparison of empirical equations for calculating potential evapotranspiration with data from Switzerland." *Water Resour. Manag.,* 16(3), 197-707.

Xu, C., Wang, J., and Li, Q. (2018). "A new method for temperature spatial interpolation based on sparse historical stations." *J. Clim.,* 31(5), 1757-1770.

Yanto, Livneh, B., and Rajagopalan, B. (2017). "Development of a gridded meteorological dataset over Java island, Indonesia 1985–2014." *Sci. Data,* 4(1), 1-10.

Zhang, Y., Liu, C., Tang, Y., and Yang, Y. (2007). "Trends in pan evaporation and reference and actual evapotranspiration across the Tibetan Plateau." *J. Geophys. Res.: Atmos.,* 112(D12).

Zhao, L., Xia, J., Xu, C. Y., Wang, Z., Sobkowiak, L., and Long, C. (2013). "Evapotranspiration estimation methods in hydrological models." *J. Geogr. Sci.,* 23(2), 359-369.

Zimmerman, D., Pavlik, C., Ruggles, A., and Armstrong, M. P. (1999). "An experimental comparison of ordinary and universal kriging and inverse distance weighting." *Math. Geol.,* 31(4), 375-390.

Zomer, R. J., Xu, J., and Trabucco, A. (2022). "Version 3 of the Global Aridity Index and Potential Evapotranspiration Database." *Sci. Data,* 9(1), 1-15.

## PUBLICATIONS FROM THE RESEARCH

**Journal**

Niranjan, S., and Nandagiri, L. (2021). "Effect of local calibration on the performance of the Hargreaves reference crop evapotranspiration equation." *J. Water Clim. Chg.*, 12(6), 2654-2673.

Niranjan, S., and Nandagiri, L. (2022). "Performance Evaluation of Simpler Reference Crop Evapotranspiration Estimation Equations With and Without Local Calibration." *J. Appl. Water Res. Eng.,* (Under Review).

Niranjan, S., and Nandagiri, L. (2023). "Development of Daily Gridded Penman-Monteith Reference Crop Evapotranspiration Data for Karnataka State, India." *ISH J. Hydraul. Eng.,* (Under Review).

**Conference**

Niranjan, S., and Nandagiri, L. (2017). "Evaluation of evapotranspiration models in different climatic regions of India." *Proc., Int. Conf. on Hydraulics, Water Resources and Coastal Eng.*, LD College of Engineering, Ahmedabad, India., 418-428.

Niranjan, S., and Nandagiri, L. (2018). "Development of a gridded Reference Crop Evapotranspiration dataset." *Natl. Conf. on New Frontiers in Civil Eng.*, IIT Bombay, Mumbai, India.

Niranjan, S., and Nandagiri, L. (2019). "Evaluation of Solar Radiation Equations for Estimating Reference Crop Evapotranspiration in different Agro-Climatic Zones of Karnataka State, India." *AGU Fall Meeting 2019*, San Francisco, U.S.A.

Niranjan, S., and Nandagiri, L. (2020). "Performance of Modified Temperature-Based Reference Crop Evapotranspiration Models across Different Agro-Climatic Zones in Karnataka State, India." *EGU General Assembly 2020*, Vienna, Austria.